



## Review article

## Methods of photovoltaic fault detection and classification: A review

Ying-Yi Hong<sup>\*</sup>, Rolando A. Pula

Department of Electrical Engineering, Chung Yuan Christian University, Taoyuan City, 32023, Taiwan



## ARTICLE INFO

## Article history:

Received 1 February 2022  
 Received in revised form 4 April 2022  
 Accepted 12 April 2022  
 Available online 4 May 2022

## Keywords:

Classification  
 Detection  
 Electrical based method  
 Fault  
 Photovoltaic system  
 Visual and thermal method

## ABSTRACT

Photovoltaic (PV) fault detection and classification are essential in maintaining the reliability of the PV system (PVS). Various faults may occur in either DC or AC side of the PVS. The detection, classification, and localization of such faults are essential for mitigation, accident prevention, reduction of the loss of generated energy, and revenue. In recent years, the number of works of PV fault detection and classification has significantly increased. These works have been reviewed by considering the categorization of detection and classification techniques. This paper improves of the categorization of methods to study the faulty PVS by considering visual and thermal method and electrical based method. Moreover, an effort is made to list all potential faults in a PVS in both the DC and AC sides. Specific PV fault detection and classification techniques are also enumerated. A possible direction for research on the PV fault detection and classification, such as quantum machine learning, internet of things, and cloud/edge computing technologies, is suggested as a guide for future emerging technologies.

© 2022 The Author(s). Published by Elsevier Ltd. This is an open access article under the CC BY-NC-ND license (<http://creativecommons.org/licenses/by-nc-nd/4.0/>).

## Contents

|   |      |
|---|------|
| 1. Introduction.....  | 5899 |
| 2. PV systems and parameters.....   | 5899 |
| 2.1. PV model.....  | 5899 |
| 2.2. PVS interconnection.....   | 5901 |
| 2.2.1. Stand-alone PVS.....   | 5901 |
| 2.2.2. Grid-connected PVS.....  | 5901 |
| 3. Types of PV faults.....  | 5901 |
| 3.1. Mismatch fault.....  | 5902 |
| 3.2. Ground-fault.....  | 5902 |
| 3.3. Line-to-line fault.....  | 5902 |
| 3.4. Arc faults.....  | 5902 |
| 3.5. Other types of faults.....   | 5902 |
| 3.5.1. Diode faults.....  | 5902 |
| 3.5.2. Junction box faults.....   | 5903 |
| 3.5.3. Hot spot.....  | 5903 |
| 4. PV fault detection and classification monitoring system.....                                 | 5903 |
| 4.1. Measured parameters.....   | 5903 |
| 4.2. Data acquisition, measurement and transmission.....  | 5903 |
| 4.3. DATA preprocessing.....  | 5903 |
| 5. Categories of PV fault detection and classification techniques.....                          | 5906 |
| 5.1. Visual and thermal methods.....  | 5907 |
| 5.1.1. Infrared/Thermal Imaging (IMI).....  | 5907 |
| 5.1.2. Visual Inspection (VI).....  | 5907 |
| 5.1.3. Electroluminescence Imaging (EI).....  | 5907 |
| 5.1.4. Lock-in Thermography (LIT).....  | 5907 |
| 5.1.5. Visual and thermal methods integrated with Artificial Intelligence Techniques (AIT)..... | 5908 |

<sup>\*</sup> Corresponding author.

E-mail address: [yyhong@ee.cycu.edu.tw](mailto:yyhong@ee.cycu.edu.tw) (Y.-Y. Hong).

|         |  |      |
|---------|--|------|
| 5.2.    | Electrical Based Methods (EBMS)                            | 5908 |
| 5.2.1.  | Climatic Data-independent Technique (CDT)                  | 5908 |
| 5.2.2.  | I–V characteristics analysis (IVCA)                        | 5908 |
| 5.2.3.  | Power Loss Analysis (PLA)                                  | 5909 |
| 5.2.4.  | Current and voltage measurement                            | 5909 |
| 5.2.5.  | Heat exchange and temperature based method                 | 5909 |
| 5.2.6.  | Voltage Randomness Estimation (VRE)                        | 5910 |
| 5.2.7.  | Voltage/current Spectral Analysis (VCSA)                   | 5910 |
| 5.2.8.  | Artificial Intelligence Technique (AIT)                    | 5910 |
| 5.2.9.  | Statistical and signal processing techniques               | 5913 |
| 5.2.10. | Hybrid methods   | 5920 |
| 5.2.11. | Other types of methods                                     | 5920 |
| 6.      | Future trends in PV fault detection and classification     | 5920 |
| 6.1.    | Quantum machine learning                                   | 5920 |
| 6.2.    | Internet of Things, cloud-based monitoring, edge computing | 5921 |
| 7.      | Conclusion   | 5922 |
|         | Declaration of competing interest                          | 5924 |
|         | Acknowledgments  | 5924 |
|         | References   | 5924 |

## 1. Introduction

The increased production of renewable energy in the recent decades can be attributed to the commitment of countries to the Kyoto protocol (de Boer, 2008). The Kyoto protocol aims to lessen the effect of climate change which is caused by increasing carbon dioxide emission. Photovoltaic systems (PVs) are one class of sources of renewable energy. In recent years, the production of energy by PVSs has been increasing, as presented in the report of the International Renewable Energy Agency (IRENA) in 2020 (Mantel et al., 2019), which showed that the installed PV capacity in that year was approximately 700,000 MW, and this value had been increasing continuously since the previous decade. The decline in the global weighted mean levelized cost of energy (LCOE) due to PVSs from 2010 to 2019 was about 82 percent (Mantel et al., 2019). This relationship between increasing installed capacity and falling weighted global LCOE can be attributed to the many advantages of the PVS, such as availability, noise-free operation, absence of pollution, ease of installation, modularity, reliability, and the possibility of installation wherever the source of energy is an obstacle-free and abundant.

Like other systems, PVSs inevitably fail at times. These failures are primarily caused by various faults, which occur in different parts/components of the PVS, such as PV modules, protection devices, interconnections, converters, and inverters. These faults are caused mostly by external operating conditions, such as dirt or soil in the modules, converter and/or inverter failures, shading conditions, manufacturing mismatches, and module aging (Mellit et al., 2018). Catastrophic faults in a PVS can be broadly categorized as line-to-line faults, arc faults, ground faults (Alam et al., 2015), and mismatch faults.

According to the data of Blume (2021), fires associated with faults in Germany are primarily caused by human error, with 38% arising from in installation errors and 17% from failures of planning. The second most significant cause (35%) of fire due to faults involves product failure and external factors are responsible for 10% of such failures. Fig. 1 displays a summarizing pie chart (Blume, 2021).

Faults in PVSs must be understood to prevent fire and the loss of vast amounts of energy. The most recent report of fires that involved a PVS in the UK (E. & I. S. Department for Business, 2021) was published in 2019. It makes different recommendations concerning the installations of PVSs to prevent catastrophic failures and provides guidelines for avoiding fires associated with PVSs. PV fault detection and classification are necessary for understanding such faults. Owing to the aforementioned advantages of PV,

interest in PVSs, especially in fault detection and classification, has been steadily increasing. Most of relevant works focus on particular areas of interest (Triki-Lahiani et al., 2018), such as the type of PVS installation, the technique used, the integration of sensors, the input parameters used in applied methods, data acquisition, the application of techniques to the system (offline/online), and integration of the proposed system. Several studies have also reviewed various approaches about fault detection and classification in PVSs. However, they considered only particular topics such as PVS interconnection and associated electrical methods (E. & I. S. Department for Business, 2021), particular parts of PVS (Alam et al., 2015), and the advantages and limitations of compared methods (Mellit et al., 2018).

This review will focus on fault detection and classification methods; and review numerous papers that may and may not have been reviewed elsewhere. This paper will also provide concise explanations, presentations, and comparisons that will elucidate the integrations, applications, and types of detection and classification and whether fault localization is involved in the technique applied.

This review is organized as follows. Section 2 will discuss types of PV system, the standard parameters used for the PV fault detection and classification, and the types of PVS interconnection. Section 3 will discuss types of faults in PVS. Section 4 describes the PV monitoring system. Section 5 will cover the typical configuration of a PV system and categorize various PV fault detection and classification techniques. Section 6 will discuss the future of the PV fault detection and classification and provide a possible direction for research. Section 7 will draw a conclusion.

## 2. PV systems and parameters

### 2.1. PV model

PV arrays comprise PV modules, which are formed by combining cells. PV array is constructed by the interconnection among PV modules in either series or parallel. Connecting modules in series increases their output voltage while connecting them in parallel increases their output current (Triki-Lahiani et al., 2018). Combining these two configurations of PV cells will increase the PV power output. A simplified PV cell equivalent model is always used to understand the electrical behavior of a PV cell, as shown in Fig. 2 (Anon, 2021b). The circuit in Fig. 2 has an ideal current source, a parallel diode connected with the current source, and a resistor in series.

## Nomenclature

### PV related terminologies

|          |   |
|----------|---|
| AC       | Alternating current                       |
| BcD      | Blocking diode                            |
| BESS     | Battery energy storage system             |
| BpD      | bypass diode                              |
| CCC      | Current carrying conductor                |
| DC       | Direct current                            |
| dI/dV    | change in current with respect to voltage |
| EVA      | Ethylene Vinyl Acetate                    |
| F1       | Partial shading fault                     |
| F3       | line-to-line fault                        |
| F31      | line-to-line (same string)                |
| F32      | line-to-line (different strings)          |
| F4       | arc fault                                 |
| F41      | series arc fault                          |
| F42      | parallel arc fault                        |
| F5       | bypass diode fault                        |
| F51      | shorted bypass diode fault                |
| F52      | shunted bypass diode                      |
| F6       | Blocking diode fault                      |
| F61      | Open-circuit blocking diode fault         |
| F62      | Short-circuit blocking diode fault        |
| GCPVS    | Grid-connected PVS                        |
| $I$      | PV current                                |
| $I_D$    | Diode current                             |
| $I_0$    | Diode saturation current                  |
| $I_{SC}$ | current (short circuit of solar cell)     |
| $I-V$    | Current-voltage                           |
| $k$      | Boltzmann's constant                      |
| MPP      | Maximum power point                       |
| MPPT     | Maximum power point tracking              |
| MW       | Megawatts                                 |
| PV       | Photovoltaic                              |
| PVS      | Photovoltaic system                       |
| $R_s$    | series intrinsic resistance               |
| SAPVS    | Stand-alone PVS                           |
| $V_T$    | thermal potential                         |

### PV fault detection and classification methods

|          |   |
|----------|---|
| ABC      | Artificial bee colony   |
| AIT      | Artificial intelligence technique                                     |
| ANFIS    | Adaptive neuro-fuzzy inference system                                 |
| ANN      | Artificial neural network   |
| a-Si     | Amorphous Silicon   |
| CART     | Classification regression tree  |
| CDT      | Climate-based techniques  |
| CNN      | Convolutional neural network  |
| DA-DCGAN | Domain adaptation with a convolutional generative adversarial network |
| DL       | Deep learning   |
| DNN      | Deep neural network   |
| DT       | decision tree   |
| DWT      | Discrete wavelet transform  |
| EBM      | Electrical-based method   |

|         |  |
|---------|--|
| ECM     | Earth capacitance measurement                      |
| EI      | Electroluminescence imaging                        |
| ELM     | Extreme learning machine                           |
| EMD     | Empirical mode decomposition                       |
| EML     | Ensemble machine learning                          |
| EWMA    | Exponentially weighted moving average              |
| FCM     | Fuzzy C-means                                      |
| FF      | Fill factor  |
| FFT     | Fast Fourier Transform                             |
| FIS     | Fuzzy inference systems                            |
| FIT     | Finite impulse response                            |
| FLC     | Fuzzy logic control                                |
| GA      | Genetic algorithm                                  |
| GAN     | Generative adversarial network                     |
| GRU     | Gated recurrent unit                               |
| IMI     | Infrared/thermal imaging                           |
| IoT     | Internet of things                                 |
| IVCA    | I–V characteristics analysis                       |
| KDE     | Kernel density estimation                          |
| k-NN    | k-nearest neighbor                                 |
| LIT     | Lock-in thermography                               |
| LSTM    | Long short-term memory                             |
| MEWMA   | Multivariate exponentially weighted moving average |
| ML      | Machine learning                                   |
| MRA     | Multiresolution analysis                           |
| MSD     | Multiresolution signal decomposition               |
| NARX    | Nonlinear autoregressive exogenous                 |
| NB      | Naïve Bayes  |
| PCA     | Principal component analysis                       |
| PLA     | Power losses analysis                              |
| PLAM    | Power losses analysis method                       |
| PNN     | Probabilistic neural network                       |
| PSO     | Particle swarm optimization                        |
| QML     | Quantum machine learning                           |
| QNN     | Quantum neural network                             |
| RBFNN   | Radial basis function neural network               |
| RF      | Random forest                                      |
| RK      | Reduced-kernel                                     |
| RNN     | Recurrent neural network                           |
| SA      | Simulated annealing                                |
| SNN     | Shallow neural network                             |
| SVM     | Support vector machine                             |
| TDR     | Time domain reflectometry                          |
| TSK-FRB | Takagi–Sugeno Kang Fuzzy rule-based                |
| VCSA    | Voltage/current spectrum analysis                  |
| VI      | Visual inspection                                  |
| VRE     | Voltage randomness estimation                      |
| VTM     | Visual and thermal method                          |

### Other abbreviations

|        |  |
|--------|--|
| BS IEC | British standard International Electrotechnical Commission |
| FTP    | File transfer protocol                                     |
| IEC    | International Electrochemical Commission                   |
| IP     | Internet protocol  |

|       |  |
|-------|--|
| IPS   | Internet protocol suite                        |
| IR    | Infrared                                       |
| IRENA | International Renewable Energy Agency          |
| LCOE  | Levelized cost of energy                       |
| NEC   | National electrical code                       |
| NREL  | National renewable energy laboratory           |
| NTP   | Network timing protocol                        |
| OSTI  | Office of scientific and technical information |
| PDI   | Potential-induced degradation                  |
| RF    | radio frequency                                |
| SMTP  | Simple mail transfer protocol                  |
| TCP   | Transmission control protocol                  |
| TFQ   | TensorFlow quantum                             |
| UDP   | Transmission control protocol                  |

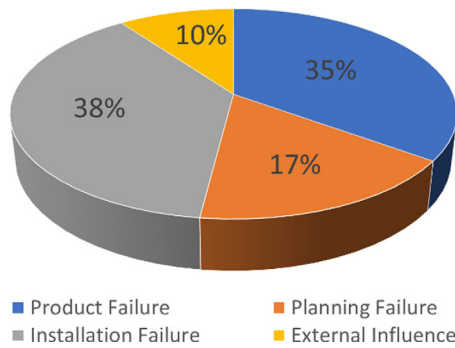


Fig. 1. Root causes of fires in PV systems in Germany.

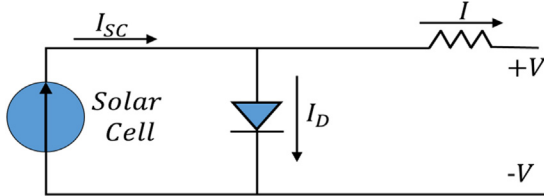


Fig. 2. Cell equivalent model.

The current  $I$  in Fig. 2 is given by Eq. (1).

$$I = I_{sc} - I_D = I_{sc} - I_0 e^{\left(\frac{V + IR_s}{nV_T}\right) - 1} \quad (1)$$

where  $I_{sc}$  is the short-circuit current of a solar cell under a certain irradiance;  $I_D$  represents the diode current;  $I_0$  represents the diode saturation current;  $R_s$  is the series intrinsic resistance to the current flow,  $V$  denotes the terminal voltage of the cell;  $n$  means the ideal constant of the diode;  $V_T$  is the thermal potential of cell (V), which is the  $m \left( \frac{kT}{q} \right)$ ;  $k$  signifies the Boltzmann's constant;  $T$  is temperature in Kelvin;  $q$  is the Coulomb constant, and  $m$  is for the number of cells in series in each module.

## 2.2. PVS interconnection

A PVS can be categorized based on its connection and installed power (Anon, 2021b). A PVS connection may be classified as stand-alone or grid-connected mode. With respect to installation sites, a PVS may be located in residential, off-shore, industrial, or utility sites.

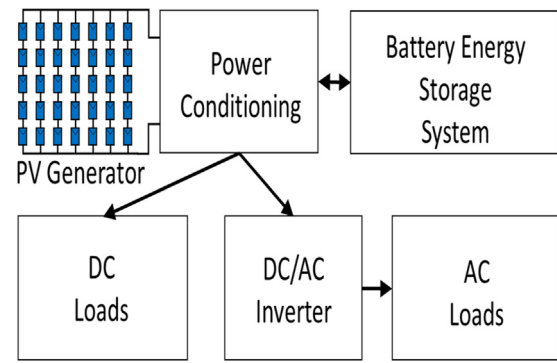


Fig. 3. Block diagram of SAPVS.

### 2.2.1. Stand-alone PVS

A stand-alone PV system (SAPVS) is generally composed of PV generators (arrays or modules) that are connected to power conditioning circuits (such as regulator, converter, protection diodes and inverter) (Kim et al., 2009), with a battery energy storage system to store surplus energy that is generated by the PVS and used during an emergency or at night. Maximum power point tracking (MPPT) is also included in the power conditioning block to provide a maximum power point (MPP). MPPT is required for the PVS to maintain the MPP owing to the intermittency of solar irradiances and temperatures. Fig. 3 presents different blocks that are associated with the standalone PV system. In the standalone PV system, the power from the power conditioning unit goes directly either to DC loads or the DC/AC inverter before going to AC loads.

### 2.2.2. Grid-connected PVS

The grid-connected PVS (GCPVS) is a PVS tied/connected to a utility grid. A typical configuration of GCPVS comprises a PV generator (PV arrays), a diode (bypass and blocking), a dc-link, DC/DC converter, DC/AC inverter, filter, step-up transformer, and power/utility grid (Anon, 2021b). The various functions of the block devices have been discussed elsewhere (Anon, 2021b). Fig. 4 displays a simplified block diagram of a GCPVS.

In Fig. 4, the DC power that is generated by the PV arrays goes to the DC/DC converter. The DC voltage in this block can be increased. The DC/DC converter also performs MPPT for the MPP operation of the PV arrays. Measured voltage and current are looped to the MPPT block to maximize output power. The output of the DC/DC converter goes to the DC/AC inverter, in which the controller delivers the power required by the grid. The output of the inverter connects first to the low-pass filter to remove harmonic frequencies other than the fundamental frequency of the system utility grid (50 Hz or 60 Hz). Filtered signals then flow to the step-up transformer before being fed into the utility grid (Kim et al., 2009).

## 3. Types of PV faults

Various kinds of fault in a PV system, either stand-alone or grid-connected, may be present in different parts of the PV system such as the PV modules, electrical devices (such as fuses, DC box, wirings, diodes-bypass/blocking, grounding system), the MPPT side, the converter, and the inverter, or in PV modules themselves (Mellit et al., 2018). Faults may be caused by either internal or external factors. Faults may also be categorized as either permanent or temporary by their duration in the PVSs (Madeti and Singh, 2017). A permanent fault (such as aging or loose/disconnected electrical wiring) is present in the

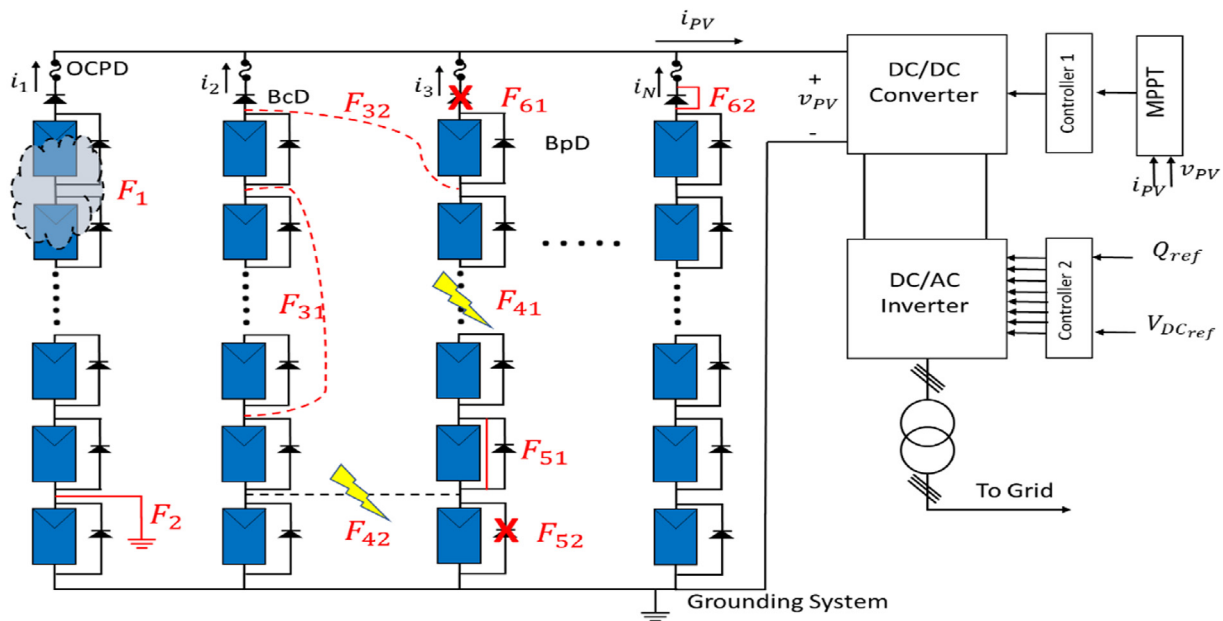


Fig. 4. Typical GCPVS with illustration of different types of faults.

system for a long time, while a temporary fault is present for only a specific period, such as dust/dirt/snow accumulations on the surface of the PV module. These shadows are caused by the nearby entities (buildings, trees, and others) or the passing overhead of clouds (Madeti and Singh, 2017). Faults have been categorized primarily in terms of their general characteristics. This section summarizes typical types of faults.

### 3.1. Mismatch fault

Mismatch faults (F1), as shown in Fig. 4, may be present if at least one module has different electrical parameters from the other modules. Such a type of fault may be temporary or permanent (Hu et al., 2014). For example, a temporary mismatch fault may be caused by the partial shading of PV modules. A permanent mismatch fault may be caused by PV degradation, defective modules, or an open circuit in the PV modules/strings (Hu et al., 2014).

### 3.2. Ground-fault

Ground faults (F2), as shown in Fig. 4, may occur when noncurrent carrying conductors (such as PV mounting racks, PV module frames, and others) are exposed to a current-carrying conductor (CCC) (Alam et al., 2015). Exposure of a noncurrent carrying conductors to a CCC is caused by melting insulation, corrosion, a cutting off of a wire, or poor wiring (Alam et al., 2015). A noncurrent carrying conductors in a PVS should be connected to an earth/ground-equipment grounding conductor as required by the National Electrical Code (NEC), to prevent the possible electrocution of people or animals (Sheehan and Coddington, 2014). However, a ground fault may also occur if an equipment ground conductor accidentally connects with a CCC.

### 3.3. Line-to-line fault

Line-to-line faults (F31 and F32), as shown in Fig. 4, are caused by unintended shorting between two potentials in a PV array (Alam et al., 2015; Pillai and Natarajan, 2019). F3 occurs between two adjacent strings (F32) or within a single string

(F31) (Mellit et al., 2018; Flicker and Johnson, 2013). A line-to-line fault under low irradiance may not be detected owing to the production of a small current that is not detected by over-current protection devices (Alam et al., 2015). The factors contributing to an undetected line-to-line fault are explained concisely elsewhere (Alam et al., 2015). A line-to-line fault in a PV array may occur because of the accidental short-circuiting of CCCs, poor insulation between connectors, a DC box string, damage caused by motion, and the failure of insulation (Mellit et al., 2018). A line-to-line fault may occur within a single string (F31) or between two neighboring strings, as shown in Fig. 4.

### 3.4. Arc faults

Arc faults (F41 and F42) typically occur in the connections/junctions that are ordinarily present in a PVS. A discontinuity between these junctions/connections and the CCCs is the typical cause of an arc fault (Mellit et al., 2018; Alam et al., 2015; Sheehan and Coddington, 2014; Pillai and Natarajan, 2019; Flicker and Johnson, 2013). Another cause is the breakdown of insulation between adjacent CCCs. Therefore, an arc fault may occur in either the DC or AC side of a PVS. Such a fault is either a series arc fault (F41) or a parallel arc fault (F42). An F41 can occur if CCCs have solder disjoints, damaged cells or corroded connectors while an F42 may occur in adjacent CCCs usually due to a breakdown of insulation (Alam et al., 2015; Pillai and Natarajan, 2019). An arc fault is typically very dangerous and may cause a fire if it is not detected quickly.

### 3.5. Other types of faults

#### 3.5.1. Diode faults

A bypass diode (BpD) has an important role in compensating for power losses and lessening the shading effect in a module (Triki-Lahiani et al., 2018). A BpD also serves as a protective device to prevent module destruction in case of a hot spot fault or other faults that reverse the bias of the module (E. & I. S. Department for Business, 2021; Schill et al., 2015; Woike et al., 1990). For example, a bypass diode fault can occur when the diode is shorted (F51) or open (shunted bypass diode) (F52) (Mandal and Kale, 2020). A blocking diode (BcD), provides reverse current



protection (Mellit et al., 2018). A blocking diode fault (F6) may result in an open BcD fault (F61) or a short-circuited BcD (F62). Fig. 4 shows such faults, too.

### 3.5.2. Junction box faults

A junction box protects the wiring between PV strings and an external terminal (Mandal and Kale, 2020). Junction box faults/failures are caused by human error, including the loose/poor fixing of the junction to the back sheet, poor wiring, and inadequate mounting or the corrosion of and penetration of moisture into connectors (Mandal and Kale, 2020; Köntges et al., 2016).

### 3.5.3. Hot spot

A hot spot is formed when the temperature of a PVS rises sufficiently high such that it results in a fire to a large-scale PVS, if it is not detected quickly (Ma et al., 2019; Schill et al., 2015). In most cases, a hot spot affects the performance and life-cycle of the affected module (s) (B.E.M.B.E.R.G.G.H.- [www.agentur-bemberg.de](http://www.agentur-bemberg.de), 2021). A hot spot fault is a mismatch fault caused directly by an imbalanced distribution of power in the PV cells in a module (Gallardo-Saavedra et al., 2019). Cells affected by a hot spot become reverse-biased, and so act as a load in a PV string/array, consuming power generated by the other cells/modules, and increasing the temperature of the affected cells (Flicker and Johnson, 2013; Ma et al., 2019).

Reviews describe more faults than the typical faults/failures that are discussed above. This review will collate all faults listed and discussed in those reviews. Table 1 summarizes all faults discussed above and faults that have been presented in other investigations (Mellit et al., 2018; Alam et al., 2015; Triki-Lahiani et al., 2018). Table 1 presents types and descriptions of faults, along with the devices that they affect and relevant references, too.

## 4. PV fault detection and classification monitoring system

A typical PV fault detection and classification monitoring system has two main parts—the PV system with sensors and the monitoring system for fault detection and classification. The significant components of the PVS are the PV array with irradiance and temperature sensors, the DC/DC converter with MPPT, and the DC/AC inverter. The locations of the sensors may vary, depending on the parameters and type of faults that are being considered. For example, the sensor can be between the PV array and the DC/DC converter, between the DC/DC converter and the DC/AC inverter, or after the DC/AC inverter.

The reading of the sensors will pass to the second part of the PV monitoring system with functions of fault detection and classification. In this part, the data from sensors may firstly be preprocessed or they may be sent directly to the data acquisition/storage stage. The next step is data transmission to the fault detection and classification stage. The next stage is the notification/alarm/action stage. The final stage may be extended into the mitigation stage. Preprocessing can be carried out either before or after data transmission. Fig. 5 shows a typical PV fault detection and classification monitoring system and the aforementioned stages.

### 4.1. Measured parameters

When the performance of a PVS is studied, measurement accuracy must meet some standard requirements, such as BS IEC 61724, also known as the “Photovoltaic System Performance Monitoring - Guidelines for measurement data exchange and analysis”. Table 2 summarizes some essential parameters and the

corresponding measurement accuracy requirements in IEC 61724.

When PV module performance is evaluated, test conditions, such as those in the IEC 61853, should be taken into account. Aside from standard testing condition (1000 W/m<sup>2</sup>, 25°C, 1.5 AM (air mass)), various weather conditions for different module performances should be considered. Table 3 shows the IEC 61853 testing conditions.

### 4.2. Data acquisition, measurement and transmission

Before fault detection and classification, data from the sensors can either be fed directly into the PV fault detection and classification system in real-time or stored. A preprocessor is then used to train the fault detection and classification algorithm. The trained algorithm is then be used for online/real-time fault detection and classification. Fault detection and classification data can also be acquired by utilizing mathematical modeling and simulating the equivalent PVS behavior. After the necessary data is obtained, it is processed and trained, and verified. The preferred algorithm is run on the data for detection and classification of the fault. Not all methods reviewed in this paper involved the use of sensors or their direct attachment to the PVS.

The measured parameters in Table 2 should be considered before the methods of PV fault detection and classification are applied. However, not all parameters in Table 2 have to be used. As mentioned, the use of parameters depends on the PVS configuration (standalone or grid-tied mode) and the preferences of the user.

Data can be transmitted using wireless or wired technology (Ansari et al., 2021). The factors in designing the communication system in a PVS are influenced by the equipment configuration, location, data traffic, cost of maintenance, and type of control system (centralized or decentralized) (Heilscher et al., 2020). The following must be considered to identify suitable communication technologies: latency, data rate, reliability, security, interoperability, and scalability (Mills-Price et al., 2014). Communication technologies are broadly separated as wired and wireless. Under wired technologies are power line communication, digital subscriber line, and optic fiber. Wireless communication technologies include ZigBee, Wi-Fi, WiMAX, the 3G/4G cellular network, satellite, LoRaWAN, and IEEE 2030.5-2018 (Smart energy profile Application Protocol) (Mills-Price et al., 2014). Table 4 summarizes these communication technologies, of which a detailed discussion can be found in Mills-Price et al. (2014).

The communication systems associated with these technologies use a well-defined protocol for exchanging messages/data. The four main categories of the communication protocol for the integration of PVS with various systems are the Internet protocol suite (IPS), Modbus, DNP3, and IEC61580 (Mills-Price et al., 2014). The IPS that are the most commonly used in power systems are the network timing protocol (NTP) for the synchronization with time, the Internet protocol (IP), the transmission control protocol (TCP), the user datagram protocol (UDP), the file transfer protocol (FTP), and the simple mail transfer protocol (SMTP).

### 4.3. DATA preprocessing

Data acquired from the sensors in a PVS may or may not be preprocessed, depending on the requirements of the applied method of PV fault detection and classification. Data preprocessing is crucial in detection and classification problems, but not all forms of data have to undergo it. For example, data preprocessing is used to remove noise, extract features, remove or minimize outliers, deal with missing attributes/values, repair

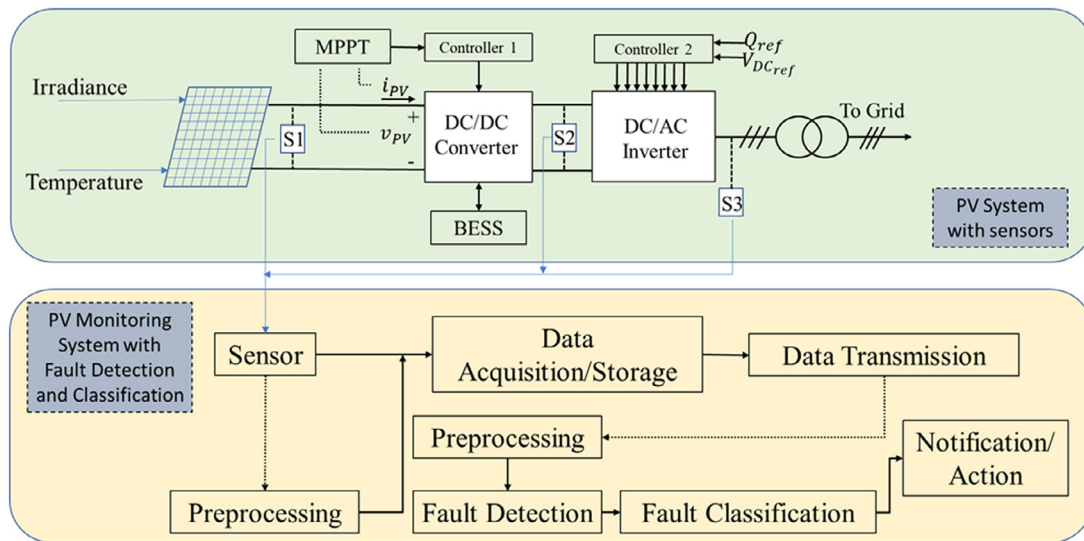
**Table 1**  
Summary of types of faults.

| Types of Faults  | Location (DC or AC) | Description/Caused  | Device affected              | Ref.  |
|--|---------------------|---|------------------------------|---|
| <b>Mismatch Fault</b>  | DC                  |   |                              |   |
| • Partial shading  |                     | • Caused by passing clouds, trees, and other infrastructure blocking the solar irradiance.  | PV Module                    | Nguyen (2015), Hu et al. (2015a), Heidari et al. (2015), Sabbaghpur Arani and Hejazi (2016) |
| • Dust accumulation  |                     | • Dust accumulation due to environment.   | PV Module                    | Nguyen (2015), Hu et al. (2015a), Heidari et al. (2015), Sabbaghpur Arani and Hejazi (2016) |
| • Bird/leaves dropping   |                     | • Caused by birds/leaves dropped by nearby trees and carried by wind.   | PV Module                    | Nguyen (2015), Hu et al. (2015a), Heidari et al. (2015), Sabbaghpur Arani and Hejazi (2016) |
| • Uniform irradiance distribution                                    |                     | • Caused by sun's natural daily cycles.   | PV Module                    | Nguyen (2015), Hu et al. (2015a), Heidari et al. (2015), Sabbaghpur Arani and Hejazi (2016) |
| • Hot spot   |                     | • Degradation of mechanical and optical properties degradation of encapsulation materials.  | PV Module                    | Nguyen (2015), Hu et al. (2015a), Heidari et al. (2015), Sabbaghpur Arani and Hejazi (2016) |
| • Modules degradation  |                     | • Steady decline in the output power of modules due to improper installation (Sharma and Chandel, 2013).  | PV Module                    | Kim et al. (2021)   |
| • Glass breakage   |                     | • Mostly occur during installation due to poor clamp geometry (sharp edges), length or position of clamps. Affects performance of the modules over performance in time due to corrosion of cell and electrical circuit caused by oxygen and penetrating water vapor (Köntges et al., 2014). | PV Module                    | Anon (2021e)  |
| • Soldering failure  |                     | • Caused by (1) Ag or Cu leaching or (2) long-term solder joint fatigue. Both may happen during soldering process.  | PV Module                    | Itoh et al. (2014b)   |
| • Busbars interconnection breakage                                   |                     | • Reduced cross-sectional surface area through which current in module can pass. Caused by mishandling packaging process, installation, hail and/or throwing of stones.   | PV Module                    | Colvin et al. (2021)  |
| • Discoloration  |                     | • A type of degradation that changes the color of ethylene vinyl acetate (EVA) between the glass and cells to usually yellowish or brown. Affects power generated within affected cells due to poor penetration of light.   | PV Module                    | Bouaichi et al. (2017)  |
| • Delamination   |                     | • Caused by loss of interfacial glass-EVA, cell-EVA, EVA-cell, and EVA-back sheet module bonds owing to formation of gaps.  | PV Module                    | Hasan et al. (2021)   |
| • Frame defects/frame breakage (broken, bend, misaligned, scratched) |                     | • Caused by loss of interfacial glass-EVA, cell-EVA, EVA-cell, and EVA-back sheet module bonds owing to formation of gaps.  | PV Module                    | Hasan et al. (2021)   |
| • modules micro crack  |                     | • Caused by excessive weight of snow formed in the PV module surface.   | PV Module                    | Anon (2021e)  |
| • cell breakage  |                     | • Caused from different processes that involve stages of PV modules, including from manufacturing, transportation, handling, installation, vibration, environmental stresses factors, poor wrong installation, improper cleaning, and maintenance.  | PV Module                    | Bdour et al. (2020)   |
|  |                     | • Caused by stresses induced in silicon wafer during in-line processing.  | PV Module                    | Popovich (2011)   |
| <b>Short circuit fault</b>   | DC                  | • Can happen in modules, BcD, and BpD. Caused by bad connection in PV cells or from manufacturing.  | PV module, BcD, BpD          | Jiang and Maskell (2015), Itoh et al. (2014a)   |
| <b>Open circuit fault</b>  | DC                  | • Caused by bad connection between PV cells, hot spots, broken cells, old cables, loose connectors in junction box, etc.  | BpD, PV module, junction box | Jiang and Maskell (2015), Itoh et al. (2014a), Chine et al. (2015)                          |
| • with bypass diode  | DC                  |   |                              |   |
| • without bypass diode   | DC                  |   |                              |   |
| <b>Bypass diode fault</b>  | DC                  | • Short-circuited or open circuit BpD   | BpD                          | Jiang and Maskell (2015), Itoh et al. (2014a), Chine et al. (2015)                          |
| <b>Line to line fault</b>  | DC                  | • Unintentional interconnections in either same string or different strings in the PV.  | PV module/string             | Alam et al. (2015), Zhao (2010)   |
| • same string  |                     |   |                              |   |
| • neighboring strings  |                     |   |                              |   |

(continued on next page)

**Table 1** (continued).

| Types of Faults  | Location (DC or AC) | Description/Caused  | Device affected                         | Ref.  |
|--|---------------------|---|---|---|
| Ground fault<br>• Upper ground fault<br><br>• Lower ground fault | DC                  | <ul style="list-style-type: none"> <li>• Unintentional connections between CCCs and to ground/neutral conductors.</li> <li>• Unintentional low impedance that mostly occurs between the CCCs of the last two modules in PV string and ground.</li> <li>• Unintentional low impedance occurs between CCC and the 2nd and 3rd modules of PV string and ground with large fed-back current.</li> </ul> | PV module/string,                       | Alam et al. (2015)                            |
| Line to Ground Fault   | DC                  | <ul style="list-style-type: none"> <li>• Unintentional connections between CCCs and ground/earth ground.</li> </ul>   | PV module/string                        | Alam et al. (2015), Zhao (2010)               |
| Junction box fault   | DC                  | <ul style="list-style-type: none"> <li>• Description provided above</li> </ul>  | Junction box                            | Mandal and Kale (2020), Köntges et al. (2016) |
| Arc fault<br>• Series<br><br>• parallel                          | DC                  | <ul style="list-style-type: none"> <li>• Caused when gap exists between CCC as results of corrosion of connectors, damage to cell, disconnection of solder, and so on.</li> <li>• Caused by insulation breakdown</li> </ul>   | PV module/string, Junction box          | Alam et al. (2015), Zhao (2010)               |
| Bridging fault   | DC                  | <ul style="list-style-type: none"> <li>• Low resistance in connections between cabling PV modules</li> </ul>  | PV module/string                        | Zhao (2010)                                   |
| MPPT failure   | DC                  | <ul style="list-style-type: none"> <li>• Caused by malfunction in charge controller of MPPT or by sensor of MPPT.</li> </ul>  | MPPT, PV module, MPPT sensor/controller | Wang et al. (2016a)                           |
| Inverter fault   | AC                  | <ul style="list-style-type: none"> <li>• Caused by malfunction/failures of any inverter component/devices such as IGBT, circuitry drivers, or capacitors</li> </ul>   | Inverter                                | Chan and Calleja (2006)                       |
| Grid failure   | AC                  | <ul style="list-style-type: none"> <li>• Caused by line tripping, failures of equipment, maintenance services, configuration of network, accident, or human error</li> </ul>  | Whole grid                              | Zhao (2010)                                   |
| Sudden natural disaster  | DC/AC               | <ul style="list-style-type: none"> <li>• Caused by storm, lightning, or any other natural disasters</li> </ul>  | Whole PVS                               | Omer (2007)                                   |

**Fig. 5.** A typical grid-tied PV fault detection and classification monitoring system.

fractured data, determine incompatibility among other used parameters, and map relationships (multiple parameters), along with other purposes (Famili et al., 1997). Most data preprocessing techniques are categorized as transformation, information gathering, and the generation of new change data (Famili et al., 1997). Data transformation may involve filtering, ordering, editing, and noise elimination. For Information gathering, processes

involve are visualization, elimination, selection, principal component analysis (PCA), and sampling (Famili et al., 1997). The generation of new data involves data engineering, time series analysis, data fusion, modeling/simulation, dimensional analysis, and constructive induction (Famili et al., 1997). Fig. 6 presents a summary of the main categories of preprocessing techniques and involved subprocesses.



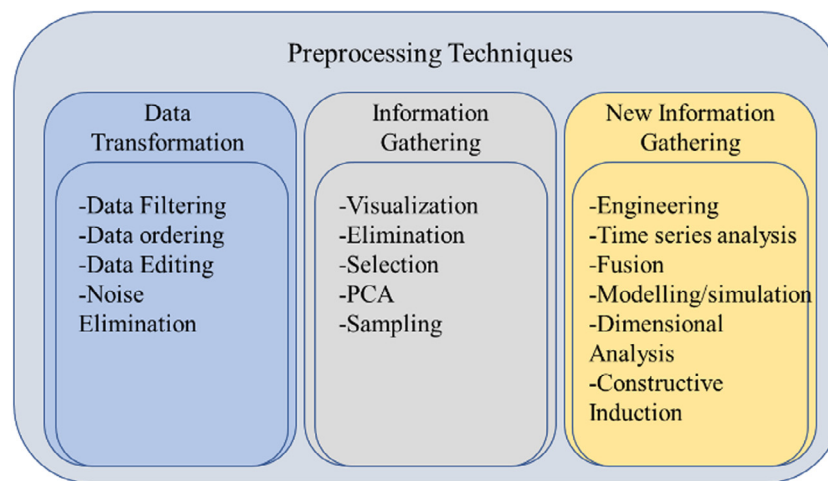


Fig. 6. Data preprocessing techniques (Famili et al., 1997).

Table 2

Standard measured parameters and recommended measurement accuracies (IEC 61724).

| Parts/Categories | Parameters                         | Unit             | Measurement accuracy requirements                            |
|------------------|------------------------------------|------------------|--|
| Meteorology      | Solar irradiance                   | W/m <sup>2</sup> | ±5%  |
|                  | Ambient air temperature            | °C               | ±1 °C  |
|                  | Wind speed                         | m/s              | ±0.5 m/s if wind speed ≤ 5 m/s<br>±10% if wind speed > 5 m/s |
| PV array         | Wind direction                     | degree           | ±5°  |
|                  | Output voltage                     | V                | ±1%  |
|                  | Output current                     | A                | ±1%  |
|                  | Output power                       | kW               | ±2%  |
|                  | Module temperature                 | °C               | ±1 °C  |
| Utility grid     | Utility voltage                    | V                | ±2%  |
|                  | Phase current from/to utility grid | A                | ±2%  |
|                  | Power from/to utility grid         | kW               | ±2%  |

Table 3

IEC 61853 testing conditions.

| Irradiance (W/m <sup>2</sup> ) | Module temperature (°C) | Air mass (AM) |
|--------------------------------|-------------------------|---------------|
| 1100                           | 25, 50, 75              | 1.5           |
| 1000                           | 15, 25, 50, 75          | 1.5           |
| 800                            | 15, 25, 50, 75          | 1.5           |
| 600                            | 15, 25, 50, 75          | 1.5           |
| 400                            | 15, 25, 50              | 1.5           |
| 200                            | 15, 25                  | 1.5           |
| 100                            | 15, 25                  | 1.5           |

Table 4

Types of communication technologies used in PVS.

| Wired communication      | Wireless communication |
|--------------------------|------------------------|
| Power line communication | ZigBee                 |
| Digital subscriber line  | Wi-Fi                  |
| Optic fiber              | WiMAX                  |
|                          | 3G/4G                  |
|                          | Satellite              |
|                          | LoRaWAN                |
|                          | IEEE 2030.5-2018       |

In the fault detection and classification research, the most commonly used preprocessing techniques are PCA (Hajji et al., 2021; Onal and Turhal, 2021), multiresolution analysis (MRA) (Yi and Etemadi, 2017a; Khoshnami and Sadeghkhani, 2018), feature extraction through normalization, different wavelet transform, and other transformations such as the Hilbert Huang transform, the s-transform, and the Fast Fourier transform (FFT) (Harrou et al., 2019b; Pedersen et al., 2019; Belaout et al., 2018; Madeti and Singh, 2018a).

## 5. Categories of PV fault detection and classification techniques

Fault detection and classification techniques can be classified into two main categories—visual and thermal methods (VTMs) and electrical-based methods (EBMs) (Tina et al., 2015). VTMs (Tsanakas et al., 2017, 2016) are used to identify panel breakage, discoloration, browning, and surface soiling. EBMs are used to determine the electrical characteristics of a PVS in module, string, or array. EBMs are also used in different parts of a PV system on either the DC or the AC side. Most relevant studies of PV fault detection and classification assert that EBMs provide a more comprehensive view of the information that is used in different methods. The majority of the faults in Table 1 can be detected and classified using EBMs.

VTMs and EBMs can be divided further into subcategories. The subcategories of VTMs are infrared/thermal imaging (IMI), visual inspection (VI), electroluminescence imaging (EI), lock-in thermography (LIT), and artificial intelligence techniques (AIT)—machine learning (ML), deep learning (DL), and hybrid methods. The subcategories of EBMs are climate data-based techniques (CDT), I-V characteristics analysis (IVCA), power losses analysis methods (PLAM), current and voltage measurement method, temperature and heat exchange based method, voltage randomness estimation (VRE), voltage/current spectrum analysis (VCSA), statistical and signal processing techniques, AIT, and hybrid techniques. AIT and hybrid VTMs and EBMs are therefore available. Fig. 7 shows fault detection and classification techniques/methods. This review focuses on both VTMs and EBMs.

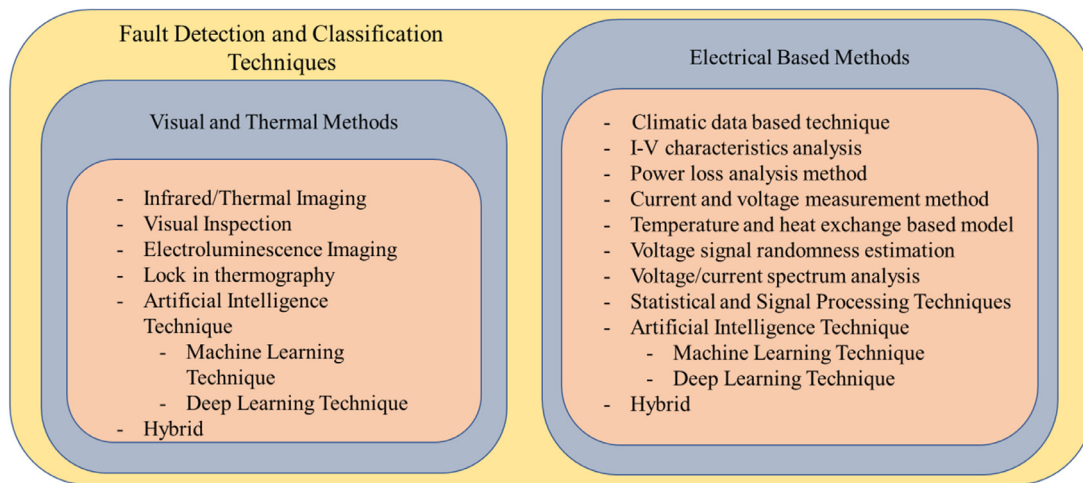


Fig. 7. Categories of fault detection and classification methods.

### 5.1. Visual and thermal methods

#### 5.1.1. Infrared/Thermal Imaging (IMI)

One of the most time-efficient techniques for fault detection and classification in the PVS and their electrical components is infrared (IR) thermal imaging (Cubukcu and Akanalci, 2020). IMI is also used for fault localization in PV modules and other parts of a PVS, such as the cabling, diodes, DC box combiner, junction boxes, connectors, and others (Haney and Burstein, 2013). IMI can also be performed even when the PVS is being operated online without affecting the entire operation of the system. No sensor has to be installed in the PVS because IMI uses an external component, an IR camera, to characterize the different electrical components and PVS modules/strings under test. IMIs can be used from small photovoltaic arrays to large photovoltaic power plants (Cubukcu and Akanalci, 2020; Haney and Burstein, 2013). Furthermore, since this type of photovoltaic fault diagnosis does not require the use of sensors, its cost is lower than other methods (Haney and Burstein, 2013).

IMI is based on local heat generation due to the Joule heating effect of shunted cells, poor connections, and short circuits (Madeti and Singh, 2017; Cubukcu and Akanalci, 2020; Haney and Burstein, 2013). The two types of IR imaging are (Madeti and Singh, 2017) (i) reverse bias imaging and (ii) forward bias imaging. Methods of the IR imaging of a PVS (Cubukcu and Akanalci, 2020) are walking, crane/lift, and drone methods. The detected, classified, and localized faults (Cubukcu and Akanalci, 2020) are heated connections (fuses/cables/breakers), hot-spots, defective strings, heated junction boxes, and broken modules. Haney and Burstein (2013) reviewed IR diagnosis in operating c-Si PV modules and the detection, classification, and localization of faults other than those identified by Cubukcu and Akanalci (Cubukcu and Akanalci, 2020). These faults were module degradation, cell cracks/microcracks/snail trails, cell breakage, loss of materials in cells, potential-induced degradation, shadowing, shorted/open cells, a broken interconnecting ribbon, faulty soldering, failed system connection, and bypass diode faults.

#### 5.1.2. Visual Inspection (VI)

In most cases, VI is the initial step in determining the condition of a PVS (including its modules and other components). Based on the results of this step, a decision is made regarding further inspection and testing (Madeti and Singh, 2017). Guidelines for visual inspection, including necessary data collection tools, are included in the International Electrochemical Commission (IEC1215 - 1987) standards and those of the National Renewable

Energy Laboratory (NREL). According to the guidelines for the VI of PV modules, the light source must have 1000 lux (Madeti and Singh, 2017). Proper visual inspection and maintenance have been elucidated (Muhammad et al., 2017). VI has the advantage of providing the on-site detection, classification, and localization of faults. Examples of faults that have been detected, classified and located (Kirchartz et al., 2009) include snail tracks, bird dropping, slight chalking, degradation, a defective junction box, corrosion of the frame, discoloration, cell cracking, and busbar discoloration. Since VI requires human intervention, VI needs a tedious procedure and is likely to cause electrical shocks to the inspectors (Madeti and Singh, 2017). However, through proper training and expertise, this method can accurately detect and classify faults at a low cost (Madeti and Singh, 2017).

#### 5.1.3. Electroluminescence Imaging (EI)

Luminescence imaging has the advantage of providing PV cell characteristics/measurements in a brief period because of its sensitivity to several detrimental effects (shunts, increased resistance) (Kirchartz et al., 2009). In contrast, the electroluminescence imaging of PV modules/PVS requires an external contact for current injection. Therefore, the emission intensity of electroluminescence images is proportional to the carrier lifetime density of the current. In most cases, this method is used in failure analysis (Madeti and Singh, 2017). Other faults, such as current imbalance distribution, cell cracks, and poor connections can also be easily detected using this method. For example, possible problems in PV modules have been detected using a drone (Alves dos Reis Benatto et al., 2020). When a drone is used, precautions, permits and guidelines must be considered, especially in a restricted area with tight security (Alves dos Reis Benatto et al., 2020).

#### 5.1.4. Lock-in Thermography (LIT)

Lock-in thermography is a non-destructive, contact-less localization technique for defects on electronic devices or other materials (Bachmann et al., 2012). The infrared camera is used synchronously as the defect activation signal. LIT produces amplitude and phase images, localizing the position and indicating the nature of a defect. LIT can also be regarded as a method for finding indirect power loss by infusing a pulsating current into a solar cell. The pulsating current heats the area where the shunt defects may occur. By adjusting the modulation of the pulsating current, different shunt defects can be easily characterized. Illumination is not an issue in this kind of test, so testing can be carried out on any day. For example, LIT has been conducted in the dark to detect solder bond failure (Asadpour et al., 2020), which

**Table 5**  
Summary of faults studied by VTMs.

| Types of faults   | Fault Diagnosis Stage |       |      | Kind of PVS |       | DC/AC Side | Measured Parameters                           | Validation Experimental/ Actual/ simulated | Testing condition Offline/online | Specific method(s) applied  | Types of Technique used | Ref.                                 |
|---|-----------------------|-------|------|-------------|-------|------------|---|--|----------------------------------|---|-------------------------|--------------------------------------|
|   | Det.                  | Clas. | Loc. | SAPVS       | GCPVS |            |   |  |                                  |   |                         |                                      |
| Crack cell, snail trails, BpD fault   | ✓                     | ✓     | ✓    |             | ✓     | DC         | - I-V curve for validation                    | Experimental actual                        | Offline, online                  | Infrared imaging, aerial triangulation and terrestrial georeferencing, Image segmentation, canny edge | IMI                     | Tsanakas et al. (2017)               |
| Hotspot, soldering problem, shading, cabling problems, heated junction box, module breakage, breaker faults | ✓                     | ✓     | ✓    |             | ✓     | DC         | Irradiance and cell temperature               | Experimental actual                        | Offline, online                  | Thermal imaging through using of lift, walking, and drone   | IMI                     | Cubukcu and Akanalci (2020)          |
| Junction box fault, corrosion, degradation, discoloration,  | ✓                     | ✓     | ✓    |             | ✓     | DC         | visual  | actual                                     | Offline, online                  | Visual inspection   | VI                      | Muhammad et al. (2017)               |
| Cracks/broken cells, interconnections problem, shunted diode  | ✓                     | ✓     | ✓    | –           | –     | DC         | –   | experimental                               | Offline, online                  | Electro-luminescence, image processing  | EI                      | Alves dos Reis Benatto et al. (2020) |
| Hot spot  | ✓                     | ✓     | ✓    | –           | –     | DC         | –   | Experimental                               | offline                          | Lock-in thermography, image processing  | LIT                     | Bachmann et al. (2012)               |
| Hot spot, series resistance, solder bond failure  | ✓                     | ✓     | ✓    | –           | –     | DC         | Comparing results with module I-V measurement | Experimental                               | Offline, online                  | Dark LIT  | LIT                     | Asadpour et al. (2020)               |
| Subsurface defect   | ✓                     | ✓     | ✓    | –           | –     | DC         | –   | Experimental                               | offline                          | LIT, CNN  | LIT, AIT/ hybrid        | Cao et al. (2020)                    |
| Defective module  | ✓                     | ✓     | ✓    |             |       | DC         | –   | Experimental                               | Offline, online                  | Thermography, parametric based model  | IMI, hybrid             | Hu et al. (2013)                     |
| Defective module  | ✓                     | ✓     | ✓    | –           | –     | DC         | –   | Experimental                               | offline                          | Eddy current thermography, CNN  | IMI, hybrid             | Du et al. (2020)                     |
| Cracked cells,  | ✓                     | ✓     | ✓    |             | ✓     | DC         | –   | Actual                                     | Online                           | IR imaging, image processing, canny edge detection  | IMI, hybrid             | Tsanakas et al. (2015a)              |
| Cracked cells   | ✓                     | ✓     | ✓    | –           | –     | DC         | –   | Experimental                               | Offline, online                  | IR imaging, canny edge detection  | IMI                     | Tsanakas et al. (2015a)              |

increases a series resistance in solar modules. Most studies of applying LIT to PV faults involve detection and localization first before classification (Cao et al., 2020). Because LIT is a nondestructive characterization method, LIT is very effective during pre-characterization to further investigate the origin of physical defects in solar cells (Cao et al., 2020).

#### 5.1.5. Visual and thermal methods integrated with Artificial Intelligence Techniques (AIT)

IMI or LIT has been integrated with AITs and a further operation is carried out to classify the detected faults/failures. Such approaches are defined herein as hybrid applications of VTMs.

A hybrid VTMs can be implemented in detection, classification, localization, or a combination of two of the primary processes involved in fault diagnosis. For example, Hu et al. (2013) combined LIT with a parameter-based model for fault detection. Du et al. (2020) combined thermography with CNN to classify faults in a Si-PV cell; their classified faults were a broken edge of a PV module, a surface impurity, scratches, cracking, a hot spot, and damage over a large area of the modules. Another exciting area of research in VTMs concerns the use of orthophotos for fault detection and classification (Tsanakas et al., 2015a). Tsanakas et al. (2015a) used image processing, including segmentation and canny edge detection to identify and classify faults, such as cracks in PV modules. Another hybrid VTM is the combination of IMI with intelligent edge detection, as proposed by Tsanakas et al. (2015b) to detect damaged PV cells.

Table 5 summarizes studies related to VTMs; the table presents the detected, classified, and located faults. Other information concerning the proposed methods/techniques is also presented, along with the kind of PVS interconnection, validation method of proposed techniques, and the type of techniques.

## 5.2. Electrical Based Methods (EBMS)

EBMs are more popular than VTMs. Table 6 summarizes PV faults studied by EBMs.

### 5.2.1. Climatic Data-independent Technique (CDT)

CDT is a method that does not include measurement of PV climatic data such as irradiance, humidity, temperature, and wind speed. Instead, CDT uses external LCR (inductance, capacitance, and resistance) meters and signal generation through injection. Takashima et al. (2006) measured the earth capacitance to detect in individual modules in the string. Faults was detected through signal generation and signal injection in PV modules was implemented in Lu et al. (2021b); faults thus detected were classified using a CNN. Another CDT used time-domain reflectometry, as proposed in Schirone et al. (1994b). An experiment was performed in which the characteristics of electrical lines were measured to detect any discontinuity, change in impedance or fault.

### 5.2.2. I–V characteristics analysis (IVCA)

The current–voltage (I–V) characteristics of the PV module are used to monitor the behavior/health of a PV system in operation. During normal operation, I–V characteristics follow a particular curve, which changes during a fault. The type and severity of a fault in a PVS significantly affect the degree of change of the I–V characteristics. Most studies of the current–voltage (I–V) characteristics for PV fault detection and classification compare the healthy I–V characteristics of the PV system with the faulty ones (Stellbogen, 1993; Fadhel et al., 2019a; Spataru et al., 2015). Stellbogen (Stellbogen, 1993) proposed the detection and classification of faults such as ground fault, short-circuiting, and faulty connections by comparing the I–V characteristics of normal strings to those of the faulty strings. Fadhel et al. (2019a) used the same method but considered only various partial shading conditions; they also used principal component analysis to improve the detection and classification of faults. Spataru et al. (2015) demonstrated a method for detecting and classifying partial shading, series resistance losses, and potential-induced degradation using fuzzy logics. Miwa et al. developed an extension of IVCA (Miwa et al., 2006) that used the negative change in current with voltage ( $-dI/dV$ ) in the I–V characteristics of the PVS.

Their proposed method detected partially shadowed PV modules. Another extension of IVCA combined the I–V characteristics to another PV parameters under observation (Chao et al., 2008). Daliello et al. (2016) extended their methods of IVCA using a correlation function and a matter–element model to detect various abnormalities in the PVS. Instead of using only the I–V characteristics of PV module, the proposed method takes its first and second derivatives to detect BpD faults and series resistance.

In the work presented in Fezzani et al. (2015), 12 types of fault were classified using the simulation model in MatLab/simscape. They were a short-circuit BpD, inverted BpD, shunted BpD, a short-circuit cell, a short-circuit module, an inverted module, modules connected with resistance, module shadowing, shadowing with open BpD, shadowing with inverter BpD, shadowing with shunted BpD, and module shadowing with series resistance (Fezzani et al., 2015). Chine et al. (2015) identified five anomalies in PV parameters. These were a reduction of short-circuit current, a reduction of open-circuit voltage, a change in output current, a change in output voltage, and a change in number of I–V peaks. By analyzing the five anomalies, the authors were able to classify the 12 faults. Like Fezzani's work in Fezzani et al. (2015), Hu et al. (2015b) used I–V and P–V characteristics, by comparing the normal I–V and P–V curves without faults to those the PV with faults. Fezzani et al. considered mismatch faults, series resistance faults, connection faults, open BpD, module shunt, and ground faults (Fezzani et al., 2015). IVCA was not only used for PV fault detection and classification but also for optimization. Hu et al. (2015b) used I–V characteristics to optimize the locations of voltage sensors. Hachana et al. (2016) combined a metaheuristic technique and denominated artificial bee colony with generated differential equation and a PV simulator assess four types of fault; these were total and partial shading, BpD faults, connection faults, and a short-circuited sub-strings fault. The parameters used were the PV I–V curves (Hachana et al., 2016). Cracks on a PV surface can be detected using IVCA and by studying the dynamic response of the I–V curve of the PV module (Wang et al., 2016b). Euclidean norm between the I–V characteristics of a normal PV array and the faulty-PV array has been used to detect interconnection resistance and various PV shading conditions (Ali et al., 2017). Faults were classified through the differential residue that was obtained by computing this Euclidean norm. Due to its simplicity, IVCA has been extensively studied in different literatures to further improve its performance by integrating with other methods, such as AITs.

### 5.2.3. Power Loss Analysis (PLA)

PLA involves the computation of the power losses in PVS of either a model-based PVS or experimental/actual setup of system under testing. Chouder and Silvestre (Chouder and Silvestre, 2010) simulated a model in MatLab/Simulink to detect and classify faults in a PVS by analyzing the DC power output using thermal capture losses, miscellaneous losses, and the current–voltage ratio. Solórzano and Egido (2013) experimentally analyzed the DC power losses to detect and classify faults, such as shading, hot-spot, module degradation, and power losses due to cabling problems. The detection process of Silvestre's work (Silvestre et al., 2013) involved comparing simulated and measured losses; classification was involved computing the error deviation between the normal condition and the faulty condition. Stauffer et al. determined the difference between the simple model-based and measured DC power outputs (Stauffer et al., 2015). The idea of PV fault detection is to raise an alarm if the difference between the measured and computed powers reaches a threshold. Although detection process is easy, the proposed method could not classify and localize faults. Additionally, unpredictable changes in irradiance can trigger problematic false alarms. By comparing

past and present conditions of a PV array, Shimakage et al. (2011) were able to detect faults, such as partial shading. Dhimish and Holmes determined measured and theoretical output power using a statistical t-test for fault detection (Dhimish and Holmes, 2016). They conducted fault localization by determining the ratio of the measured or the theoretical power to the voltage output. They considered connection failure, partial shading in a string, a faulty PV module in a string, a faulty PV module with partial shading in a string, two defective PV modules in a string, two faulty PV modules with partial shading in a string, a faulty string, and a faulty MPPT (Dhimish and Holmes, 2016).

### 5.2.4. Current and voltage measurement

Another way of finding an anomaly/fault in a PVS is to measure the current and voltage in a module, string, or array, or at the output terminal in the DC side of the PVS. For example, Huang and Guo (2009) detected faults using a microcontroller by determining the difference between the maximum current value and other current values in PV modules. They located the faults by calculating the deviation between the measured current in the branches of PV modules. Gokmen et al. (2013) measured the PV operating voltage and ambient temperature for detecting faults; they claimed that their proposed method could identify the difference between the partial shading condition and other types of studied fault conditions. Mahendran et al. (2015) used an Arduino microcontroller to measure PV panel voltage, PV temperature and PV resistance. They compared the measured values to the predicted values to detect a fault condition in the experimental PV setup. Dhar et al. (2018) proposed a PVS circuit to interrupt and detect an arc fault. The detected arc-fault was classified using differential current methods and then the fault was located using a non-iterative Moore Penrose pseudo technique. Silvestre et al. (2014) simulated PV cell model with five parameters, based on measured voltage and current using MatLab/Simulink. The measured voltage and current were used as indicators of faults in a system and validated experimentally. Chen and Wang (2018) detected faults by measuring multiple output signals (current, voltage, power) in a PV string and obtained the time correlation between faulty signals and other signals using an autoregression model. They also performed a generalized local likelihood ratio test for fault localization.

Most of the proposed methods for fault detection and classification are based on supervised learning, so data labeling must precede their application. Zhao et al. (2015) minimized labeled data using graph-based semi-supervised learning for PV fault detection and classification. The parameters in their proposed algorithm (Zhao et al., 2015) are the instantaneous short-circuit current and the open-circuit voltage of the reference module, measured in the inverters. A method of language theory, Petri-NET, has been used to analyze the output power and current of a PV system for fault detection and isolation (Muñoz et al., 2015). Davarifar et al. correctly classified faults by measuring voltage and current and examining the I–V characteristics (Davarifar et al., 2013a).

### 5.2.5. Heat exchange and temperature based method

A by-product or after-effect of faults in a PVS is the generated heat by either increasing resistance in the section in which the fault occurs or increasing the flow of current (Madeti and Singh, 2017). Thermal imaging techniques, as discussed with reference to VTMs, can also be used to detect heat exchange. The faulty parts of a PVS yield higher heat thermographic signatures than in other parts of the system. Hu et al. (2013) calculated the total heat exchange, ambient temperature, and natural adequate supply of solar energy along with the output heat signature of the thermal camera to generate a parametric model for fault detection.



### 5.2.6. Voltage Randomness Estimation (VRE)

As mentioned elsewhere (Madeti and Singh, 2017), VRE fault detection design is specifically for arc faults; it involves statistical methods and filters to analyze measured signals. This method requires finite impulse response (FIT) bandpass filters and mathematical calculations. The FIT and results of signal distortion mathematical calculation are compared to a threshold level to identify anomalies, such as arc faults. For example, Schimpf and Norum (Schimpf and Norum, 2009) used analog and digital signals to analyze measured signals to determine fault conditions.

### 5.2.7. Voltage/current Spectral Analysis (VCSA)

Another method specifically for detecting arc faults is VCSA. In VCSA, lower-frequency content is analyzed to detect arc faults (Madeti and Singh, 2017) because the response in an arc fault is related to inverse of frequency. Different factors must be considered in setting the desired operating frequency in this technique. For example, variable irradiance, partial shading, noise from other components, and external noise may interfere with the set operating frequency of the system. Some studies (Johnson et al., 2011a; Johnson and Kang, 2012; Seo et al., 2012) have suggested a frequency range of 1–100 kHz. One arc detector (Haeblerlin and Real, 2007) can be tuned to several frequencies using a resonant circuit for various conditions and operations. The arc frequency of the arc fault detector is not present under normal operating conditions.

### 5.2.8. Artificial Intelligence Technique (AIT)

AIT has seen a wide range of uses in various disciplines in recent decades. These include medicine, engineering, socio-economics, natural language processing, astronomy, behaviors sciences, and many others. AIT is a powerful tool that has been exploited in various areas of researches into PV systems, including forecasting and prediction. Mellit and Kalogirou (2008) reviewed various forecasting techniques that used AI to predict PV power generation.

Many researchers have used different AITs to solve various problems, including the detection of faults in PVSs. An example of an AIT for fault diagnosis, which used a forward error backpropagation neural network, was provided by Wu et al. (2009). They used an algorithm to monitor signals from various power devices, including overcurrent, undervoltage, and overheating signals. The other PV panel parameters of the algorithm were solar array output undervoltage and overvoltage and grid undervoltage. Coleman and Zalewski proposed a method for finding the cause of a detected fault (Coleman and Zalewski, 2011) using a Bayesian belief network. Their framework validated the fault detection sensors' readings and mapped the results to the Bayesian belief network using Netica API. Syafaruddin and Hiyama (2011) diagnosed faults using a feedforward artificial neural network (ANN) with one hidden layer. Their proposed method was applied to 12 short-circuit faults at different irradiance and temperature levels using DC voltage as inputs to the proposed ANN. Finally, Ducange et al. (2011) used the Takagi–Sugeno Kang Fuzzy Rule-based (TSK-FRB) algorithm which estimates the power output of a PVS from available meteorological data. The idea was to compare the output DC power of the PV panel under a normal/no-fault condition the measured DC power under fault condition. The results were then passed through a rule-based system generated by a fuzzy logic system and applied a certain threshold to determine whether a fault has occurred. Some AITs generally require many sensors to collect data in a large PVS, resulting in a high cost. Furthermore, most AITs perform model training by giving a dataset that is specific to a PVS configuration. However, the return of investment in terms of accuracy, scalability, social approval, and security is very high.

**5.2.8.1. Machine learning.** A subfield of AIT is machine learning (ML) which does not depend on hard-coding to improve the accuracy of its applications. Some famous ML algorithms are k-nearest neighbor (k-NN), decision tree (DT), random forest (RF), and support vector machine (SVM). A multi-resolution signal decomposition (MSD) for feature extraction (Yi and Etemadi, 2017b, 2016) has been coupled with SVM to detect line-to-line faults. Xia et al. (2018) combined wavelet decomposition with SVM to detect series DC arc faults. Cho et al. (2020) used SVM and four years of measured data to detect and classify faults in the strings and inverters. A binary SVM classifier (normal and abnormal classes) was presented (Harrou et al., 2019a) to detect abnormalities in output DC and power through by a PSIM simulation of an installed grid-connected PVS. Islanding and grid faults in a PVS have been detected through simulation (Baghaee et al., 2020). Jufri et al. (2019) proposed a method that combined regression and SVM to classify the abnormal power output of a studied PVS; the method also provided binary classification (normal and abnormal). Miao et al. (2021) used SVM and empirical mode decomposition (EMD) to detect DC arc faults. A discrete wavelet transforms (DWT) was combined with multi-resolution singular spectrum entropy to extract features from AC side of PVS of the three-phase voltage signal of the AC side (Ahmadipour et al., 2019). The extracted features were then input to a proposed SVM to classify grid faults; these were single phase-to-ground, phases-to-phase, phase-to-ground, and three phase-to-ground faults. Wang et al. (2019) used an optimized SVM with grid search and k-fold cross-validation to detect short-circuit, open-circuit, and shading faults in PV arrays. The input parameters of the SVM were I–V characteristics curves, short-circuit current, open-circuit voltage, maximum power-current, and maximum power-voltage. A least-squared SVM in the Bayesian framework was used and experimentally tested (Sun et al., 2017) to detect and classify short-circuit, open-circuit, and abnormal aging faults. Badr et al. (2019) combined rule-based fault detection with SVM to detect and classify six fault types in a PV array by simulating a grid-tied PVS. A genetic algorithm (GA) has been used to optimize an SVM (Eskandari et al., 2020b) to detect line-to-line faults in a PVS using the I–V characteristics of the PV system as inputs. Zhang et al. (2017) used particle swarm optimization (PSO) to optimize a SVM for weather prediction and the detection of faults in a PVS. A multi-class SVM has been used (Wang et al., 2017) to detect and classify line-to-line faults and abnormal degradation faults in a PV module. Wang et al. (2017) introduced two features (fill factor (FF) and the type of fault factor) in detection and classification criteria. Chang et al. (2014) implemented a cloud-based monitoring system that was integrated with SVM for fault detection. Chen et al. (2018b) used PCA to preprocess data before use in SVM. Their method detected and classified three types of fault: open circuit, short circuit, and partial shading faults. Another study involving SVM (Gao et al., 2017) used EMD and SVM with the artificial bee colony (ABC) algorithm for optimization. For every 15-minutes intervals, EMD extracted important features, which were input to an ABC-based SVM, of signals. Winston et al. (2021) and Zhao et al. (2012) found that SVM outperformed the feedforward neural network in detecting micro-cracks and hot spot faults in a PVS.

DT has been used to detect line-to-line, open module, and partial shading faults. It has been used to detect faults in the PV array level of the studied PVS with the irradiance, temperature, voltage, and current of the PV array as inputs. Another study used DT (Benkercha and Moulahoum, 2018) in an experimental test in a small-scale grid-tied PVS. The input parameters were ambient temperature, solar irradiance, and the ratio of the calculated power to the measured power. The model-specific type of DT successfully detected and classified string, short circuit, and line-to-line faults. DT with the AdaBoost algorithm has been



used (Madani et al., 2012) to detect islanding in a microgrid with a PV farm.

Another ML technique that has been used for PV fault detection and classification is the kNN. Madeti and Singh proposed a kNN to detect and classify open-circuit faults, line-to-line faults, partial shading with BpD, partial shading without BpD, and partial shading with inverted BpD (Madeti and Singh, 2018b). Sabbaghpur Arani and Hejazi (2021) presented a Bayesian kNN, which was experimentally determined through simulation to detect a line-to-line fault and an open-circuit fault. kNN-based Shewhart and exponentially weighted moving average schemes with non-parametric and parametric thresholds have been presented (Rezgui et al., 2014; Harrou et al.). Experimental data have been used as inputs to kNN for detecting and classifying open-circuit faults, line-to-line faults, partial shading with and without BpD, and partial shading with inverted BpD (Madeti and Singh, 2018c). To improve fault detection and localization, Patil and Hinge (2019) combined three algorithms: MSD-for signal preprocessing, fuzzy logic system and kNN.

RF is one of the most widely used ML techniques for classification of fault in a PVS. For example, Chen et al. (2018a) used an ensemble-type RF to detect and classify line-to-line faults, degradation, and open-circuit and partial shading conditions. The input parameters of the proposed RF algorithm (Chen et al., 2018a) were the string voltage and current that were implemented through simulation and experiments. Dhibi et al. (2020) proposed two reduced-kernel-RF classifiers—the Euclidean distance RK-RF and the k-means clustering RK-RF. Dhibi et al. (2021b) used an interval-reduced kernel PCA for feature extraction using RF. The RF method was used in a grid-tied PVS simulated in a Chroma PV and grid simulator to detect and classify five types of fault. Ziane et al. (2020) used RF to detect and classify other partial shading conditions in a grid-tied PVS. Yun et al. (2021) used RF to detect open-circuit, short-circuit, hotspot, aging, and partial shading faults. The kernel PCA has been widely used for feature extraction (Dhibi et al., 2021a; Bird et al., 2019; Ndjakomo Essiane et al., 2021). Then, the extracted features were used to input to the RF. Verch et al. (2021) used RF with PCA for PV fault detection and classification. A classification regression tree (CART) RF was implemented (Gong et al., 2020) to classify partial shading, aging, open circuit, and short-circuit faults. In that work (Gong et al., 2020), CART-RF outperformed three ML techniques: DT, SVM, and kNN. The performance of the ML technique usually depends on how the model is tuned, the use of feature extraction, and the characteristics of the data. For example, in one study (Dhimish, 2021), discriminant classifiers outperformed DT, SVM, and kNN in detecting hot-spot faults.

Fuzzy logic system was another ML that is commonly used for PV fault detection and classification in combination with various algorithms. For example, the MRA and fuzzy inference system (FIS) were proposed and presented to detect short-circuit faults in the DC side of a PVS (Yi and Etemadi, 2017a). Zaki et al. (2019) used fuzzy logic control (FLC) to detect normal and faulty conditions in a PVS. A fuzzy C-means (FCM) clustering technique was applied to cluster and classify six different fault conditions (Zhao et al., 2018). The method was carried out experimentally in a PV array using the PV parameters. Spataru et al. (2012) used FLC to detect short-circuit faults in LabView. The method applied was a comparison between the measured values of the installed PV and the simulated equivalent model. A fuzzy classifier has been used to detect series resistances that were generated by partial shading (Spataru et al., 2012). Natsheh and Samara (2020) used a nonlinear autoregressive exogenous input (NARX) to detect and classify faults in PVS with customizable granularity. The fuzzy NARX was found to be able to detect and classify the different intensities of partial shading. Vieira et al.

(2020) used a Sugeno-type fuzzy logic system after the detection of ANN in determining the number of faulty modules in a PV array. An adaptive neuro-fuzzy inference system (ANFIS) using Mamdani-type FLC was used to detect different types of hot spot (Dhimish and Badran, 2019); it used three input parameters, which were percentage power loss, short-circuit current, and open-circuit voltage. To detect series losses, BpD faults and BcD faults, a neuro-fuzzy classifier was implemented in Belaout et al. (2016). To differentiate normal and faulty PV operations, a neuro-fuzzy algorithm was used in the study conducted by Bonsignore et al. (2014). An ANFIS was developed to detect and classify five faults using current, voltage, irradiance, temperature and weather data as inputs in Abbas and Zhang (2021). To increase the accuracy of the IVCA method in detection, a fuzzy logic system has been used in Dhimish et al. (2017b). An improved multi-class adaptive neuro-fuzzy classifier was proposed to classify five types of fault in Belaout et al. (2018a). Samara and Natsheh (2020) used NARX neural network with Sugeno fuzzy inference to detect and classify open and short-circuit degradation, MPPT failure, and partial shading. A combination of variational-mode decomposition, improved multi-scale fuzzy entropy and SVM, was proposed to detect arc faults in a PVS (Wang et al., 2021). In Grichting et al. (2015), a cascaded fuzzy logic was employed to detect arc faults. Dhimish et al. (2017a) used a fuzzy logic system at the end of a six-layer detection algorithm to classify several faults in a PVS.

Several ML techniques other than those discussed above can be found in the literature. One of these is the probabilistic neural network (PNN) (Garoudja et al., 2017a). This method has two stages; the first is the identification of the unknown electrical parameters of the one-diode model of PV cell using the best-so-far algorithm. Then, based on the identified parameters, the PV array is simulated and experimentally tested in PSIM/Matlab. The second and final stage is the use of the PNN for the detection and classification of faults. The PNN has also been used to detect and classify open-circuit, line-to-line, ground, and arc faults (Garoudja et al., 2017a). Another ML technique is the ML-based Gaussian process regression (Fazai et al., 2019a), which has been simulated and experimentally validated. The method can detect and classify mismatch faults, BpD faults, and mixed faults with high accuracy. Basnet et al. used data-mining techniques and then fed the preprocessed data into a PNN for the fault detection and classification in PVS (Basnet et al., 2020). An improved method, based on an ML technique with hierarchical classification, was presented in Eskandari et al. (2021) to detect and classify line-to-line and line-to-ground faults. The simulated annealing (SA) algorithm was utilized to optimize the improved RBF kernel extreme learning machine (ELM) (Wu et al., 2017). That method was implemented in simulations and effectively detected and classified short circuits, aging, and partial shadings. Chen et al. (2017) and Sun et al. (2018b) used the kernel ELM with Nelder–Mead simplex optimization and IVCA for PV fault detection and classification. By applying PCA only to the I–V curve of the PVS, Fadhel et al. (2019b) were able to detect and classify PV under normal conditions and shaded conditions. Aljahdali et al. (2019) claimed that they could detect, classify, and locate open-circuit, short-circuit, and hot-spot faults using the existing ML toolbox in Matlab through simulations. Machine learning-based statistical hypothesis testing with a generalized likelihood ratio test algorithm was used (Fazai et al., 2019b) to detect the normal and abnormal operations of a PVS. T-squared and weighted squared errors have been applied for fault detection (Attouri et al., 2020), before PCA (Fadhel et al., 2019c) was used for feature extraction; and then SVM was employed to classify five faults. Li et al. (2021b) used Grammian angular field and recurrence plot of the corrected and resampled values of the I–V curve before using the data in different ML techniques. The performances of ANN, SVM,

DT, RF, kNN, and Naïve Bayesian algorithm in detecting seven types of fault were evaluated. Another ML technique with data mining has been used (Benavides et al., 2021) for fault detection. Rouani et al. (2021) applied vertices principal component analysis to detect effectively partial shading conditions. Babasaki and Higuchi (2018) mentioned the use of the ML technique to detect a fault in a PV string but did not mention the type of ML used. A combination of ensemble machine learning (EML) model and I–V characteristics has been implemented (Eskandari et al., 2020a) to detect and classify line-to-line faults. This proposed method, which was simulated and experimentally tested, outperformed other ML techniques with an average testing and validation accuracies of 99% and 99.5%. EML has also been employed (Le et al., 2020) to detect series dc arc-faults experimentally. A model with two cascaded DTs was implemented in He et al. (2021) with PV electrical parameters as inputs. The first DT was used to detect faults and then the second DT was used to differentiate other faults during partial shading. A wavelet transform and RBF with a dynamic fusion kernel were used (Kurukuru et al., 2020) to detect 13 faults in a PV module and array, boost converter and inverter. Binary classification with ML has been used (Haba, 2019) for fault diagnosis, but the ML method was not specified. In the same study, a supervised ELM method was implemented to detect and classify faults (Kapucu and Cubukcu, 2021). An impressive RBF-based ANN was found (Hussain et al., 2020a) to have an accuracy of 98.1%. In a comparative study of ML techniques (Livera et al., 2018), kNN outperformed the DT, SVM, and FIS.

**5.2.8.2. Neural networks.** Neural networks have been categorized (Li et al., 2021a) into shallow neural networks (SNNs) and deep neural networks (DNNs) (Gao, 2021; Patil and Bindu, 2021). SNNs include RBF (Pedersen et al., 2019; Eskandari et al., 2021; Kurukuru et al., 2020; Kapucu and Cubukcu, 2021), ELM (Chen et al., 2017; Sun et al., 2018b; Kapucu and Cubukcu, 2021; Ndjakomo Essiane et al., 2021), PNN (Dhimish et al., 2017a; Basnet et al., 2020), the Elmann neural network (Liu and Yu, 2017), and the wavelet neural network. The ANNs used in PV fault detection and classification can be classified into pure ANNs, modified or enhanced ANNs, and ANNs combined with other methods. A pure ANN has been used for PV fault detection and classification (Syafaruddin and Hiyama, 2011; Basnet et al., 2020; Mekki et al., 2016; Laamami et al., 2017; Rao et al., 2019; Jazayeri et al., 2017; Jenitha and Immanuel Selvakumar, 2017; Chine et al., 2016; Sofiah et al., 2021; Samara and Natsheh, 2019; Kara Mostefa Khelil et al., 2020; Hwang et al., 2019; Sabri et al., 2018; Haque et al., 2019; Muralidharan, 2020; Guejia Burbano et al., 2021; Djalab et al., 2020). Enhanced ANNs and ANNs combined with other methods have also been proposed and implemented (Jiang and Maskell, 2015; Natsheh and Samara, 2020; Hussain et al., 2020b; Ganeshprabu and Geethanjali, 2016; Fadhel et al., 2019d; Karma-charya and Gokaraju, 2019; Janarthanan et al., 2021; Jones et al., 2015; Usman et al., 2020; Li et al., 2019).

DL is a subset of ML, a multilayered neural network that accepts and learns a vast amount of data. DL is much more powerful than ML, and a DL algorithm contains more than one hidden layer, explaining the use of the word “deep”. Fig. 8 displays the relationship among AI, ML, and DL (Copeland, 2021).

Several DL frameworks that have been used for PV fault detection and classification, as follows.

- Convolutional neural network (CNN),
- Long-short term memory (LSTM),
- recurrent neural network (RNN),
- generative adversarial network (GAN), and
- autoencoder-decoder.

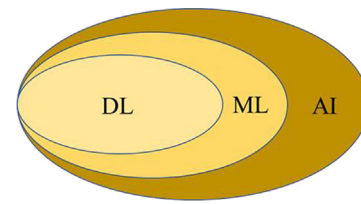


Fig. 8. Relationship among AI, ML, and DL (Copeland, 2021).

DL includes DNN (Khondoker et al., 2018) and other types of multilayered intelligent systems such as CNN (Cao et al., 2020; Du et al., 2020; Lu et al., 2021b). A CNN that belongs to VTMs or LIT, has been implemented (Platon et al., 2015; Deutsch et al., 2019; Sun et al., 2018a). In Fig. 9, taken from (Li et al., 2019), the depth of a proposed CNN structure was applied for classification of faults. As an EBM, a CNN has been used for PV fault detection and classification (Zaki et al., 2021) with three indicators, which are normalized PV array current, normalized PV voltage, and fill factor. That proposed method has been experimentally tested to detect line-to-line, open-circuit, and shading faults. Omran et al. (2020) used CNN to detect series arc faults in a PVS through simulation using PSCAD. The method had an accuracy of 98.9% and outperformed other ML techniques. A combination of continuous-wave transform and an existing pre-trained CNN—AlexNet has been used to detect and classify faults (Aziz et al., 2020). That proposed method used the I–V characteristics of a PVS to detect and classify faults, including arc, line-to-line, open circuit, partial-shading faults, and faults that occur during partial shading. Malik et al. (2021) used a pre-trained CNN and ResNet50 to detect and classify faults with a spectrogram of DC voltage as inputs. A ResNet CNN with a squeeze and excitation network, optimized with Bayesian optimization has been presented (Fu et al., 2020). A combination of CNN with a gated recurrent unit (GRU), which uses I–V characteristics, solar irradiance, and temperature as inputs, has also been introduced (Lu et al., 2021a). Several CNNs for PV fault detection and classification under EBMs have been implemented in Aziz et al. (2020), Lu et al. (2019a), Gao and Wai (2020), Chen et al. (2019).

LSTM RNN has been used to detect a high-impedance fault in a PVS connected to an IEEE 13-bus system (Veerasamy et al., 2021). That method outperformed KNN, SVM, DT, and NB with a classification accuracy of 91.21%. Appiah et al. (2019) used LSTM in a PV array to detect line-to-line and hot-spot faults. An example of the use of GAN used domain adaptation with a convolutional generative adversarial network (DA-DCGAN) to detect DC series arc faults (Lu et al., 2019b). Fig. 10 shows the structure of the used DA-DCGAN. An attached auto-encoder and clustering have been applied to I–V curves of a PVS to detect three types of short-circuit fault, two types of degradation fault, a partial shading with BpD open-circuit fault, a partial shading with BpD short-circuit fault, and a short circuit with degradation (Liu et al., 2021).

**5.2.8.3. Benchmark methods and parameter settings.** Since AITs provide promising results for PV fault detection and classification, many baseline or benchmark methods have been used for showing the comparative results. To fairly compare the performance of different methods, the method parameter setting is crucial. Table 7 shows these baseline or benchmark methods and their corresponding parameter settings along with test results. It can be found that DT, kNN and SVM are the most popular baseline/benchmark methods.

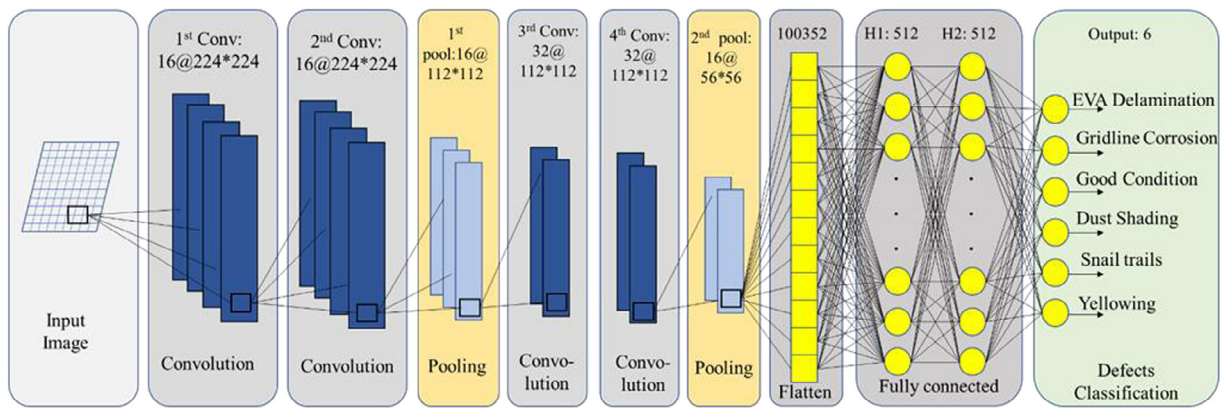


Fig. 9. Example structure of CNN used in PV fault detection and classification, showing depth of DL (Li et al., 2019).

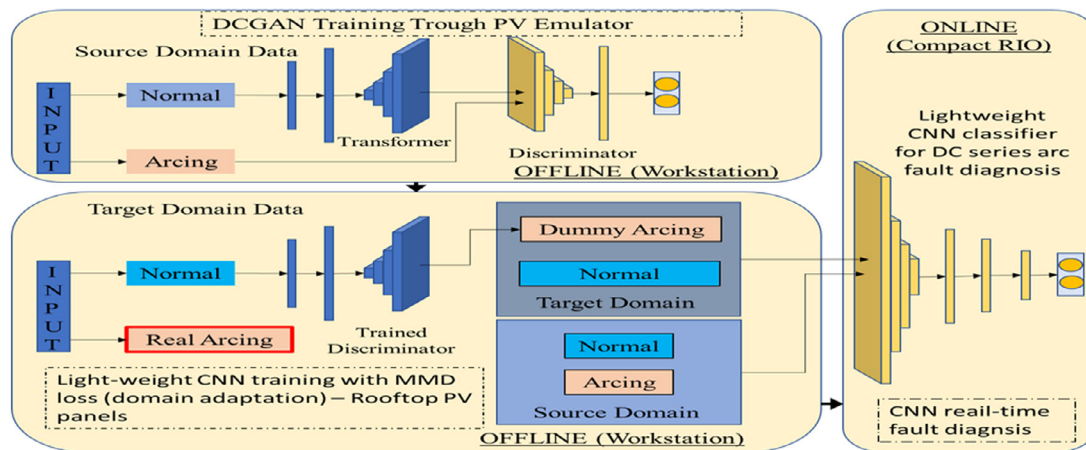


Fig. 10. GAN structure used by Lu et al. (2019b).

### 5.2.9. Statistical and signal processing techniques

Waveform signals provide references in the various signal processing methods such as Earth Capacitance Measurement (ECM), Time Domain Reflectometry (TDR) and Speared Spectrum TDR (Mellit et al., 2018). The TDR method can be used for fault detection and localization, but it depends on installation conditions, PV component materials, module mounting, and wiring. The principal purpose of TDR is to identify malfunctions on the PV module in a PV array (Takashima et al., 2006).

The disconnection of a PV module in a string can be detected using ECM and TDR techniques (Takashima et al., 2006, 2008). ECM can be used to determine the position of disconnection on a PV module in a string, disregarding the effects of a change of irradiance. TDR can locate degradation, including the escalation of series resistance between a PVS and other faults. In one study, the use of an ECM was not restricted to crystalline Si PV module as it was also used to an amorphous silicon (a-Si) PV module. TDR can be used to detect circuit breaks, insulation malfunctions, and wiring problems such as open circuits and inverse polarity (Schirone et al., 1994a).

A frequency analyzer can be used to measure radio frequency propagation. The suggested frequency of the arc-fault circuit interpreter is below 100 kHz based on the RF effects in a PVS. Johnson et al. have established the usefulness of PV arc detection testing with comprehensive topologies and a PVS (Johnson et al., 2011b).

Gonzalez et al. took a systematic approach to investigate a DC-DC boost converter and a voltage source full-bridge inverter about the extent of some significantly quantifiable frequency

components. The method can identify detachment of the positive point of a DC link capacitor and the short circuiting of the diode booster and boost converter switch. The limitations of the signal approach arise from the problem of singly determining the site of the faults because of the similarity between its signatures and the standard restrictions on sensor measurements. However, the partitions of faults in a group of similar signatures are more advantageous than examining the whole PVS because doing so reduces the group of components (Gonzalez et al., 2011).

Davarifar et al. proposed a method for detecting faults in a PVS based on an analysis of power loss of the PV by signal processing (Davarifar et al., 2013b). They provided a real-time current universal circuit-based model of a photovoltaic panel and a model residual that was based on a Sequential Probability Ratio Test (SPRT) framework for electrical fault diagnosis. Guasch et al. presented a method for automatically detecting abnormalities in a PVS, reducing the amount of data to be obtained for fault detection (Guasch et al., 2003). The algorithm accurately detected several failures, such as series resistance in connections and current leakage to the ground. Vergura et al. provided a procedure for generating descriptive and inferential statistics to determine errors in PV plants (Vergura et al., 2009). They demonstrated that the ANOVA and Kruskal-Wallis test effectively identified errors in operational setups and the reduced availability of measured energy.

Garoudja et al. developed a model-based fault detection method to identify the shading of PV modules and faults called the exponentially weighted moving average (EWMA) control chart. It was used to detect the performance of PV systems



**Table 6**  
Summary of PV faults studied by EBMs.

| Types of faults  | Fault Diagnosis Stage |      |     | Kind of PVS |       | DC/AC | Measured Parameters  | Validation Experimental/ Actual/ simulated | Testing condition Offline/online | Specific method(s) applied   | Types of Technique used | Ref.                         |
|--|-----------------------|------|-----|-------------|-------|-------|--|--|----------------------------------|--|-------------------------|------------------------------|
|  | Det                   | Clas | Loc | SAPVS       | GCPVS |       |  |  |                                  |  |                         |                              |
| Open module in strings   | ✓                     | ✓    | ✓   | ✓           | –     | DC    | Voltage signal from TDR  | Experimental                               | online                           | Time domain reflectometry (TDR), earth capacitance measurement   | CDT                     | Takashima et al. (2006)      |
| module breakage, module contact defectiveness and module bypass diode failure                          | ✓                     | ✓    |     | ✓           | –     | DC    | Measurement of high frequency voltage generator to the PV module | Experimental                               | Offline/online                   | chaos synchronization detection method (CSDM) w/ (CNN),  | CDT, hybrid             | Lu et al. (2021b)            |
| Open and short circuit   | ✓                     | ✓    | ✓   | ✓           | –     | DC    | TDR response measurements  | Experimental                               | Offline/online                   | TDR measurement  | CDT                     | Schirone et al. (1994b)      |
| Ground fault, short circuit, faulty connections, partial shading                                       | ✓                     | –    | –   | ✓           | –     | DC    | I–V characteristics  | simulated                                  | Offline                          | Comparison of actual and simulation measurement (faulty and normal)  | IVCA                    | Stellbogen (1993)            |
| Partial shading  | ✓                     | ✓    | –   | ✓           | –     | DC    | I–V characteristics  | Experimental                               | Offline                          | PCA for data representation and fault classification   | IVCA                    | Fadhel et al. (2019a)        |
| Increased series resistance, degradation, partial shading  | ✓                     | ✓    | –   | –           | ✓     | DC    | I–V characteristics  | Experimental/actual                        | Offline/online                   | Fuzzy logic for classification   | IVCA                    | Spataru et al. (2015)        |
| Partial shading  | ✓                     | ✓    | –   | ✓           | –     | DC    | I–V characteristics  | Experimental/actual                        | Online                           | –dI/dV in the I–V characteristics  |                         | Miwa et al. (2006)           |
| Faulty module in PV  | ✓                     | ✓    | –   | ✓           | –     | DC    | I–V characteristics  | Simulated                                  | Online                           | Extended correlation w/ matter–element model   | IVCA                    | Chao et al. (2008)           |
| Partial shading, hotspot   | ✓                     | –    | –   | ✓           | –     | DC    | I–V characteristics  | Experimental                               | Online                           | bypass approach  | IVCA                    | Daliento et al. (2016)       |
| F1, series resistance faults, connection faults, open BcD, module shunt, and ground faults             | ✓                     | –    | –   | ✓           | –     | DC    | I–V and P–V characteristics                                      | Simulated                                  | Online                           | I–V and P–V measurements   | IVCA                    | Fezzani et al. (2015)        |
| Shorted BpD, Partial shading   | ✓                     | ✓    | ✓   | ✓           | –     | DC    | I–V characteristics  | Experimental                               | Online                           | Voltage sensor reading of I–V characteristics  | IVCA                    | Hu et al. (2015b)            |
| total and partial shading, BpD faults, connection faults, and short-circuited sub-strings fault        | ✓                     | ✓    | –   | ✓           | –     | DC    | I–V characteristics  | Experimental                               | Online                           | metaheuristic technique denominated artificial bee colony with deferential equation                                  | IVCA                    | Hachana et al. (2016)        |
| Crack module   | ✓                     | –    | –   | –           | ✓     | DC    | I–V characteristics  | Experimental                               | Online                           | Dynamic I–V Characteristics measurement with modified particle swarm optimization algorithm                          | IVCA                    | Wang et al. (2016b)          |
| Partial shading and increase series resistance   | ✓                     | ✓    | –   | –           | –     | DC    | I–V characteristics  | Experimental                               | Online                           | Comparison of faulty and normal PV through I–V characteristics   | IVCA                    | Ali et al. (2017)            |
| Faulty string, partial shading   | ✓                     | ✓    | –   | –           | ✓     | DC    | Power calculation through I–V characteristics                    | Experimental                               | Online                           | thermal capture losses and miscellaneous capture losses computation  | PLAM                    | Chouder and Silvestre (2010) |
| Partial shading, dirt, hot-spot, module degradation, and power losses due to cabling problems          | ✓                     | ✓    | –   | ✓           | –     | DC    | MPP and power losses measurement                                 | Experimental                               | Online                           | Normalized MPP calculation for detection, rule-based approach  | PLAM                    | Solórzano and Egidio (2013)  |
| Partial shading, ground fault, line-to-line, BcD fault, faulty strings, short circuit fault, BpD fault | ✓                     | ✓    | –   | –           | ✓     | DC    | I–V characteristics  | Experimental                               | Online                           | Comparison of measured and simulated power losses  | PLAM                    | Silvestre et al. (2013)      |
| Cabling failures, aging, cell breakage   | ✓                     | –    | –   | ✓           | –     | DC    | DC power   | Experimental                               | Online                           | Comparison of Normalized error computation and normalized error analysis of DC power output from simulated to actual | PLAM                    | Stauffer et al. (2015)       |
| PV module fault, bypass diode fault, and blocking diode fault  | ✓                     | –    | –   | –           | ✓     | DC/AC | I–V, P–V characteristics, AC power                               | Experimental                               | Online                           | comparing the past and present conditions of the PV array (AC power, Performance ratio, and power difference)        | PLAM                    | Shimakage et al. (2011)      |
| Partial shading, faults during partial shading   | ✓                     | ✓    | –   | –           | ✓     |       | P–V characteristics  | Experimental                               | Online                           | Power ratio rule   | PLAM                    | Dhimish and Holmes (2016)    |
| Faulty module  | ✓                     |      | ✓   | ✓           | –     | DC    | Current and voltage measurement                                  | Experimental                               | Online                           | Comparison of Imppp from different branch of strings   | CVMM                    | Huang and Guo (2009)         |
| Short circuit, open circuit faults   | ✓                     | –    | –   | ✓           | –     | DC    | PV voltage and ambient temperature                               | Experimental                               | Online                           | Probability estimation of sliding window voltage   | CVMM                    | Gokmen et al. (2013)         |
| Mismatch faults  | ✓                     | –    | –   | –           | –     | DC    | PV voltage, temperature, resistances                             | Experimental                               | Online                           | Measurement of voltage, temperature, and resistances of PV panel through microcontroller                             | CVMM                    | Mahendran et al. (2015)      |

(continued on next page)

Table 6 (continued).

| Types of faults  | Fault Diagnosis Stage |      |     | Kind of PVS |       | DC/AC | Measured Parameters   | Validation Experimental/ Actual/ simulated | Testing condition Offline/online | Specific method(s) applied  | Types of Technique used | Ref.   |
|--|-----------------------|------|-----|-------------|-------|-------|---|--|----------------------------------|---|-------------------------|--|
|  | Det                   | Clas | Loc | SAPVS       | GCPVS |       |   |  |                                  |   |                         |  |
| DC series arc fault  | ✓                     | ✓    | ✓   | –           | ✓     | DC    | Current measurement   | Simulated                                  | Online                           | Differential current methods—detection, non-iterative Moore Penrose pseudo technique—localization       | CVCM                    | Dhar et al. (2018)   |
| Faulty strings (open circuit)  | ✓                     | –    | –   | –           | ✓     | DC    | PV voltage and current  | Experimental                               | Online                           | Threshold settings of voltage and current   | CVCM                    | Silvestre et al. (2014)  |
| Partial shading, line-to-line faults, ground faults  | ✓                     | ✓    | ✓   | –           | ✓     | DC    | PV current, voltage, power                                      | Simulated                                  | Online                           | time correlation between the faulty signals and among other signals using the autoregression (AR) model | CVCM                    | Chen and Wang (2018)   |
| Open circuit fault and line-to-line fault  | ✓                     | ✓    | –   | ✓           | –     | DC    | PV instantaneous short circuit current and open-circuit voltage | Experimental                               | Online                           | graph-based semi-supervised learning  | CVCM                    | Zhao et al. (2015)   |
| Partial shading, inverter control fault,   | ✓                     | ✓    | ✓   | –           | ✓     | DC    | Output current and power  | Experimental                               | Online                           | Petri-NET   | CVCM                    | Muñoz et al. (2015)  |
| Short circuit, open circuit, mismatch, ground fault, partial shading, hotspot                      | ✓                     | –    | –   | –           | –     | DC    | PV voltage and current  | Experimental                               | Online                           | I-V and P-V measurement analysis  | CVCM                    | Davarifar et al. (2013a)   |
| DC arc fault   | ✓                     | –    | –   | –           | –     | DC    | Voltage measurement   | Experimental                               | Online                           | Module based arc detector   | VRE                     | Schimpf and Norum (2009)   |
| Arc faults   | ✓                     | –    | –   | ✓           | –     | DC    | Frequency measurement   | Experimental                               | Online                           | Measurement of RF frequencies   | VCSA                    | Johnson et al. (2011a), Johnson and Kang (2012), Seo et al. (2012), Haeblerlin and Real (2007) |
| Partial shading, damage cell, series resistance, open circuit, short circuit                       | ✓                     | ✓    | –   | –           | ✓     | DC/AC | Measurement of over current, under-voltage, and overheating     | Experimental                               | Online                           | Back propagation neural network   | AIT, ML                 | Wu et al. (2009)   |
| Devices failures   | ✓                     | ✓    | –   | –           | ✓     | DC/AC | Monitoring of sensor's parameters                               | Simulated                                  | Offline                          | Bayesian belief network (BBN)   | AIT, ML                 | Coleman and Zalewski (2011)  |
| Short circuit fault  | ✓                     | –    | ✓   | –           | –     | DC    | I-V and P-V characteristics                                     | Experimental                               | Offline                          | feed-forward neural network   | AIT, ML                 | Syafaruddin and Hiyama (2011)  |
| Cell breakage, water infiltration, partial shading   | ✓                     | ✓    | –   | –           | –     | DC    | Temperature, power, irradiance, current and voltage of PV       | Simulated                                  | Online                           | Takagi-Sugeno Fuzzy Rule-Based (TSK-FRB)  | AIT, ML                 | Ducange et al. (2011)  |
| Line-to-line fault   | ✓                     | –    | –   | ✓           | ✓     | DC    | PV's open circuit voltage, short circuit current Vmpp, Impp,    | Experimental                               | Online                           | Multiresolution Signal Decomposition and Two-Stage Support Vector Machine                               | AIT, ML                 | Yi and Etemadi (2017b)   |
| Line-to-line fault   | ✓                     | –    | –   | –           | ✓     | DC    | PV's open circuit voltage, short circuit current Vmpp, Impp,    | Simulated                                  | Online                           | SVM   | AIT, ML                 | Yi and Etemadi (2016)  |
| DC arc fault   | ✓                     | ✓    | –   | –           | ✓     | DC    | Current frequency measurement                                   | Experimental                               | Online                           | wavelet decomposition and SVM, PCA for features extraction  | AIT, ML                 | Xia et al. (2018)  |
| String fault, inverter fault   | ✓                     | ✓    | –   | –           | ✓     | DC    | Daily power measurements  | Experimental                               | Online                           | SVM   | AIT, ML                 | Cho et al. (2020)  |
| Faulty PV  | ✓                     | –    | –   | –           | ✓     | DC    | Vmpp and Impp   | Experimental                               | Offline                          | One class SVM   | AIT, ML                 | Harrou et al. (2019a)  |
| Islanding  | ✓                     | –    | –   | –           | ✓     | AC    | Frequency, real power, reactive power, Irms, Vrms, Ithd, Vthd   | Experimental                               | Online                           | SVM   | AIT, ML                 | Baghaee et al. (2020)  |
| PV abnormal behavior (faults not specified)  | ✓                     | –    | –   | –           | –     | DC    | PV power, voltage, current, irradiance, and temperature         | Simulated                                  | Online                           | Regression and SVM  | AIT, ML                 | Jufri et al. (2019)  |
| DC arc fault   | ✓                     | –    | –   | ✓           | –     | DC    | Current and current frequency                                   | Experimental                               | Online                           | EMD and SVM   | AIT, ML                 | Miao et al. (2021)   |
| Single phase to ground, double phases to ground, phase to phase, and three phase to grounds faults | ✓                     | ✓    | –   | –           | ✓     | AC    | Three-phase voltage   | Experimental                               | Online                           | Wavelet Multi-Resolution Singular Spectrum Entropy and SVM  | AIT, ML                 | Ahmadipour et al. (2019)   |
| Open circuit, short circuit, partial shading   | –                     | ✓    | –   | –           | –     | DC    | I-V characteristic curves, Isc, Voc, Impp, Pmpp, Vmpp           | Simulated                                  | Online                           | SVM, grid search, and k-fold cross-validation   | AIT, ML                 | Wang et al. (2019)   |

(continued on next page)



Table 6 (continued).

| Types of faults   | Fault Diagnosis Stage |      |     | Kind of PVS |       | DC/AC  | Measured Parameters                  | Validation Experimental/ Actual/ simulated | Testing condition Offline/online | Specific method(s) applied  | Types of Technique used | Ref.   |
|---|-----------------------|------|-----|-------------|-------|--------|--------------------------------------|--|----------------------------------|---|-------------------------|--|
|   | Det                   | Clas | Loc | SAPVS       | GCPVS |        |                                      |  |                                  |   |                         |  |
| short circuit, open circuit, aging  | –                     | ✓    | –   | –           | –     | DC     | I–V characteristic                   | Experimental                               | Online                           | LSSVM in the Bayesian framework                                       | AIT, ML                 | <a href="#">Sun et al. (2017)</a>                                    |
| Line-to-line, partial shading, open circuit, MPPT failure   | ✓                     | ✓    | –   | –           | ✓     | DC     | PV power                             | Simulated                                  | Online                           | SVM   | AIT, ML                 | <a href="#">Badr et al. (2019)</a>                                   |
| Line-to-line  | ✓                     | ✓    | –   | –           | –     | DC     | I–V characteristics                  | Simulated                                  | Online                           | SVM, GA   | AIT, ML                 | <a href="#">Eskandari et al. (2020b)</a>                             |
| Not specified   | ✓                     | –    | –   | –           | –     | DC     | PV power                             | Simulated                                  | Online                           | SVM, PSO  | AIT, ML                 | <a href="#">Zhang et al. (2017)</a>                                  |
| Degradation, line-to-line   | –                     | ✓    | –   | –           | –     | DC     | I–V and P–V characteristics,         | Simulated                                  | Online                           | Multiclass SVM  | AIT, ML                 | <a href="#">Wang et al. (2017)</a>                                   |
| Partial shading   | ✓                     | ✓    | –   | –           | ✓     | DC     | PV power                             | Experimental                               | Online                           | Cloud based monitoring with SVM                                       | AIT, ML                 | <a href="#">Chang et al. (2014)</a>                                  |
| Open circuit, short circuit, partial shading  | ✓                     | ✓    | –   | –           | ✓     | DC     | Impp, Vmpp                           | Experimental                               | Online                           | PCA, SVM  | AIT, ML                 | <a href="#">Chen et al. (2018b)</a>                                  |
| Partial shading   | ✓                     | ✓    | –   | –           | ✓     | AC     | AC power                             | Experimental                               | Online                           | EMD, SVM, ABD   | AIT, ML                 | <a href="#">Gao et al. (2017)</a>                                    |
| Line-to-line, open, partial shading   | ✓                     | ✓    | –   | –           | ✓     | DC     | Idc, Vdc, irradiance, temperature    | Experimental                               | Online                           | DT  | AIT, ML                 | <a href="#">Zhao et al. (2012)</a>                                   |
| String fault, short circuit, line-to-line   | ✓                     | ✓    | –   | –           | ✓     | DC     | Idc, Vdc                             | Experimental                               | Online                           | C4.5 DT   | AIT, ML                 | <a href="#">Benkercha and Moulaboum (2018)</a>                       |
| islanding   | ✓                     | –    | –   | –           | ✓     | AC     | Power                                | Simulated                                  | Online                           | DT with AdaBoost algorithm  | AIT, ML                 | <a href="#">Madani et al. (2012)</a>                                 |
| open circuit faults, line-to-line faults, partial shading w/ BpD, partial shading w/o BpD, and partial shading w/ inverted BpD    | ✓                     | –    | –   | –           | ✓     | DC     | I–V characteristics                  | Simulated                                  | Online                           | kNN   | AIT, ML                 | <a href="#">Madeti and Singh (2018b)</a>                             |
| Line-to-line, pen circuit   | ✓                     | ✓    | –   | –           | ✓     | DC     | I–V characteristics                  | Simulated                                  | Online                           | Bayesian kNN  | AIT, ML                 | <a href="#">Sabbagh-pur Arani and Hejazi (2021)</a>                  |
| Short circuit, open circuit, partial shading  | ✓                     | ✓    | –   | –           | ✓     | DC     | Vdc, Idc                             | Experimental                               | Online                           | kNN-based Shewhart, EWMA with parametric and non-parametric threshold | AIT, M                  | <a href="#">Rezgui et al. (2014)</a> , <a href="#">Harrou et al.</a> |
| open-circuit faults, line-to-line partial shading w/ and w/o BpD, and partial shading w/ inverted BpD                             | ✓                     | ✓    | –   | –           | ✓     | DC     | I–V characteristics                  | Simulated                                  | Online                           | kNN   | AIT, M                  | <a href="#">Madeti and Singh (2018c)</a>                             |
| Line-to-line, line-to-ground  | ✓                     | ✓    | ✓   | –           | ✓     | DC     | I–V characteristics                  | Simulated                                  | Online                           | MSD, fuzzy logic, kNN   | AIT, ML                 | <a href="#">Patil and Hinge (2019)</a>                               |
| line-to-line degradation, open circuit, partial shading   | ✓                     | ✓    | –   | –           | ✓     | DC     | Idc, Vdc                             | Experimental                               | Online                           | Ensemble RF   | AIT, ML                 | <a href="#">Chen et al. (2018a)</a>                                  |
| Inverter fault, islanding, connector failure, partial shading   | ✓                     | ✓    | –   | –           | ✓     | DC/AC  | Idc, Vdc, Iac, Vac                   | Simulated/ Experimental                    | Online                           | Euclidean distance RK–RF and k-means clustering RK–RF, PCA            | AIT, ML                 | <a href="#">Dhibi et al. (2021b)</a>                                 |
| Inverter fault (open circuit), islanding, connector failure   | ✓                     | ✓    | –   | –           | ✓     | DC/ AC | Idc, Vdc, Iac, Vac                   | Simulated/ Experimental                    | Online                           | IRKPCA, RF  | AIT, ML, hybrid         | <a href="#">Dhibi et al. (2020)</a>                                  |
| Partial shading   | ✓                     | –    | –   | –           | ✓     | DC     | Idc, Vdc, irradiance, temperature    | Experimental                               | Online                           | RF  | AIT, ML                 | <a href="#">Ziane et al. (2020)</a>                                  |
| Aging, cell breakage, hotspot, short circuit, open circuit  | ✓                     | ✓    | –   | –           | –     | DC     | Idc, Vdc, irradiance, temperature    | Simulated                                  | Offline                          | RF  | AIT, ML                 | <a href="#">Yun et al. (2021)</a>                                    |
| Inverter fault (open circuit), islanding, connector failure   | ✓                     | ✓    | –   | –           | ✓     | DC/ AC | Idc, Vdc, irradiance, temperature    | Simulated                                  | Online                           | IKPCA-RF  | AIT, ML                 | <a href="#">Dhibi et al. (2021a)</a>                                 |
| Not specified   | ✓                     | –    | –   | –           | ✓     | DC     | Pdc                                  | Simulated                                  | Offline                          | RF, SVM, ANN  | AIT, ML                 | <a href="#">Bird et al. (2019)</a>                                   |
| Degradation, soiling, partial shading, short circuit  | ✓                     | –    | –   | –           | –     | DC     | Pdc, Idc, Vdc, Voc, Isc, temperature | Simulated                                  | Offline                          | PCA, ANN, RF  | AIT, ML                 | <a href="#">Verch et al. (2021)</a>                                  |
| partial shading, aging, open circuit, and short circuit faults  | ✓                     | ✓    | –   | –           | –     | DC     | I–V characteristics                  | Simulated                                  | Online                           | CART-RF   | AIT, ML                 | <a href="#">Gong et al. (2020)</a>                                   |
| hotspot   | ✓                     | –    | –   | –           | ✓     | DC     | Pdc                                  | Experimental                               | Online                           | DT, DC, SVM, kNN  | AIT, ML                 | <a href="#">Dhimish (2021)</a>                                       |
| Partial shading w/o BpD failure, partial shading w/ BpD failure, short circuit, open circuit, snow falling, birds/leaves dropping | ✓                     | ✓    | –   | –           | ✓     | DC     | I–V characteristics                  | Experimental                               | Online                           | FLC   | AIT, ML                 | <a href="#">Zaki et al. (2019)</a>                                   |
| Partial shading, open circuit, short circuit  | ✓                     | ✓    | –   | ✓           | ✓     | DC     | I–V and PV characteristics           | Experimental                               | Online                           | FCM, FLC  | AIT, ML                 | <a href="#">Zhao et al. (2018)</a>                                   |
| Faulty modules, partial shading   | ✓                     | ✓    | –   | –           | ✓     | DC     | Power and voltage ratio              | Experimental                               | Online                           | FLC   | AIT, ML                 | <a href="#">Dhimish et al. (2017c)</a>                               |
| Increase series resistances, partial shading  | ✓                     | –    | –   | –           | –     | DC     | I–V characteristics                  | Experimental                               | Online                           | FIS   | AIT, ML                 | <a href="#">Spataru et al. (2012)</a>                                |

(continued on next page)

Table 6 (continued).

| Types of faults  | Fault Diagnosis Stage |        |        | Kind of PVS |        | DC/AC    | Measured Parameters           | Validation Experimental/ Actual/ simulated | Testing condition Offline/online | Specific method(s) applied   | Types of Technique used | Ref.  |
|--|-----------------------|--------|--------|-------------|--------|----------|-------------------------------|--|----------------------------------|--|-------------------------|---|
|  | Det                   | Clas   | Loc    | SAPVS       | GCPVS  |          |                               |  |                                  |  |                         |   |
| Partial shading  | ✓                     | ✓      | –      | –           | –      | DC       | Idc, Vdc                      | Simulated                                  | Online                           | Tree Search Fuzzy NARX neural network                                  | AIT, ML                 | Natsheh and Samara (2020)   |
| Short circuit strings. Open circuit strings  | ✓                     | ✓      | –      | –           | ✓      | DC       | Irradiance, temperature, Pmmp | Experimental                               | Online                           | Sugeno type fuzzy with ANN   | AIT, ML                 | Vieira et al. (2020)  |
| hotspot  | ✓                     | –      | –      | –           | ✓      | DC       | PPL, Isc, Voc                 | Experimental                               | Online                           | ANFIS Mandami type fuzzy   | AIT, ML                 | Dhimish and Badran (2019)   |
| series losses, BpD faults, and BcD faults  | ✓                     | ✓      | –      | –           | –      | DC       | Pmmp, Voc                     | Simulated                                  | Online                           | Neuro-fuzzy  | AIT, ML                 | Belaout et al. (2016)   |
| Upper ground fault, lower ground fault, partial shading, short circuit diode               | ✓                     | ✓      | –      | –           | –      | DC       | I–V characteristics           | Simulated                                  | Online                           | Neuro-fuzzy  | AIT, ML                 | Bonsignore et al. (2014)  |
| Open circuit, line-to-line   | ✓                     | ✓      | –      | –           | ✓      | DC       | I–V characteristics           | Simulated                                  | Online                           | Grid partition, subtractive clustering, ANFIS                          | AIT, ML                 | Abbas and Zhang (2021)  |
| Partial shading, faulty modules w/ partial shading, faulty modules w/o partial shading     | ✓                     | ✓      | –      | –           | ✓      | DC       | I–V characteristics           | Experimental                               | Online                           | FLC  | AIT, ML                 | Dhimish et al. (2017b)  |
| Partial shading, increase series resistance, BpD short circuit, BpD open, PV short circuit | ✓                     | ✓      | –      | ✓           | –      | DC       | I–V characteristics           | Experimental                               | Online                           | MC-NFC (ANFIS)   | AIT, ML                 | Belaout et al. (2018a)  |
| Faulty panel, partial shading  | ✓                     | ✓      | –      | ✓           | –      | DC       | Idc, Vdc                      | Simulated                                  | Online                           | NARX neural network, Linguistic fuzzy rule                             | AIT, ML                 | Samara and Natsheh (2020)   |
| Arc faults   | ✓                     | –      | –      | –           | ✓      | DC       | Idc                           | Experimental                               | Online                           | Variational mode decomposition, multi-scale fuzzy entropy, SVM         | AIT, ML                 | Wang et al. (2021)  |
| Arc faults   | ✓                     | –      | –      | –           | ✓      | DC       | Idc, Vdc                      | Simulated                                  | Online                           | Cascaded Fuzzy   | AIT, ML                 | Grichting et al. (2015)   |
| Faulty modules, partial shading  | ✓                     | ✓      | –      | –           | ✓      | DC       | Power and voltage ratio       | Experimental                               | Online                           | Six layers of rule based approach                                      | AIT, ML                 | Dhimish et al. (2017a)  |
| Open circuit string, open circuit string   | ✓                     | ✓      | –      | –           | ✓      | DC       | I–V characteristics           | Experimental                               | Online                           | best-so-far ABC and PNN  | AIT, ML                 | Garoudja et al. (2017a)   |
| Mismatch fault, BpD fault  | ✓                     | ✓      | –      | –           | ✓      | DC       | I–V and P–V characteristics   | Experimental                               | Online                           | generalized likelihood ratio test                                      | AIT, ML                 | Fazai et al. (2019a)  |
| Open module fault, line-to-line  | ✓                     | ✓      | –      | –           | ✓      | DC       | I–V characteristics           | Experimental/ simulated                    | Online                           | PNN  | AIT, ML                 | Basnet et al. (2020)  |
| Line-to-line, line-to-ground   | ✓                     | ✓      | –      | ✓           | –      | DC       | I–V characteristics           | Experimental                               | Online                           | SVM, Naïve Bayes (NB), logistic regression                             | AIT, ML                 | Eskandari et al. (2021)   |
| Short circuit, open circuit, partial shading   | ✓                     | ✓      | –      | –           | –      | DC       | I–V characteristics           | Simulated                                  | Online                           | SA-RBF ELM   | AIT, ML                 | Wu et al. (2017)  |
| Partial shading, short circuit, open circuit, degradation                                  | ✓                     | ✓      | –      | –           | –      | DC       | I–V characteristics           | Experimental                               | Online                           | Optimized kernel ELM, Nelder–Mead Simplex optimization                 | AIT, ML                 | Chen et al. (2017)  |
| Partial shading  | ✓                     | –      | –      | ✓           | –      | DC       | I–V characteristics           | Experimental                               | Online                           | PCA,   | SSPA                    | Fadhel et al. (2019b), Aljahdali et al. (2019), Fadhel et al. (2019c) |
| Hotspot open circuit, short circuit  | ✓                     | ✓      | –      | –           | –      | DC       | I–V characteristics           | Simulated                                  | Online                           | Classification learner app in MATLAB                                   | AIT, ML                 | Aljahdali et al. (2019)   |
| Mismatch fault, BpD fault  | ✓                     | ✓      | –      | –           | ✓      | DC       | Idc, Vdc, Pdc                 | Simulated                                  | Online                           | Gaussian process regression GLRT                                       | AIT, ML                 | Fazai et al. (2019b)  |
| Increase series resistance   | ✓                     | ✓      | –      | –           | ✓      | DC       | Idc, Pdc                      | Simulated                                  | Online                           | PCA, T squared, squared weighting average, SVM                         | AIT, ML                 | Attouri et al. (2020)   |
| Open circuit, short circuit, degradation, partial shading                                  | ✓                     | ✓      | –      | –           | –      | DC       | I–V characteristics           | Experimental                               | Online                           | GAF, recurrence plot, ANN, SVM, DT, RF, kNN, Naïve Bayesian classifier | AIT, ML                 | Li et al. (2021b)   |
| Not specified  | ✓                     | ✓      | –      | –           | ✓      | DC       | I–V characteristics           | Experimental                               | Online                           | Supervised learning, regression  | AIT, ML                 | Benavides et al. (2021)   |
| Partial shading  | ✓                     | ✓      | –      | –           | ✓      | DC       | I–V characteristics           | Experimental                               | Online                           | Vertices PCA   | AIT, ML                 | Rouani et al. (2021)  |
| Partial shading, cell breakage   | –                     | ✓      | –      | –           | ✓      | DC       | I–V characteristics           | Simulated                                  | Online                           | ANN  | AIT, ML                 | Babasaki and Higuchi (2018)   |
| Line-to-line   | ✓                     | ✓      | –      | –           | –      | DC       | I–V characteristics           | Simulated                                  | Online                           | ELM, NB, SVM, kNN  | AIT, ML                 | Eskandari et al. (2020a)  |
| Series arc fault open-circuit, short-circuit, partial shading, degradation, BpD fault      | ✓<br>✓                | ✓<br>✓ | –<br>– | –<br>–      | –<br>– | DC<br>DC | Idc<br>I–V characteristics    | Experimental<br>Simulated                  | Online<br>Online                 | ELM fine-tuning Naïve Bayesian model                                   | AIT, ML<br>AIT, ML      | Le et al. (2020)<br>He et al. (2021)                                  |
| Open circuit fault, short circuit fault, partial shading                                   | ✓                     | ✓      | –      | –           | ✓      | DC       | I–V characteristics           | Simulated                                  | Online                           | Wavelet transform, RBFN  | AIT, ML                 | Kurukuru et al. (2020)  |
| Panel degradation  | ✓                     | ✓      | –      | –           | ✓      | DC       | Idc, Vdc, Pdc                 | Simulated                                  | offline                          | Logistic regression classifier   | AIT, ML                 | Haba (2019)   |
| Partial shading, short circuited PV  | ✓                     | ✓      | –      | –           | –      | DC       | Idc, Vdc                      | Experimental                               | Online                           | ELM  | AIT, ML                 | Kapucu and Cubukcu (2021)   |
| Open module  | ✓                     | ✓      | –      | –           | ✓      | DC       | Pdc                           | Simulated                                  | Offline                          | RBF-based ANN  | AIT, ML                 | Hussain et al. (2020a)  |

(continued on next page)

Table 6 (continued).

| Types of faults   | Fault Diagnosis Stage |      |     | Kind of PVS |       | DC/AC | Measured Parameters                   | Validation Experimental/ Actual/ simulated | Testing condition Offline/online | Specific method(s) applied           | Types of Technique used | Ref.                                   |
|---|-----------------------|------|-----|-------------|-------|-------|---------------------------------------|--|----------------------------------|--------------------------------------|-------------------------|--|
|   | Det                   | Clas | Loc | SAPVS       | GCPVS |       |                                       |  |                                  |                                      |                         |  |
| Open module, short module, inverter failure,  | ✓                     | ✓    | –   | –           | ✓     | DC    | Pdc                                   | Experimental                               | Online                           | DT, kNN, SVM, FIS                    | AIT, ML                 | Livera et al. (2018)                   |
| Open module, short module, partial shading  | ✓                     | ✓    | –   | –           | ✓     | DC    | I–V and P–V characteristics           | Experimental                               | Online                           | KPCA                                 | AIT, ML                 | Ndjakomo Essiane et al. (2021)         |
| Short module, open module, aging, partial shading   | ✓                     | ✓    | –   | –           | –     | DC    | I–V characteristics                   | Simulated                                  | Online                           | Kernel based ELM                     | AIT, ML                 | Sun et al. (2018b)                     |
| Micro crack, hotspot  | ✓                     | ✓    | –   | –           | –     | DC    | PPL, Voc, Isc, temperature, impedance | Experimental                               | Online                           | SVM, ANN                             | AIT, ML                 | Winston et al. (2021)                  |
| Partial shading   | ✓                     | ✓    | –   | –           | –     | DC    | Irradiance, temperature, Idc, Vdc     | Experimental                               | Online                           | ANN                                  | AIT, ML                 | Mekki et al. (2016)                    |
| Inversed module, partial shading  | ✓                     | ✓    | –   | ✓           | –     | DC    | Pdc                                   | Simulated                                  | Online                           | ANN                                  | AIT, ML                 | Laamami et al. (2017)                  |
| Partial shading, degradation, ground fault, arc fault   | ✓                     | ✓    | –   | ✓           | ✓     | DC    | I–V characteristics                   | Experimental                               | Online                           | Cyber–physical systems, ANN, k-means | AIT, ML                 | Rao et al. (2019)                      |
| Faulty operation (not specified)  | ✓                     | –    | –   | –           | ✓     | DC    | Pdc, Irradiance                       | Simulated                                  | Offline                          | ANN                                  | AIT, ML                 | Jazayeri et al. (2017)                 |
| Line-to-line, degradation, open module circuit  | ✓                     | ✓    | –   | –           | –     | DC    | Pdc                                   | Simulated                                  | Offline                          | ANN                                  | AIT, ML                 | Jenitha and Immanuel Selvakumar (2017) |
| Short circuit, inversed BpD, shunted BpD, open circuit, Increase series resistance, partial shading, partial shading w/ faulted BpD, partial shading w/ series resistance | ✓                     | ✓    | –   | –           | ✓     | DC    | I–V characteristics                   | Experimental                               | Online                           | ANN                                  | AIT, ML                 | Chine et al. (2016)                    |
| Short circuit   | ✓                     | –    | –   | –           | ✓     | AC    | Pac                                   | Simulated                                  | Online                           | ANN                                  | AIT, ML                 | Soffiah et al. (2021)                  |
| Faulty module   | ✓                     | –    | –   | –           | –     | DC    | Idc, Vdc                              | Simulated                                  | Online                           | ANN                                  | AIT, ML                 | Samara and Natshah (2019)              |
| Open circuit, partial shading   | ✓                     | ✓    | –   | –           | –     | DC    | Idc, Vdc                              | Experimental                               | Online                           | ENN                                  | AIT, ML                 | Liu and Yu (2017)                      |
| Line-to-line, line-to-ground, open circuit,   | ✓                     | ✓    | –   | ✓           | –     | DC    | Pdc                                   | Simulated                                  | Offline                          | MLP, CNN                             | AIT, ML                 | Gao (2021)                             |
| Short circuit, open circuit   | ✓                     | ✓    | –   | –           | ✓     | DC    | Impp, Vmpp, Pmpp                      | Experimental                               | Online                           | ANN                                  | AIT, ML                 | Kara Mostefa Khelil et al. (2020)      |
| Faulty module (damage)  | ✓                     | –    | –   | –           | –     | DC    | I–V characteristics                   | Experimental                               | Online                           | Adaptive resonance theory 2 NN, MLP  | AIT, ML                 | Hwang et al. (2019)                    |
| BpD open circuit, BpD short circuit, BcD open circuit, BcD short circuit  | ✓                     | ✓    | –   | ✓           | –     | DC    | I–V and P–V characteristics           | Simulated                                  | Online                           | PCA, DNN                             | AIT, ML                 | Sabri et al. (2018)                    |
| Short circuit, open circuit   | ✓                     | ✓    | –   | ✓           | –     | DC    | I–V characteristics                   | Experimental                               | Online                           | ANN                                  | AIT, ML                 | Haque et al. (2019)                    |
| Partial shading, open circuit, short circuit  | ✓                     | ✓    | –   | –           | ✓     | DC    | I–V characteristics                   | Simulated                                  | Online                           | ANN                                  | AIT, ML                 | Muralidharan (2020)                    |
| degradation   | ✓                     | ✓    | –   | –           | –     | DC    | I–V characteristics                   | Simulated                                  | Offline/Online                   | ANN                                  | AIT, ML                 | Guejia Burbano et al. (2021)           |
| Hotspot, BpD open, BpD short, BcD open, BcD short, line-to-ground fault, line-to-line   | ✓                     | ✓    | –   | ✓           | –     | DC    | I–V and P–V characteristics           | Simulated                                  | Online                           | MLP                                  | AIT, ML                 | Djalab et al. (2020)                   |
| Open module   | ✓                     | ✓    | –   | –           | ✓     | DC    | Irradiance, Pdc                       | Experimental                               | Online                           | ANN                                  | AIT, ML                 | Hussain et al. (2020b)                 |
| Short circuit, partial shading, aging   | ✓                     | ✓    | ✓   | –           | –     | DC    | I–V characteristics                   | Simulated                                  | Online                           | ANN and Memetic Algorithm            | AIT, ML                 | Ganeshprabu and Geethanjali (2016)     |
| Partial shading   | ✓                     | ✓    | –   | ✓           | –     | DC    | I–V characteristics                   | Experimental                               | Online                           | PCA,                                 | AIT, ML                 | Fadhel et al. (2019d)                  |
| Ground fault, line-to-line  | ✓                     | ✓    | ✓   | –           | ✓     | DC    | Vdc                                   | Simulated                                  | Online                           | MRA, DWT, ANN                        | AIT, ML                 | Karmacharya and Gokaraju (2019)        |
| Partial shading, faulty modules   | ✓                     | ✓    | –   | –           | ✓     | DC    | I–V characteristics                   | Simulated                                  | Online                           | RBFSNN and type 2 fuzzy systems      | AIT, ML                 | Janarthanan et al. (2021)              |
| Mismatch fault  | ✓                     | ✓    | –   | –           | ✓     | DC    | Idc, Vdc, Pdc                         | Simulated                                  | Online                           | LAPART                               | AIT, ML                 | Jones et al. (2015)                    |
| Phase-ground, phase to phase fault  | ✓                     | ✓    | ✓   | –           | ✓     | AC    | Iac, Vac, Pac                         | Experimental                               | Online                           | ANN                                  | AIT, ML                 | Usman et al. (2020)                    |
| Dust, encapsulation, delamination, corrosion, snail trails, yellowing   | ✓                     | ✓    | ✓   | ✓           | ✓     | DC    | Images                                | Experimental/actual                        | Offline/Online                   | CNN                                  | AIT, ML, DL             | Li et al. (2019)                       |
| Microcracks, degradation, cell breakage   | ✓                     | ✓    | ✓   | ✓           | ✓     | DC    | Images                                | Experimental/actual                        | Offline/Online                   | LIT, CNN                             | AIT, ML, DL             | Deitsch et al. (2019)                  |
| Cell breakage, microcracks  | ✓                     | ✓    | ✓   | ✓           | ✓     | DC    | Images                                | Experimental/actual                        | Offline/Online                   | ELM, CNN                             | AIT, ML, DL             | Sun et al. (2018a)                     |
| Partial shading, line-to-line, open circuit   | ✓                     | ✓    | –   | ✓           | ✓     | DC    | I–V and P–V characteristics           | Experimental                               | Online                           | CNN, meta-heuristic algorithm        | AIT, ML, DL             | Zaki et al. (2021)                     |
| Arc fault   | ✓                     | ✓    | –   | ✓           | –     | DC    | I–V characteristics                   | Simulated                                  | Online                           | CNN                                  | AIT, ML, DL             | Omran et al. (2020)                    |

(continued on next page)

Table 6 (continued).

| Types of faults  | Fault Diagnosis Stage |      |     | Kind of PVS |       | DC/AC | Measured Parameters                       | Validation Experimental/ Actual/ simulated | Testing condition Offline/online | Specific method(s) applied                                       | Types of Technique used | Ref.                     |
|--|-----------------------|------|-----|-------------|-------|-------|---|--|----------------------------------|--|-------------------------|--------------------------|
|  | Det                   | Clas | Loc | SAPVS       | GCPVS |       |   |  |                                  |  |                         |                          |
| Partial shading, open circuit, line-to-line, arc fault,  | ✓                     | ✓    | –   | ✓           | –     | DC    | Pdc                                       | Simulated                                  | Online                           | Scalogram, CNN   | AIT, ML, DL             | Aziz et al. (2020)       |
| Open circuit, line-to-line,  | ✓                     | ✓    | –   | –           | ✓     | DC    | Idc, Vdc                                  | Experimental                               | Online                           | CNN  | AIT, ML, DL             | Lu et al. (2019a)        |
| Line-to-line, partial shading, open circuit  | ✓                     | ✓    | –   | –           | ✓     | DC    | Idc, Vdc                                  | Experimental                               | Online                           | Dual-channel CNN   | AIT, ML, DL             | Lu et al. (2021a)        |
| Arc fault  | ✓                     | ✓    | –   | –           | –     | DC    | Idc, Vdc                                  | Simulated                                  | Online                           | CNN  | AIT, ML, DL             | Patil and Bindu (2021)   |
| Partial shading w/ BpD, Partial shading w/ reversed BpD, short circuit, increase series resistance     | ✓                     | ✓    | –   | –           | –     | DC    | I–V characteristics                       | Experimental                               | Online                           | CNN w/ residual GRU  | AIT, ML, DL             | Gao and Wai (2020)       |
| Ground fault, arc fault  | ✓                     | ✓    | –   | –           | –     | DC    | I–V characteristics, Pmmp                 | Simulated                                  | Online                           | MLP  | AIT, ML, DL             | Khondoker et al. (2018)  |
| Short circuit, open circuit, combined short circuit and open circuit.                                  | ✓                     | ✓    | –   | –           | ✓     | AC    | Iac, Vac                                  | Simulated                                  | Online                           | ResNET (CNN) , transfer learning                                 | AIT, ML, DL             | Malik et al. (2021)      |
| Partial shading, short circuit, degradation, open circuit  | ✓                     | ✓    | –   | –           | –     | DC    | I–V characteristics                       | Experimental                               | Online                           | ResNET (CNN), autoencoder–decoder                                | AIT, ML, DL             | Chen et al. (2019)       |
| High impedance, line to ground, Line-to-line-to ground, line–line to line-to-ground                    | ✓                     | ✓    | –   | –           | ✓     | AC    | Iac, Vac                                  | Simulated                                  | Online                           | LSTM RNN   | AIT, ML, DL             | Fu et al. (2020)         |
| Line-to-line, partial shading,   | ✓                     | ✓    | –   | –           | –     | DC    | I–V characteristics                       | Simulated                                  | Online                           | LSTM   | AIT, ML, DL             | Veerasamy et al. (2021)  |
| Line-to-line, partial shading,   | ✓                     | ✓    | –   | –           | –     | DC    | I–V characteristics                       | Simulated                                  | Online                           | LSTM   | AIT, ML, DL             | Appiah et al. (2019)     |
| Series arc fault   | ✓                     | ✓    | –   | –           | ✓     | DC    | Idc                                       | Experimental                               | Online                           | DA-DCGAN   | AIT, ML, DL             | Lu et al. (2019b)        |
| Short circuit, degradation, partial shading, partial shading w/ BpD open, partial shading w/ BpD short | ✓                     | ✓    | –   | –           | ✓     | DC    | I–V characteristics                       | Experimental                               | Online                           | Stacked autoencoder  | AIT, ML, DL             | Liu et al. (2021)        |
| Boost converter faults   | ✓                     | ✓    | –   | –           | ✓     | DC    | I–V characteristics                       | Simulated                                  | Online                           | Signal frequency analysis  | SSPA                    | Gonzalez et al. (2011)   |
| Fault occurrence (not specified)   | ✓                     | –    | –   | –           | –     | DC    | Power losses                              | Experimental                               | Online                           | Sequential Probability Ratio Test                                | SSPA                    | Davarifar et al. (2013b) |
| Arc fault  | ✓                     | –    | –   | –           | ✓     | DC    | Idc                                       | Experimental                               | Online                           | Signal analysis  | SSPA                    | Johnson et al. (2011b)   |
| Inverter Failure   | ✓                     | –    | –   | –           | –     | DC    | Pdc                                       | Experimental                               | Online                           | Analysis of Variance, Kruskal–Wallis Test                        | SSPA                    | Guasch et al. (2003)     |
| Open circuit, short circuit  | ✓                     | –    | –   | ✓           | –     | DC    | Idc, Vdc                                  | Simulated                                  | Online                           | Signal analysis w/ rule-based                                    | SSPA                    | Vergura et al. (2009)    |
| Short, open circuit  | ✓                     | ✓    | –   | –           | ✓     | DC    | Vdc                                       | Experimental                               | Online                           | Time-domain reflectometry  | SSPA                    | Schirone et al. (1994a)  |
| Open circuit,  | ✓                     | ✓    | –   | –           | –     | DC    | Vdc                                       | Experimental                               | Online                           | Time-domain reflectometry  | SSPA                    | Takashima et al. (2008)  |
| Partial shading, short circuit, open circuit   | ✓                     | –    | –   | –           | ✓     | DC    | I–V characteristics                       | Experimental                               | Online                           | EWMA   | SSPA                    | Garoudja et al. (2017b)  |
| Partial shading, dust, bird drop, short circuit, pen circuit, aging                                    | ✓                     | ✓    | –   | –           | ✓     | DC    | I–V characteristics                       | Experimental                               | Online                           | Multivariate EWMA  | SSPA                    | Harrou et al. (2017)     |
| Inverter fault, grid anomaly, mismatch fault, MPPT fault, converter fault,                             | ✓                     | ✓    | –   | –           | ✓     | DC/AC | I–V characteristics, Iac, Vac             | Experimental                               | Online                           | PCA-KDE-based multivariate KL divergence                         | SSPA                    | Bakdi et al. (2021)      |
| Faulty string  | ✓                     | –    | –   | –           | ✓     | DC    | Historical data, I–V characteristics, Pdc | Simulated                                  | Offline                          | RT, ANN, Multi-gene GA, Gaussian process, SVM, Sugeno type fuzzy | AIT, ML, hybrid         | Rodrigues et al. (2020)  |
| Line-to-line, increase series resistance, degradation, partial shading, open circuit                   | ✓                     | ✓    | –   | –           | ✓     | DC    | I–V characteristics                       | Experimental                               | Online                           | Rotation forest ELM  | AIT, hybrid             | Han et al. (2019)        |
| Aging, short circuit, soiling, partial shading w/ reversed BpD, partial w/ open BpD                    | ✓                     | ✓    | –   | –           | –     | DC    | I–V characteristics                       | Experimental                               | Online                           | ABC and ELM  | AIT, hybrid             | Huang et al. (2019)      |
| Partial shading , faulty PV  | ✓                     | ✓    | –   | –           | –     | DC    | I–V characteristics                       | Simulated                                  | Online                           | N-semi supervised fuzzy semi supervised learning                 | AIT, hybrid             | Murugesan et al. (2020)  |
| Inverter fault   | ✓                     | ✓    | –   | –           | –     | DC    | Historical data (I–V characteristics)     | Simulated                                  | Offline                          | Support vector regression, model-based prediction                | hybrid                  | Gradwohl et al. (2021)   |

(continued on next page)

(Garoudja et al., 2017b). Harrou et al. used a statistical monitoring approach, multivariate EWMA (MEWMA) to monitor the PVS (Harrou et al., 2017). They focused on the advantages of the one-diode model and EWMA for fault detection. They generated

a series of residuals of current, voltage and power from measurements of temperature and irradiance. Differences between measurements and predictions of the residuals yielded the MPP. MEWMA was used to monitor the DC side of a PV system and identify partial shading.

Table 6 (continued).

| Types of faults  | Fault Diagnosis Stage |      |     | Kind of PVS |       | DC/AC | Measured Parameters                             | Validation Experimental/ Actual/ simulated | Testing condition Offline/online | Specific method(s) applied            | Types of Technique used        | Ref.   |
|--|-----------------------|------|-----|-------------|-------|-------|---|--|----------------------------------|---------------------------------------|--------------------------------|--|
|  | Det                   | Clas | Loc | SAPVS       | GCPVS |       |   |  |                                  |                                       |                                |  |
| Inverter fault   | ✓                     | –    | –   | –           | ✓     | AC    | Iac, Vac  | Simulated                                  | Online                           | Inverter based fault detection        | other                          | Smith et al. (1997), de Araujo Ribeiro et al. (2003), Rodríguez-Blanco et al. (2011), Salehifar et al. (2014), Fang et al. (2015)  |
| Islanding fault  | ✓                     | –    | –   | –           | ✓     | AC    | Iac, Vac  | Simulated                                  | Online                           | Equipment based detection             | other                          | Ezzy et al. (2007), Kunte and Gao (2008), Llaría et al. (2009), Mahat et al. (2011), Econect (2001), Chowdhury et al. (2009), Zeineldin et al. (2006), Hu and Sun (2009), Yin (2005) |
| Open circuit, short circuit, degradation, Soiling, Potential-induced degradation | ✓                     | ✓    | –   | –           | –     | DC    | Weather satellite data                          | Simulated                                  | Offline                          | RNN                                   | AIT, DL                        | Van Gompel et al. (2022)   |
| Glass breakage, dust, corrosion, snail trails, yellowing                         | ✓                     | ✓    | ✓   | ✓           | ✓     | DC    | Images  | Experimental/ Actual                       | Online/Offline                   | Deep embedded restricted cluster, CNN | AIT, DL, hybrid, future trends | Li et al. (2020)   |
| Partial shading, line-to-line  | ✓                     | ✓    | –   | –           | –     | DC    | I <sub>dc</sub> , V <sub>dc</sub> , Temperature | Experimental                               | Online                           | Explainable Artificial Intelligence   | AIT, DL, hybrid, future trends | Sairam et al. (2021)   |

### 5.2.10. Hybrid methods

The definition of hybrid EBM technique is any method that combines any techniques in subclasses of EBMs. In general, most EBMs are hybrid. For example, Bakdi et al. (2021) proposed a PCA with Kullback–Leibler Divergence and recursive smooth kernel density estimation (KDE) for PV fault detection and classification. A hybrid of ML techniques was proposed using a fuzzy system with the five trained ML techniques of regression tree, ANN, multi-gene genetic programming, the Gaussian process, and SVM (Rodrigues et al., 2020). Another example of a hybrid ML technique is rotation forest with bootstrap (Dhibi et al., 2020). PCA with ELM was the hybrid ML technique used for the detection of faults (Han et al., 2019). A hybrid ABC and ELM design has been implemented experimentally to detect five types of fault (Huang et al., 2019). Another method is based on the N-semi-regular fuzzy semi-supervised learning system that is based on the N-semi graph with few labeled data (Murugesan et al., 2020). An approach that used physical and statistical models and physics-based fault diagnosis has also been proposed (Gradwohl et al., 2021).

### 5.2.11. Other types of methods

Other methods cannot be categorized, as mentioned by Madeti and Singh (2017), because several techniques used particular converters. Some of them can be found in Smith et al. (1997), de Araujo Ribeiro et al. (2003), Rodríguez-Blanco et al. (2011), Salehifar et al. (2014), Fang et al. (2015). The faults can be categorized by DC side and AC side in Madeti and Singh (2017). Madeti and Singh emphasized fault detection in the AC side. Islanding fault detection techniques are subdivided into two groups remote islanding and local islanding (Madedi and Singh, 2017). Remote techniques include (a) system state monitoring (Balaguer-Álvarez and Ortiz-Rivera, 2010; I. Llaría et al., 2009), (b) switch state monitoring (Mahat et al., 2008; Ezzy et al., 2007; Kunte and Gao, 2008; Llaría et al., 2009; Mahat et al., 2011), and inter tripping (Econect, 2001; Chowdhury et al., 2009). The local islanding technique can be passive technique, active, or hybrid. The passive methods are under/over voltage and under/over frequency (Zeineldin et al., 2006), voltage phase jump detection (Hu and Sun, 2009), and harmonic measurement (Yin, 2005). Active techniques include impedance measurement (Mahat et al., 2008) and slide-mode frequency shift (Zeineldin et al., 2006).

## 6. Future trends in PV fault detection and classification

### 6.1. Quantum machine learning

Based on the published literature and research, new methods for PV fault detection and classification will continue to be developed and improved, especially those associated with AITs and hybrid methods. This steady advance can be attributed to improvements in computing capabilities, increasing internet speed, development of communication infrastructure, the improvement of interfacing agents (software and hardware), the creation of new and improved AI models and parameters, and so on. One discipline that has been a center of attention in the last few decades is quantum computing which has shown much promising direction in recent years. Quantum computing (QC) is advancing toward handling very complex problems and holds the promise of solving them quickly (Steane, 1998).

Quantum Machine Learning (QML), as defined by Biamonte et al. (2017), is software in which quantum algorithms are used in the implementation of computation. QML is also used to extend the application of ML in quantum computers (Bergholm et al., 2020). Since quantum computers are costly and not yet fully commercialized, several quantum computer simulators have been developed for running tests, simulations, and problem-solving to understand how a quantum computer treats inputs and presents outputs (Fingerhuth et al., 2018). Since IBM and other institutions have provided access to quantum computers for running experiments through cloud computing interfaces, research on the use of QML, hybrid QC, and ML is expected to grow in the next few years. Several leading platforms for providing ML libraries have also been developed, such as TensorFlow Quantum (TFQ) (Ho, 2009), providing a QML model for solving prediction and classification problems. TFQ and other platforms for QML can be used to prepare quantum datasets, evaluate quantum neural network (QNN) models, sample or average data, evaluate classical NN models, and evaluate gradients and update parameters (Ho, 2009). One way of using the quantum computer involves the QML framework. For example, Sama (2021) demonstrated the use of PennyLane's QML framework as an integrator to several backend quantum simulators and real quantum computers. His experiment used a hybrid approach to image classification with a pre-trained ResNet-18 model to classify faces with and without a mask. The results



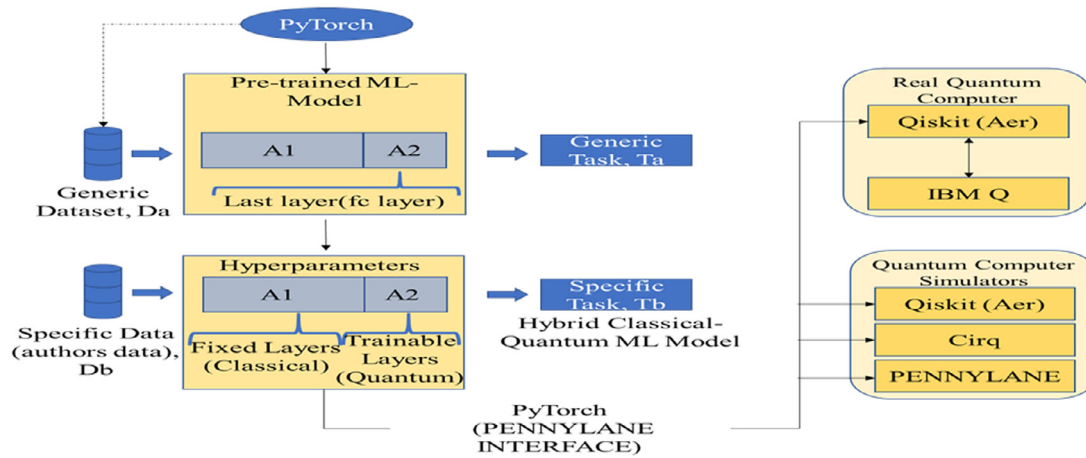


Fig. 11. Framework for developing hybrid classical QML model (Sama, 2021).

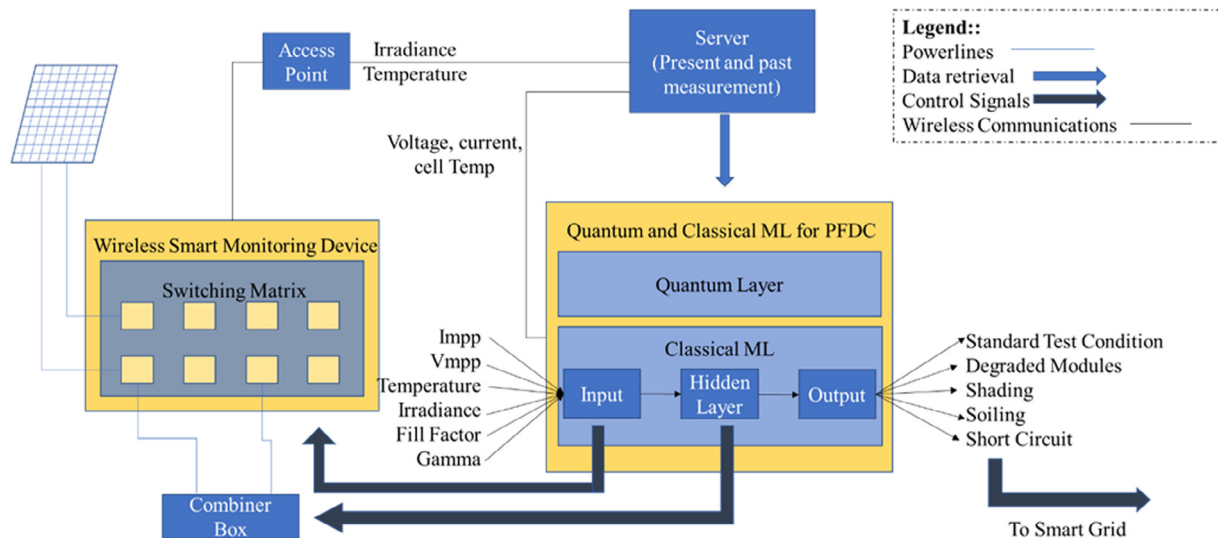


Fig. 12. Implemented framework for smart PV fault detection using QML (Uehara et al., 2021).

of their simulations on different quantum computer simulators used are auspicious: achieved accuracies for Qiskit-IBM, Cirq-Google and PennyLane interface are 97.0833%, 97.5%, and 97.5%, respectively. Fig. 11 presents the framework that was used (Sama, 2021). As can be seen, the hybrid quantum classical model was used with an integrating framework (PennyLane) for quantum computer simulators and a real computer.

The idea presented above can also be applied in different detections and classification problems, such as PV fault detection and classification. One example of the application illustrated in Fig. 11 was provided by Uehara et al. (2021). Their PV fault detection was designed for two qubits, an intelligent monitoring device. Different QNNs were considered to optimize the best results of the experiment. Fig. 12 presents the implemented framework using quantum and classical hybrid ML for PV fault detection (Uehara et al., 2021).

## 6.2. Internet of Things, cloud-based monitoring, edge computing

Internet of Things (IoT) has existed for several years and has had various applications. IoT was already used for PV fault detection and classification as a means of data transfer. For example,

Natsheh and Samara (2020) used IoT to receive data wirelessly before ML was used to detect and classify PV faults. This technology has a promise direction and continues to grow and developed steadily. Its infrastructure has been exploited to monitor PVS in different settings. In the next few years, interconnections among architectures and power generation infrastructure are expected to progress further. Some cities are already implementing “smart grid” with IoT technologies.

A PVS is usually in its grid-connected mode. The monitoring of connected systems in a grid must be considered in its design. Data collection, data analysis, and performance evaluations are typically parts of such systems. Centralized data logging is needed for organized data management. Centralized data logging, monitoring, and analysis can also predict anomalies and apply to any fault in grid-connected mode, including a PVS. For this purpose, cloud-based monitoring is already in use but not yet fully exploited for PV fault detection and classification. Some cloud-based monitoring systems for PVS were presented (Uehara et al., 2021; Vandemark, 2020). The technical report of the Office of Scientific and Technical Information (OSTI) of the U.S. Department of Energy in partnership with NREL and an industry partner (Sunfig) summarized the viability of developed real-time

**Table 7**

Baseline/benchmark methods along with parameter settings and test results.

| Studied faults   | Baseline/benchmark method  |   | Results  |
|--|--|---|--|
|  | Method name  | Method parameter settings   |  |
| Open-circuit fault<br>Short-circuit fault<br>Temporary shading                                   | SVM Harrou et al. (2019a)  | Regularization Coefficient (C) = 2.0;<br>kernel parameter (gamma) = 0.05;<br>kernel function = radial basis function  | 2nd to highest accuracy in detection of three short-circuited modules  |
| Hot spot fault<br>Micro crack  | Feed Forward Back Propagation Neural Network Winston et al. (2021)   | Input shape = $1 \times 6$ ; Number of hidden layers = 9; Number of neurons in hidden layer = 8; activation function = Sigmoid; learning rate = 0.6; momentum rate = 0.6;   | Lower in accuracy than the proposed SVM method   |
| Line-to-line fault<br>String degradation<br>Array degradation<br>Partial shading<br>Open circuit | Decision Tree (DT) Chen et al. (2018a)   | Number of tree = 376; Number of randomly selected features = 1  | 2nd to highest in accuracy compared with Regression Forest Perfect accuracies in diagnosing in both one and two open string faults   |
| Shorted module fault<br>Partial shading<br>Open module fault                                     | Back Propagation Neural Network; Clustering Technique Zhao et al. (2018)   | Number of membership functions = 24   | Lowest accuracy of detection compared with fuzzy C-means clustering  |
| Open-circuit fault<br>Short-circuit Fault<br>Line-to-line fault                                  | ANFIS Abbas and Zhang (2021)   | Fuzzy Inference System (FIS) = Sugeno; Inputs = 7; Output = 1; Number of membership functions = 2; Cluster radius = pi function; No. of epochs = 10   | 2nd to highest in training and testing error   |
| Short-circuit fault<br>Open-circuit fault  | Feed-forward Neural Network Garoudja et al. (2017a)  | Detection Network:<br>- back propagation<br>- hidden Layer = 25<br>- activation function = Sigmoid<br>- training epochs = 100<br>Diagnosis Network:<br>- back propagation<br>- hidden layer = 40<br>- activation function = Sigmoid<br>- training epochs = 100  | <ul style="list-style-type: none"> <li>• accuracy in detecting no-fault condition is 87.14%</li> <li>• accuracy in detecting faulty cases is 100%</li> <li>• proposed Probabilistic Neural Network with 100% accuracies in both cases above</li> <li>• accuracy to diagnose ten-module short-circuited fault is 92.12%</li> <li>• accuracy to diagnose open-circuited fault is 100%</li> <li>• proposed probabilistic neural network got accuracy of 100% in all three fault conditions</li> </ul> |
| Degradation<br>Short-circuit fault<br>Partial shading<br>Open-circuit fault                      | Kernel based Extreme Learning Machine Chen et al. (2017)   | Regularization Coefficient (C) = [(0.1, 1, 10, 50)]; kernel parameter (gamma) = [(10, 10, 10, 50)]  | Lower accuracy with unoptimized values of [C, gamma] compared with optimized kernel based extreme learning machine.  |
| Partial shading<br>Open-circuit fault<br>Short-circuit fault<br>Degradation                      | K-Nearest Neighbor (kNN) Li et al. (2021b)<br>Decision Tree (DT) Li et al. (2021b)<br>Regression forest (RF) Li et al. (2021b)<br>Naïve Bayesian (NB) classifier Li et al. (2021b) | Number of neighbors = optimized;<br>Distance metric = Euclidean, City block, or Chebyshev<br>Max number of splits = optimized;<br>Split criterion = Gini's diversity index<br>Max number of split = optimized;<br>Minimum number of leaf nodes = optimized<br>Distribution type = Gaussian or Kernel; Kernel smoothing window width = optimized | 2nd to worst in all types of datasets 4th to best in all types of datasets 3rd to best in all types of datasets the worst in all types of datasets   |

(continued on next page)

series resistance algorithm for monitoring series resistance in PVS (Vandemark, 2020).

Edge computing is an emerging computing paradigm for data processing close to the source of those data and allows for easy online defect detection (Li et al., 2020). Edge computing can also handle lightweight ML algorithms, which have a reaction time of milliseconds and can be applied in real-time. Li et al. (2020) used edge computing in unmanned aerial vehicles for PV fault detection and classification.

Sairam et al. (2021) realized edge computing-based PV fault detection and classification through the use of an irradiance-based three diode model and Boost to build what the authors

called explainable AI—a detailed framework with local interpretable model-agnostic explanations (fault caused determination). The interconnections among IoT, edge devices, and the cloud can be mapped to the whole edge computing framework, visualized in Fig. 13.

## 7. Conclusion

This reviewed methods for PV fault detection and classification. They were having tabulated and categorized by PV system interconnections, types of fault detected, classified, or even localized, measured parameters, stage of diagnosis, methods,

Table 7 (continued).

| Studied faults  | Baseline/benchmark method   |   |  |
|---|---|---|--|
|   | Method name   | Method parameter settings   | Results  |
| Line-to-line fault  | SVM <a href="#">Eskandari et al. (2020a)</a> (Regularization Coefficient (C) and kernel parameter (gamma)) kNN <a href="#">Eskandari et al. (2020a)</a> | Detection Parameters:<br>- C = 2.25; gamma = 0.3;<br>- kernel function = radial basis function<br><br>Classification Parameters:<br>- C = 100; gamma = auto;<br>- kernel function = radial basis function<br><br>Detection Parameters:<br>- number of neighbors = 5;<br>- power parameters = 1<br><br>Classification Parameters:<br>- number of neighbors = 4;<br>- power parameters = 1  | Worst in classifying line-to-line fault using 5 different derived parameters of I–V curves of PV 2nd to best in detection of line-to-line fault compared with ensemble learning machine  |
| Partial shading<br>Partial shading with open-circuit bypass diode<br>Short-circuit fault String with two shunted modules                                    | Power Losses Analysis <a href="#">Chine et al. (2016)</a>   | Simulated captured losses = 0.0037; measured captured losses = 0.18; current ratio = 1; voltage ratio = 1.33. Simulated captured losses = 0.0037; measured captured losses = 0.18; current ratio = 2.7; voltage ratio = 0.88. Simulated captured losses = 0.0037; measured captured losses = 0.16; current ratio = 1.01; voltage ratio = 1.27. Simulated captured losses = 0.0037; measured captured losses = 0.15; current ratio = 1.03; voltage ratio = 1.22. | Output: faulty modules Output: faulty strings Output: faulty modules Output: faulty modules  |
| Open module fault<br>Open module with partial shading   | Multilayered Perceptron (MLP) <a href="#">Hussain et al. (2020b)</a>  | Number of neurons in hidden layer = 10; activation function = Sigmoid; number of hidden layers = 3; epochs = 1000.  | 2nd to fastest to train and 2 <sup>nd</sup> to highest in accuracy compared with RBFNN   |
| Line-to-line fault<br>Open-circuit fault<br>Arc fault Partial Shading<br>Fault in Partial Shading   | Long short-Term Memory (LSTM) <a href="#">Aziz et al. (2020)</a> , Bi-LSTM <a href="#">Aziz et al. (2020)</a>   | Input feature dimension = 16; nodes in each LSTM input layer = 100; nodes in fully-connected layer = 40; nodes of the softmax layer = 3. Input feature dimension = 16; nodes in each LSTM input layer = 100; nodes in fully-connected layer = 40; nodes of the softmax layer = 3  | Accuracy 64.45% (noise-less data) Accuracy 63.45% (noisy data) Accuracy 62.75% (noise-less data) Accuracy 61.00% (noisy data)  |
| Partial shading<br>Degradation<br>Short-circuit fault<br>Open-circuit fault   | Convolutional Neural Network (CNN) <a href="#">Chen et al. (2019)</a>   | Input layer = $40 \times 4 \times 1$ ; 1st convolution: 2D CNN (window size (k) = $4 \times 4$ ; Number of convolution (C) = 1; stride (s) = 1); 2nd Convolution: 1D CNN (k = 3; C = 3; s = 2); 3rd Convolution: 1D CNN (k = 3; C = 5; s = 1); Maxpool1D: k = 2; s = 2; 4th Convolution: 1D CNN (k=3; C = 16; s = 1) Maxpool1D: k = 4; s = 1; Fully-connected layers = 10; Neurons in hidden layer = 16.  | Perfect accuracy in both partial shading and short circuit fault classification; 2 <sup>nd</sup> to highest in overall accuracy compared with convolutional autoencoder, and proposed method ResNet (perfect accuracy in all types of fault) |
| High Impedance fault<br>Line-to-ground fault (AC)<br>Line-to-line fault (AC)<br>Line-to-line-ground fault (AC)<br>Line-to-line to line-to-ground fault (AC) | kNN <a href="#">Veerasamy et al. (2021)</a> SVM <a href="#">Veerasamy et al. (2021)</a> Decision Tree <a href="#">Veerasamy et al. (2021)</a>           | Number of neighbors = 3; Power parameters = 1 Regularization Coefficient=2.25; kernel parameter (gamma) =0.3; kernel function = radial basis function; multiclass method = one-vs-one Number of tree = 7; Number of randomly selected features = 4; instances of DT = 2; value of fold parameters = 3.  | 2nd to highest in accuracy out of 5 methods 3rd to highest in accuracy out of 5 methods 2nd to worst in accuracy out of 5 methods  |

experiments, and mode of implementation; references were given for each. Based on the gathered information, artificial intelligence, visual and thermal method, electrical based method dominated other techniques in terms of accuracy, the detection of faults, response time, the number of publications, hybridization with other methods, and consistency of improvements. The number of AITs in the literature has increased dramatically over the last three years.

The superiority of a technique for PV fault detection and classification depends on reaction time, types of fault detected,

communication media used, data/parameters of PV used, implementation of the technique, and scalability. PV fault detection and classification in a PVS is continually improving. The application of quantum machine learning is the possible future trend because the computing power increases faster as quantum computers are developed. Infusion of monitoring architectures and IoT, cloud and edge computing technology may also represent a significant future development to perform PV fault detection and classification.

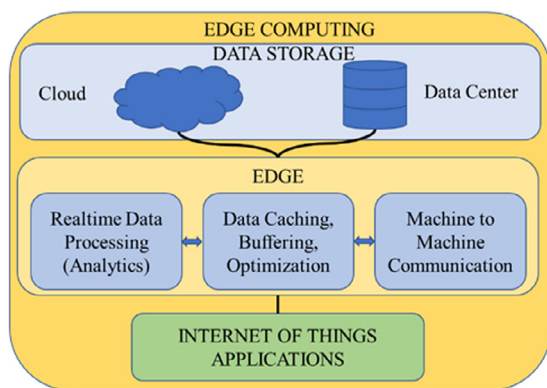


Fig. 13. Edge computing framework based on work of Chalimov (2020).

### Declaration of competing interest

The authors declare that they have no known competing financial interests or personal relationships that could have appeared to influence the work reported in this paper.

### Acknowledgments

The authors would like to thank the Ministry of Science and Technology, Taiwan, for financially supporting this research under Grant MOST 110-3116-F-008-001 and 111-3116-F-008-001.

### References

- Abbas, M., Zhang, D., 2021. A smart fault detection approach for PV modules using adaptive neuro-fuzzy inference framework. *Energy Rep.* 7, 2962–2975.
- Ahmadipour, M., Hizam, H., Othman, M., Mohd Radzi, M., Chireh, N., 2019. A fast fault identification in a grid-connected photovoltaic system using wavelet multi-resolution singular spectrum entropy and support vector machine. *Energies* 12 (13), 2508.
- Alam, M.K., Khan, F., Johnson, J., Flicker, J., 2015. A comprehensive review of catastrophic faults in PV arrays: Types, detection, and mitigation techniques. *IEEE J. Photovolt.* 5 (3), 982–997.
- Ali, M.H., Rabhi, A., Hajjaji, A.E., Tina, G.M., 2017. Real time fault detection in photovoltaic systems. *Energy Procedia* 111, 914–923.
- Aljahdali, S., Alsaheel, S., Fattah, M., Alshehri, M., 2019. Machine learning as an efficient diagnostic tool for fault detection and localization in solar photovoltaic arrays.
- Anon, 2021b. [https://backend.orbit.dtu.dk/ws/portalfiles/portal/192237454/machine\\_learning\\_pr\\_pastebin](https://backend.orbit.dtu.dk/ws/portalfiles/portal/192237454/machine_learning_pr_pastebin). [Online]. Available: <https://pastebin.com/LFp119uK>. (Accessed: 04 November 2021).
- Anon, 2021e. Review of failures of photovoltaic modules - iea-pvps.org. [Online]. Available: [https://iea-pvps.org/wp-content/uploads/2020/01/IEAPVPS\\_T1301\\_2014\\_Review\\_of\\_Failures\\_of\\_Photovoltaic\\_Modules\\_Final.pdf](https://iea-pvps.org/wp-content/uploads/2020/01/IEAPVPS_T1301_2014_Review_of_Failures_of_Photovoltaic_Modules_Final.pdf). (Accessed: 04 November 2021).
- Ansari, S., Ayob, A., Lipu, M.S., Saad, M.H., Hussain, A., 2021. A review of monitoring technologies for solar PV systems using data processing modules and transmission protocols: Progress, challenges and prospects. *Sustainability* 13 (15), 8120.
- Appiah, A., Zhang, X., Ayawli, B., Kyeremeh, F., 2019. Long short-term memory networks based automatic feature extraction for photovoltaic array fault diagnosis. *IEEE Access* 7, 30089–30101.
- Asadpour, R., Sulas-Kern, D.B., Johnston, S., Meydbray, J., Alam, M.A., 2020. Dark lock-in thermography identifies solder bond failure as the root cause of series resistance increase in fielded solar modules. *IEEE J. Photovolt.* 10 (5), 1409–1416. <http://dx.doi.org/10.1109/JPHOTOV.2020.3003781>.
- Attouri, K., Hajji, M., Mansouri, M., Harkat, M.-F., Kouadri, A., Nounou, H., Nounou, M., 2020. Fault detection in photovoltaic systems using machine learning technique. In: 2020 17th International Multi-Conference on Systems, Signals & Devices. SSD.
- Aziz, F., Ul Haq, A., Ahmad, S., Mahmoud, Y., Jalal, M., Ali, U., 2020. A novel convolutional neural network-based approach for fault classification in photovoltaic arrays. *IEEE Access* 8, 41889–41904.
- Babasaki, T., Higuchi, Y., 2018. Using PV string data to diagnose failure of solar panels in a solar power plant. In: 2018 IEEE International Telecommunications Energy Conference (INTELEC).
- Bachmann, J., Buerhop-Lutz, C., Steim, R., Schilinsky, P., Hauch, J.A., Zeira, E., B. Christoh, J., 2012. Highly sensitive non-contact shunt detection of organic photovoltaic modules. *Sol. Energy Mater. Sol. Cells* 101, 176–179.
- Badr, M.M., Hamad, M.S., Abdel-Khalik, A.S., Hamdy, R.A., 2019. Fault detection and diagnosis for photovoltaic array under grid connected using support vector machine. In: 2019 IEEE Conference on Power Electronics and Renewable Energy. CPERE, pp. 546–553.
- Baghaee, H., Mlakic, D., Nikolovski, S., Dragicevic, T., 2020. Support vector machine-based islanding and grid fault detection in active distribution networks. *IEEE J. Emerg. Sel. Top. Power Electron.* 8 (3), 2385–2403.
- Bakdi, A., Bounoua, W., Guichi, A., Mekhilef, S., 2021. Real-time fault detection in PV systems under MPPT using PMU and high-frequency multi-sensor data through online PCA-kde-based multivariate KL divergence. *Int. J. Electr. Power Energy Syst.* 125, 106457.
- Balaguer-Álvarez, I., Ortiz-Rivera, E., 2010. Survey of distributed generation islanding detection methods. *IEEE Latin Am. Trans.* 8 (5), 565–570.
- Basnet, B., Chun, H., Bang, J., 2020. An intelligent fault detection model for fault detection in photovoltaic systems. *J. Sensors* 2020, 1–11.
- Bdour, M., Dalala, Z., Al-Addous, M., Radaideh, A., Al-Sadi, A., 2020. A comprehensive evaluation on types of microcracks and possible effects on power degradation in photovoltaic solar panels. *Sustainability* 12 (16), 6416.
- Belaout, A., Krim, F., Mellit, A., 2016. Neuro-fuzzy classifier for fault detection and classification in photovoltaic module. In: 2016 8th International Conference on Modelling, Identification and Control. ICMIC, pp. 144–149.
- Belaout, A., Krim, F., Mellit, A., Talbi, B., Arabi, A., 2018. Multiclass adaptive neuro-fuzzy classifier and feature selection techniques for photovoltaic array fault detection and classification. *Renew. Energy* 127, 548–558.
- Belaout, A., Krim, F., Mellit, A., Talbi, B., Arabi, A., 2018a. Multiclass adaptive neuro-fuzzy classifier and feature selection techniques for photovoltaic array fault detection and classification. *Renew. Energy* 27, 548–558.
- B.E.M.B.E.R.G.G.H.- www.agentur-bemberg.de, 2021. 11 Common solar panel defects and how to avoid them, WINAICO. [Online]. Available: <https://www.winaico.com/us/blog/common-solar-panel-defects/>. (Accessed: 04 November 2021).
- Benavides, D.J., Arévalo-Cordero, P., González, L.G., Hernández-Callejo, L., Jurado, F., Aguado, J.A., 2021. Method of monitoring and detection of failures in PV system based on machine learning. *Revista Facultad de Ingeniería Universidad de Antioquia* (102), 26–43.
- Benkercha, R., Moulaoum, S., 2018. Fault detection and diagnosis based on C4.5 decision tree algorithm for grid connected PV system. *Sol. Energy* 173, 610–634.
- Bergholm, V., Izaac, J., Schuld, M., Gogolin, C., Alam, M.S., Ahmed, S., Arrazola, J.M., Blank, C., Delgado, A., Jahangiri, S., McKiernan, K., Meyer, J.J., Niu, Z., Száva, A., Killoran, N., 2020. PennyLane: Automatic differentiation of hybrid quantum-classical computations [WWW Document]. arXiv.org. URL <https://arxiv.org/abs/1811.04968> (accessed 4.26.22).
- Biamonte, J., Wittek, P., Pancotti, N., Rebentrost, P., Wiebe, N., Lloyd, S., 2017. Quantum machine learning. *Nature* 549 (7671), 195–202. [Accessed 10 2021].
- Bird, M., Acha, S., Brun, N.L., Shah, N., 2019. Assessing the modelling approach and datasets required for fault detection in photovoltaic systems. In: 2019 IEEE Industry Applications Society Annual Meeting. pp. 1–6.
- Blume, L., 2021. Fire safety for PV systems, sunny. SMA corporate blog, 02-may-2019. [Online]. Available: <https://www.sma-sunny.com/en/fire-safety-for-pv-systems/>. (Accessed: 04 November 2021).
- de Boer, Y., 2008. Kyoto protocol reference manual on accounting of emissions and assigned amounts [www document]. unfccc.int. URL <https://unfccc.int/documents/34558> (accessed 4.26.22).
- Bonsignore, L., Davarifar, M., Rabhi, A., Tina, G.M., Elhajjaji, A., 2014. Neuro-fuzzy fault detection method for photovoltaic systems. *Energy Procedia* 62, 431–441.
- Bouaichi, A., Merrouni, A.A., El Hassani, A., Naimi, Z., Ikken, B., Ghennoui, A., Benazzou, A., El Amrani, A., Messaoudi, C., 2017. Experimental evaluation of the discoloration effect on PV-modules performance drop. *Energy Procedia* 119, 818–827.
- Cao, Y., Dong, Y., Cao, Y., Yang, J., Yang, M.Y., 2020. Two-stream convolutional neural network for non-destructive subsurface defect detection via similarity comparison of lock-in thermography signals. *NDT & E Int.* 112, 102246.
- Chalimov, A., 2020. The impact of edge computing on IoT: The main benefits and real-life use cases: Eastern peak [WWW Document]. Eastern Peak - Technology Consulting & Development Company. URL <https://easternpeak.com/blog/the-impact-of-edge-computing-on-iot-the-main-benefits-and-real-life-use-cases/> (accessed 4.26.22).
- Chan, F., Calleja, H., 2006. Reliability: a new approach in design of inverters for PV systems. In: Proceedings of the 10th IEEE International Power Electronics Congress. CIEP '06, pp. 97–102.
- Chang, H., Lin, S., Kuo, C., Yu, H., 2014. Cloud monitoring for solar plants with support vector machine based fault detection system. *Math. Probl. Eng.* 2014, 1–10.
- Chao, K.-H., Ho, S.-H., Wang, M.-H., 2008. Modeling and fault diagnosis of a photovoltaic system. *Electr. Power Syst. Res.* 78 (1), 97–105.



- Chen, Z., Chen, Y., Wu, L., Cheng, S., Lin, P., 2019. Deep residual network based fault detection and diagnosis of photovoltaic arrays using current–voltage curves and ambient conditions. *Energy Convers. Manage.* 198, 111793.
- Chen, Z., Han, F., Wu, L., Yu, J., Cheng, S., Lin, P., Chen, H., 2018a. Random forest based intelligent fault diagnosis for PV arrays using array voltage and string currents. *Energy Convers. Manage.* 178, 250–264.
- Chen, L., Wang, X., 2018. Adaptive fault localization in photovoltaic systems. *IEEE Trans. Smart Grid* 9 (6), 6752–6763. <http://dx.doi.org/10.1109/TSG.2017.2722821>.
- Chen, Z., Wu, L., Cheng, S., Lin, P., Wu, Y., Lin, W., 2017. Intelligent fault diagnosis of photovoltaic arrays based on optimized kernel extreme learning machine and I-V characteristics. *Appl. Energy* 204, 912–931.
- Chen, L., et al., 2018b. Fault diagnosis and classification for photovoltaic arrays based on principal component analysis and support vector machine. *IOP Conf. Ser.: Earth Environ. Sci.* 188, 012089.
- Chine, W., Mellit, A., Lughi, V., Malek, A., Sulligoi, G., Massi Pavan, A., 2016. A novel fault diagnosis technique for photovoltaic systems based on artificial neural networks. *Renew. Energy* 90, 501–512.
- Chine, W., Mellit, A., Pavan, A.M., Lughi, V., 2015. Fault diagnosis in photovoltaic arrays. In: 2015 International Conference on Clean Electrical Power. ICCEP, pp. 67–72. <http://dx.doi.org/10.1109/ICCEP.2015.7177602>.
- Cho, K., Jo, H., Kim, E., Park, H., Park, J., 2020. Failure diagnosis method of photovoltaic generator using support vector machine. *J. Electr. Eng. Technol.* 15 (4), 1669–1680.
- Choudier, A., Silvestre, S., 2010. Automatic supervision and fault detection of PV systems based on power losses analysis. *Energy Convers. Manage.* 51 (10), 1929–1937.
- Chowdhury, S., Chowdhury, S., Crossley, P., 2009. Islanding protection of active distribution networks with renewable distributed generators: A comprehensive survey. *Electr. Power Syst. Res.* 79 (6), 984–992.
- Coleman, A., Zalewski, J., 2011. Intelligent fault detection and diagnostics in solar plants. In: Proceedings of the 6th IEEE International Conference on Intelligent Data Acquisition and Advanced Computing Systems. pp. 948–953.
- Colvin, D.J., Schneller, E.J., Davis, K.O., 2021. Impact of interconnection failure on photovoltaic module performance. *Prog. Photovolt., Res. Appl.* 29 (5), 524–532.
- Copeland, M., 2021. The difference between AI, Machine Learning, and deep learning? [WWW Document]. <https://blogs.nvidia.com/>. URL <https://blogs.nvidia.com/blog/2016/07/29/whats-difference-artificial-intelligence-machine-learning-deep-learning-ai/> (accessed 4.26.22).
- Cubukcu, M., Akanalci, A., 2020. Real-time inspection and determination methods of faults on photovoltaic power systems by thermal imaging in Turkey. *Renew. Energy* 147 (Part 1), 1231–1238. <http://dx.doi.org/10.1016/j.renene.2019.09.075>.
- Daliento, S., Di Napoli, F., Guerriero, P., d'Alessandro, V., 2016. A modified bypass circuit for improved hot spot reliability of solar panels subject to partial shading. *Sol. Energy* 134, 211–218.
- Davarifar, M., Rabhi, A., El Hajjaji, A., 2013a. Comprehensive modulation and classification of faults and analysis their effect in DC side of photovoltaic system. *Energy Power Eng.* 5, 230–236.
- Davarifar, M., Rabhi, A., El-Hajjaji, A., Dahmane, M., 2013b. Real-time model base fault diagnosis of PV panels using statistical signal processing. In: IEEE Int Conf Renew Energy Res Appl. ICRERA, pp. 599–604.
- de Araujo Ribeiro, R., Jacobina, C., da Silva, E., Lima, A., 2003. Fault detection of open-switch damage in voltage-fed PWM motor drive systems. *IEEE Trans. Power Electron.* 18 (2), 587–593.
- Deitsch, S., Christlein, V., Berger, S., Buerhop-Lutz, C., Maier, A., Gallwitz, F., Riess, C., 2019. Automatic classification of defective photovoltaic module cells in electroluminescence images. *Sol. Energy* 185, 455–468.
- Dhar, S., Patnaik, R.K., Dash, P.K., 2018. Fault detection and location of photovoltaic based DC microgrid using differential protection strategy. *IEEE Trans. Smart Grid* 9 (5), 4303–4312. <http://dx.doi.org/10.1109/TSG.2017.2654267>.
- Dhibi, K., Fezai, R., Bouzrara, K., Mansouri, M., Nounou, H., Nounou, M., Trabelsi, M., 2021a. Enhanced RF for fault detection and diagnosis of uncertain PV systems. In: 2021 18th International Multi-Conference on Systems, Signals & Devices. SSD.
- Dhibi, K., Fezai, R., Mansouri, M., Trabelsi, M., Bouzrara, K., Nounou, H., Nounou, M., 2021b. A hybrid fault detection and diagnosis of grid-tied PV systems: Enhanced random forest classifier using data reduction and interval-valued representation. *IEEE Access* 9, 64267–64277.
- Dhibi, K., Fezai, R., Mansouri, M., Trabelsi, M., Kouadri, A., Bouzara, K., Nounou, H., Nounou, M., 2020. Reduced kernel random forest technique for fault detection and classification in grid-tied PV systems. *IEEE J. Photovolt.* 10 (6), 1864–1871.
- Dhimish, M., 2021. Defining the best-fit machine learning classifier to early diagnose photovoltaic solar cells hot-spots. *Case Stud. Therm. Eng.* 25, 100980.
- Dhimish, M., Badran, G., 2019. Photovoltaic hot-spots fault detection algorithm using fuzzy systems. *IEEE Trans. Device Mater. Reliab.* 19 (4), 671–679.
- Dhimish, M., Holmes, V., 2016. Fault detection algorithm for grid-connected photovoltaic plants. *Sol. Energy* 137, 236–245.
- Dhimish, M., Holmes, V., Mehrdadi, B., Dales, M., 2017a. Diagnostic method for photovoltaic systems based on six layer detection algorithm. *Electr. Power Syst. Res.* 151, 26–39.
- Dhimish, M., Holmes, V., Mehrdadi, B., Dales, M., 2017b. Multi-layer photovoltaic fault detection algorithm. *High Voltage* 2 (4), 244–252.
- Dhimish, M., Holmes, V., Mehrdadi, B., Dales, M., Mather, P., 2017c. Photovoltaic fault detection algorithm based on theoretical curves modelling and fuzzy classification system. *Energy* 140, 276–290.
- Djalab, A., Rezaoui, M., Mazouz, L., Teta, A., Sabri, N., 2020. Robust method for diagnosis and detection of faults in photovoltaic systems using artificial neural networks. *Period. Polytech. Electr. Eng. Comput. Sci.* 64 (3), 291–302.
- Du, B., He, Y., He, Y., Duan, J., Zhang, Y., 2020. Intelligent classification of silicon photovoltaic cell defects based on eddy current thermography and convolution neural network. *IEEE Trans. Ind. Inform.* 16 (10), 6242–6251. <http://dx.doi.org/10.1109/TII.2019.2952261>.
- Ducange, P., Fazzolari, M., Lazzarini, B., Marcelloni, F., 2011. An intelligent system for detecting faults in photovoltaic fields. In: 2011 11th International Conference on Intelligent Systems Design and Applications. pp. 1341–134.
- E. & I. S. Department for Business, 2021. Fire incidents involving solar panels, GOV.UK, 19-Mar-2019. [Online]. Available: <https://www.gov.uk/government/publications/fire-incidents-involving-solar-panels>. (Accessed: 04 November 2021).
- Ecconect, 2001. Assessment of islanded operation of distribution networks and measures for protection. *Polymer Contents* 830–877.
- Eskandari, A., Milimonfared, J., Aghaei, M., 2020a. Line-line fault detection and classification for photovoltaic systems using ensemble learning model based on I-V characteristics. *Sol. Energy* 211 (2020), 354–365.
- Eskandari, A., Milimonfared, J., Aghaei, M., 2021. Fault detection and classification for photovoltaic systems based on hierarchical classification and machine learning technique. *IEEE Trans. Ind. Electron.* 68 (12), 12750–12759.
- Eskandari, A., Milimonfared, J., Aghaei, M., Reinders, A.H.M.E., 2020b. Autonomous monitoring of line-to-line faults in photovoltaic systems by feature selection and parameter optimization of support vector machine using genetic algorithms. *Appl. Sci.* 10 (16), 5527.
- Ezzt, M., Marei, M., Abdel-Rahman, M., Mansour, M., 2007. A hybrid strategy for distributed generators islanding detection. In: Power Engineering Society Conference and Exposition in Africa, PowerAfrica'07. pp. 1–7.
- Fadhel, S., Delpha, C., Diallo, D., Bahri, I., Migan, A., Trabelsi, M., Mimouni, M.F., 2019a. Pv shading fault detection and classification based on I-V curve using principal component analysis: Application to isolated PV system. *Sol. Energy* 179, 1–10.
- Fadhel, S., Delpha, C., Diallo, D., Bahri, I., Migan, A., Trabelsi, M., Mimouni, M.F., 2019b. Pv shading fault detection and classification based on I-V curve using principal component analysis: Application to isolated PV system. *Sol. Energy* 179, 1–10.
- Fadhel, S., Delpha, C., Diallo, D., Bahri, I., Migan, A., Trabelsi, M., Mimouni, M.F., 2019c. Pv shading fault detection and classification based on I-V curve using principal component analysis: Application to isolated PV system. *Sol. Energy* 179, 1–10.
- Fadhel, S., Delpha, C., Diallo, D., Bahri, I., Migan, A., Trabelsi, M., Mimouni, M., 2019d. Pv shading fault detection and classification based on IV curve using principal component analysis: Application to isolated PV system. *Sol. Energy* 179, 1–10.
- Famili, A., Shen, W.-M., Weber, R., Simoudis, E., 1997. Data preprocessing and intelligent data analysis. *Intell. Data Anal.* 1 (1), 3–23.
- Fang, J., Li, W., Li, H., Xu, X., 2015. Online inverter fault diagnosis of buck-converter BLDC motor combinations. *IEEE Trans. Power Electron.* 30 (5), 2674–2688.
- Fazai, R., Abodayeh, K., Mansouri, M., Trabelsi, M., Nounou, H., Nounou, M., Georgiou, G.E., 2019a. Machine learning-based statistical testing hypothesis for fault detection in photovoltaic systems. *Sol. Energy* 190, 405–413.
- Fazai, R., Mansouri, M., Abodayeh, K., Trabelsi, M., Nounou, H., Nounou, M., 2019b. Machinelearning-based statistical hypothesis testing for fault detection. In: 2019 4th Conference on Control and Fault Tolerant Systems. SysTol, pp. 38–43.
- Fezzani, A., Mahammed, I.H., Drid, S., Chrifi-alaoui, L., 2015. Modeling and analysis of the photovoltaic array faults. In: 2015 3rd International Conference on Control, Engineering & Information Technology. CEIT, pp. 1–9. <http://dx.doi.org/10.1109/CEIT.2015.7232983>.
- Fingerhuth, M., Babej, T., Wittek, P., 2018. Open source software in quantum computing. *PLOS ONE* 13, <http://dx.doi.org/10.1371/journal.pone.0208561>.
- Flicker, J., Johnson, J., 2013. Electrical simulations of series and parallel PV arc-faults. In: 2013 IEEE 39th Photovoltaic Specialists Conference. PVSC, pp. 3165–3172. <http://dx.doi.org/10.1109/PVSC.2013.6745127>.
- Fu, S., Cai, F., Wang, W., 2020. Fault diagnosis of photovoltaic array based on SE-ResNet. *J. Phys.: Conf. Ser. IOP Publishing* 1682 (1), 012004.
- Gallardo-Saavedra, S., Hernández-Callejo, L., Duque-Perez, O., 2019. Analysis and characterization of PV module defects by thermographic inspection. *Revista Facultad de Ingeniería Universidad de Antioquia* (93), 92–104.



- Ganeshprabu, B., Geethanjali, M., 2016. Dynamic monitoring and optimization of fault diagnosis of photo voltaic solar power system using ANN and memetic algorithm. *Circuits Syst.* 7 (11), 3531–3540.
- Gao, W., 2021. PV array fault detection based on deep neural network. In: 2021 IEEE Green Technologies Conference. GreenTech, pp. 42–47.
- Gao, W., Wai, R., 2020. A novel fault identification method for photovoltaic array via convolutional neural network and residual gated recurrent unit. *IEEE Access* 8, 159493–159510.
- Gao, X., Yang, S., Pan, S., 2017. Optimal parameter selection for support vector machine based on artificial bee colony algorithm: A case study of grid-connected PV system power prediction. *Comput. Intell. Neurosci.* 2017, 1–14.
- Garoudja, E., Chouder, A., Kara, K., Silvestre, S., 2017a. An enhanced machine learning based approach for failures detection and diagnosis of PV systems. *Energy Convers. Manage.* 151, 496–513.
- Garoudja, E., Harrou, F., Sun, Y., Kara, K., Chouder, A., Silvestre, S., 2017b. Statistical fault detection in photovoltaic systems. *Sol Energy* 150, 485–499.
- Gokmen, N., Karatepe, E., Silvestre, S., Celik, B., Ortega, P., 2013. An efficient fault diagnosis method for PV systems based on operating voltage-window. *Energy Convers. Manage.* 73, 350–360.
- Gong, S., Wu, X., Zhang, Z., 2020. Fault diagnosis method of photovoltaic array based on random forest algorithm. In: 2020 39th Chinese Control Conference. CCC, pp. 4249–4254.
- Gonzalez, M., Raison, B., Bacha, S., Bun, Long., 2011. Fault diagnosis in a grid-connected photovoltaic system by applying a signal approach. In: IECON 2011–37th Annual Conference of the IEEE Industrial Electronics Society.
- Gradwohl, C., Dimitrievska, V., Pittino, F., Muehleisen, W., Montvay, A., Langmayr, F., Kienberger, T., 2021. A combined approach for model-based PV power plant failure detection and diagnostic. *Energies* 14 (5), 1261.
- Grichting, B., Goette, J., Jacomet, M., 2015. Cascaded fuzzy logic based arc fault detection in photovoltaic applications. In: 2015 International Conference on Clean Electrical Power. ICCEP, pp. 178–183.
- Guasch, D., Silvestre, S., Calatayud, R., 2003. Automatic failure detection in photovoltaic systems. In: Proceedings of the 3rd IEEE World Conference on Photovoltaic Energy Conversion. pp. 2269–2271.
- Guejia Burbano, R., Petrone, G., Manganiello, P., 2021. Early detection of photovoltaic panel degradation through artificial neural network. *Appl. Sci.* 11 (19), 8943.
- Haba, C., 2019. Monitoring solar panels using machine learning techniques. In: 2019 8th International Conference on Modern Power Systems. MPS, pp. 1–6.
- Hachana, O., Tina, G.M., Hemsas, K.E., 2016. PV array fault diagnostic technique for BIPV systems. *Energy Build.* 126, 263–274.
- Haeberlin, H., Real, M., 2007. Arc detector for remote detection of dangerous arcs on the DC side of PV plants.
- Hajji, M., Harkat, M.-F., Kouadri, A., Abodayeh, K., Mansouri, M., Nounou, H., Nounou, M., 2021. Multivariate feature extraction based supervised machine learning for fault detection and diagnosis in photovoltaic systems. *Eur. J. Control* 59, 313–321.
- Han, F., et al., 2019. An intelligent fault diagnosis method for PV arrays based on an improved rotation forest algorithm. *Energy Procedia* 158, 6132–6138.
- Haney, J., Burstein, A., 2013. PV system operations and Maintenance Fundamentals [WWW Document]. <http://www.solarabcs.org>. URL <http://www.solarabcs.org/about/publications/reports/operations-maintenance/pdfs/SolarABCs-35-2013.pdf> (accessed 4.26.22).
- Haq, A., Bharath, K., Khan, M., Khan, I., Jaffery, Z., 2019. Fault diagnosis of photovoltaic modules. *Energy Sci. Eng.* 7 (3), 622–644.
- Harrou, F., Dairi, A., Taghezouit, B., Sun, Y., 2019a. An unsupervised monitoring procedure for detecting anomalies in photovoltaic systems using a one-class support vector machine. *Sol. Energy* 179, 48–58.
- Harrou, F., Sun, Y., Taghezouit, B., Saidi, A., Hamlati, M.-E., 2017. Reliable fault detection and diagnosis of photovoltaic systems based on statistical monitoring approaches. *Renew. Energy*.
- Harrou, F., Taghezouit, B., Sun, Y., 2019b. Improved KNN-based monitoring schemes for detecting faults in PV systems. *IEEE J. Photovolt.* 9 (3), 811–821.
- Harrou, F., Taghezouit, B., Sun, Y., 2019b. Robust and flexible strategy for fault detection in grid-connected photovoltaic systems. *Energy Convers. Manage.* 180, 1153–1166.
- Hasan, A.A., Ahmed Alkahtani, A., Shahahmadi, S.A., Nur E. Alam, M., Islam, M.A., Amin, N., 2021. Delamination-and electromigration-related failures in solar panels—A review. *Sustainability* 13 (12), 6882.
- He, W., Yin, D., Zhang, K., Zhang, X., Zheng, J., 2021. Fault detection and diagnosis method of distributed photovoltaic array based on fine-tuning naive Bayesian model. *Energies* 14 (14), 4140.
- Heidari, N., Gwamuri, J., Townsend, T., Pearce, J.M., 2015. Impact of snow and ground interference on photovoltaic electric system performance. *IEEE J. Photovolt.* 5 (6), 1680–1685.
- Heilscher, G., Reindl, T., Zhan, Y., Idbi, B., Guerrero, R., 2020. Communication and control for high PV penetration under smart grid environment - IEA-PVPS [WWW Document]. IEA. URL <https://iea-pvps.org/key-topics/communication-and-control-for-high-pv-penetration-under-smart-grid-environment/> (accessed 4.26.22).
- Ho, A., 2009. Announcing TensorFlow quantum: An open source library for quantum machine learning, google AI blog. [Online]. Available: <https://ai.googleblog.com/2020/03/announcing-tensorflow-quantum-open.html>. (Accessed: 10 November 2021).
- Hu, Y., Cao, W., Ma, J., Finney, S.J., Li, D., 2014. Identifying PV module mismatch faults by a thermography-based temperature distribution analysis. *IEEE Trans. Device Mater. Reliab.* 14 (4), 951–960. <http://dx.doi.org/10.1109/TDMR.2014.2348195>.
- Hu, Y., Gao, B., Song, X., Tian, G.Y., Li, K., He, X., 2013. Photovoltaic fault detection using a parameter based model. *Sol. Energy* 96, 96–102.
- Hu, W., Sun, Y., 2009. A compound scheme of islanding detection according to inverter. In: Power and Energy Engineering Conference, Asia-Pacific. pp. 1–4.
- Hu, Y., Zhang, J., Cao, W., Wu, J., Tian, G.Y., Finney, S.J., Kirtley, J.L., 2015a. Online two-section PV array fault diagnosis with optimized voltage sensor locations. *IEEE Trans. Ind. Electron.* 62 (11), 7237–7246.
- Hu, Y., et al., 2015b. Online two-section PV array fault diagnosis with optimized voltage sensor locations. *IEEE Trans. Ind. Electron.* 62 (11), 7237–7246. <http://dx.doi.org/10.1109/TIE.2015.2448066>.
- Huang, Z., Guo, L., 2009. Research and implementation of microcomputer online fault detection of solar array. In: 2009 4th International Conference on Computer Science & Education. pp. 1052–1055. <http://dx.doi.org/10.1109/ICCSE.2009.5228541>.
- Huang, J., Wai, R., Yang, G., 2019. Design of hybrid artificial bee colony algorithm and semi-supervised extreme learning machine for PV fault diagnoses by considering dust impact. *IEEE Trans. Power Electron.* 35 (7), 7086–7099.
- Hussain, M., Dhimish, M., Holmes, V., Mather, P., 2020a. Deployment of AI-based RBF network for photovoltaics fault detection procedure. *AIMS Electron. Electr. Eng.* 4 (1), 1–18.
- Hussain, M., Dhimish, M., Titarenko, S., Mather, P., 2020b. Artificial neural network based photovoltaic fault detection algorithm integrating two bi-directional input parameters. *Renew. Energy* 155, 1272–1292.
- Hwang, H., Kim, B., Cho, T., Lee, I., 2019. Implementation of a fault diagnosis system using neural networks for solar panel. *Int. J. Control Autom. Syst.* 17 (4), 1050–1058.
- I. Llaría, A., Cúrea, O., Jimenez, J., Camblong, H., 2009. Survey on microgrids: analysis of technical limitations to carry out new solutions. In: Power Electronics and Applications, EPE'09. 13th European Conference. pp. 1–8.
- Itoh, U., Yoshida, M., Tokuhisa, H., Takeuchi, K., Takemura, Y., 2014a. Solder joint failure modes in the conventional crystalline si module. *Energy Procedia* 55, 464–468.
- Itoh, U., Yoshida, M., Tokuhisa, H., Takeuchi, K., Takemura, Y., 2014b. Solder joint failure modes in the conventional crystalline si module. *Energy Procedia* 55, 464–468.
- Janarthanan, R., Maheshwari, R., Shukla, P., Shukla, P., Mirjalili, S., Kumar, M., 2021. Intelligent detection of the PV faults based on artificial neural network and type 2 fuzzy systems. *Energies* 14 (20), 6584.
- Jazayeri, K., Jazayeri, M., Uysal, S., 2017. Artificial neural network-based all-sky power estimation and fault detection in photovoltaic modules. *J. Photon. Energy* 7 (2), 025501.
- Jenitha, P., Immanuel Selvakumar, A., 2017. Fault detection in PV systems. *Appl. Solar Energy* 53 (3), 229–237.
- Jiang, L.L., Maskell, D.L., 2015. Automatic fault detection and diagnosis for photovoltaic systems using combined artificial neural network and analytical based methods. In: 2015 International Joint Conference on Neural Networks. IJCNN.
- Johnson, J., Kang, J., 2012. Arc-fault detector algorithm evaluation method utilizing prerecorded arcing signatures. In: 2012 38th IEEE Photovoltaic Specialists Conference. pp. 001378–001382.
- Johnson, J., Kuszmaul, S., Bower, W., Schoenwald, D., 2011a. Using PV module and line frequency response data to create robust arc fault detectors. In: Proceedings of the 26th European Photovoltaic Solar Energy Conference and Exhibition. pp. 5–09.
- Johnson, J., Pahl, B., Luebke, C., Pier, T., Miller, T., Strauch, J., Kuszmaul, S., Bower, W., 2011b. Photovoltaic DC arc fault detector testing at sandia national laboratories. In: Proceedings of the 37th IEEE Photovoltaic Specialists Conference. PVSC, pp. 3614–3619.
- Jones, C., Stein, J., Gonzales, S., King, B., 2015. Photovoltaic system fault detection and diagnostics using laterally primed adaptive resonance theory neural network. In: 2015 IEEE 42nd Photovoltaic Specialist Conference. PVSC, pp. 1–6.
- Jufri, F., Oh, S., Jung, J., 2019. Development of photovoltaic abnormal condition detection system using combined regression and support vector machine. *Energy* 176, 457–467.
- Kapucu, C., Cubukcu, M., 2021. A supervised ensemble learning method for fault diagnosis in photovoltaic strings. *Energy* 227, 120463.
- Kara Mostefa Khelil, C., Amrouche, B., Benyoucef, A., Kara, K., Chouder, A., 2020. New intelligent fault diagnosis (IFD) approach for grid-connected photovoltaic systems. *Energy* 211, 118591.
- Karmacharya, I., Gokaraju, R., 2019. Fault location in ungrounded photovoltaic system using wavelets and ANN. *IEEE Trans. Power Deliv.* 33 (2), 549–559.

- Khondoker, F., Rao, S., Spanias, A., Tepedelenlioglu, C., 2018. Photovoltaic array simulation and fault prediction via multilayer perceptron models. In: 2018 9th International Conference on Information, Intelligence, Systems and Applications. IISA, pp. 1–5.
- Khoshnami, A., Sadeghkhani, I., 2018. Two-stage power-based fault detection scheme for photovoltaic systems. *Sol. Energy* 176, 10–21.
- Kim, S.-K., Jeon, J.-H., Cho, C.-H., Kim, E.-S., Ahn, J.-B., 2009. Modeling and simulation of a grid-connected PV generation system for electromagnetic transient analysis. *Sol. Energy* 83 (5), 664–678.
- Kim, J., Rabelo, M., Padi, S.P., Yousuf, H., Cho, E.-C., Yi, J., 2021. A review of the degradation of photovoltaic modules for life expectancy. *Energies* 14 (14), 4278.
- Kirchartz, T., Helbig, A., Reetz, W., Reuter, M., Werner, J.H., Rau, U., 2009. Reciprocity between electroluminescence and quantum efficiency used for the characterization of Silicon solar cells. *Prog. Photovolt., Res. Appl.* 17 (6), 394–402.
- Köntges, M., Kurtz, S., Packard, C., Jahn, U., Berger, K., Kato, K., Friesen, T., Liu, H., Iseghem, M.V., Wohlgemuth, J., Miller, D., Kempe, M., Hacke, P., Reil, F., Bogdansk, N., Herrmann, W., Buerhop-Lutz, C., Razongles, G., Friesen, G., 2014. Review of failures of photovoltaic modules - iea-pvps [www document]. <https://iea-pvps.org>. URL [https://iea-pvps.org/wp-content/uploads/2020/01/IEA-PVPS-T13-01\\_2014\\_Review\\_of\\_Failures\\_of\\_Photovoltaic\\_Modules\\_Final.pdf](https://iea-pvps.org/wp-content/uploads/2020/01/IEA-PVPS-T13-01_2014_Review_of_Failures_of_Photovoltaic_Modules_Final.pdf) (accessed 4.26.22).
- Köntges, M., Siebert, M., Morlier, A., Illing, R., Bessing, N., Wegert, F., 2016. Impact of transportation on silicon wafer-based photovoltaic modules. *Prog. Photovolt., Res. Appl.* 24 (8), 1085–1095.
- Kunte, R., Gao, W., 2008. Comparison and review of islanding detection techniques for distributed energy resources. In: Power Symposium, NAPS'08. 40th North American. pp. 1–8.
- Kurukuru, V.S.B., Blaabjerg, F., Khan, M.A., Haque, A., 2020. A novel fault classification approach for photovoltaic systems. *Energies* 13 (2), 308.
- Laamami, S., Benhamed, M., Sbita, L., 2017. Artificial neural network-based fault detection and classification for photovoltaic system. In: 2017 International Conference on Green Energy Conversion Systems. GECS, pp. 1–7.
- Le, V., Yao, X., Miller, C., Tsao, B., 2020. Series DC arc fault detection based on ensemble machine learning. *IEEE Trans. Power Electron.* 35 (8), 7826–7839.
- Li, B., Delpha, C., Diallo, D., Migan-Dubois, A., 2021a. Application of artificial neural networks to photovoltaic fault detection and diagnosis: A review. *Renew. Sustain. Energy Rev.* 138, 110512.
- Li, B., Delpha, C., Migan-Dubois, A., Diallo, D., 2021b. Fault diagnosis of photovoltaic panels using full I–V characteristics and machine learning techniques. *Energy Convers. Manage.* 248, 114785.
- Li, X., Li, W., Yang, Q., Yan, W., Zomaya, A.Y., 2020. Edge-computing-enabled unmanned module defect detection and diagnosis system for large-scale photovoltaic plants. *IEEE Internet Things J.* 7 (10), 9651–9663.
- Li, X., Yang, Q., Lou, Z., Yan, W., 2019. Deep learning based module defect analysis for large-scale photovoltaic farms. *IEEE Trans. Energy Convers.* 34 (1), 520–529.
- Liu, Y., Ding, K., J. Zhang, Li, Y., Yang, Z., Zheng, W., Chen, X., 2021. Fault diagnosis approach for photovoltaic array based on the stacked auto-encoder and clustering with IV curves. *Energy Convers. Manage.* 245, 114603.
- Liu, G., Yu, W., 2017. A fault detection and diagnosis technique for solar system based on elman neural network. In: 2017 IEEE 2nd Information Technology, Networking, Electronic and Automation Control Conference. ITNEC, pp. 473–480.
- Livera, A., Theristis, M., Makrides, G., Sutterluetti, J., Georgiou, G., 2018. Advanced diagnostic approach of failures for grid-connected photovoltaic (PV) systems. In: 35th European Photovoltaic Solar Energy Conference and Exhibition At: Brussels.
- Llaria, A., Curea, O., Jimenez, J., Camblong, H., 2009. Survey on microgrids: analysis of technical limitations to carry out new solutions. In: Power Electronics and Applications, EPE'09. 13th European Conference. pp. 1–8.
- Lu, X., Lin, P., Cheng, S., Fang, G., He, X., Chen, Z., Wu, L., 2021a. Fault diagnosis model for photovoltaic array using a dual-channels convolutional neural network with a feature selection structure. *Energy Convers. Manage.* 248, 114777.
- Lu, X., Lin, P., Cheng, S., Lin, Y., Chen, Z., Wu, L., Zheng, Q., 2019a. Fault diagnosis for photovoltaic array based on convolutional neural network and electrical time series graph. *Energy Convers. Manage.* 196, 950–965.
- Lu, S., Sirojan, T., Phung, B.T., Zhang, D., Ambikairajah, E., 2019b. DA-DCGAN: An effective methodology for DC series arc fault diagnosis in photovoltaic systems. *EEE Access* 7, 45831–45840.
- Lu, S.-D., Wang, M.-H., Wei, S.-E., Liu, H.-D., Wu, C.-C., 2021b. Photovoltaic module fault detection based on a convolutional neural network. *Processes* 9 (9), 1635.
- Ma, M., Liu, H., Zhang, Z., Yun, P., Liu, F., 2019. Rapid diagnosis of hot spot failure of crystalline silicon PV module based on I–V curve. *Microelectron. Reliab.* 101, 113402.
- Madani, S.S., Abbaspour, A., Beiraghi, M., Dehkordi, P.Z., Ranjbar, A.M., 2012. Islanding detection for PV and DFIG using decision tree and AdaBoost algorithm. In: 2012 3rd IEEE PES Innovative Smart Grid Technologies Europe. ISGT Europe.
- Madeti, S.R., Singh, S.N., 2017. A comprehensive study on different types of faults and detection techniques for solar photovoltaic system. *Sol. Energy* 158, 161–185.
- Madeti, S.R., Singh, S.N., 2018a. Modeling of PV system based on experimental data for fault detection using KNN method. *Sol. Energy* 173, 139–151.
- Madeti, S.R., Singh, S.N., 2018b. Modeling of PV system based on experimental data for fault detection using KNN method. *Sol. Energy* 173, 139–151.
- Madeti, S., Singh, S., 2018c. Modeling of PV system based on experimental data for fault detection using kNN method. *Sol. Energy* 173, 139–151.
- Mahat, P., Chen, Z., Bak-Jensen, B., 2008. Review of islanding detection methods for distributed generation, electric utility deregulation and restructuring and power technologies. In: DRPT Third International Conference. pp. 2743–2748.
- Mahat, P., Chen, Z., Bak-Jensen, B., 2011. Review on islanding operation of distribution system with distributed generation. In: Power and Energy Society General Meeting. pp. 1–8.
- Mahendran, M., Anandharaj, V., Vijayavel, K., Winston Prince, D., 2015. Permanent mismatch fault identification of photovoltaic cells using arduino. *ICTACT. J. Microelectron.* 1 (2), 79–82, 2015.
- Malik, A., Haque, A., Satya Bharath, K., Jaffery, Z., 2021. Transfer Learning-Based Novel Fault Classification Technique for Grid-Connected PV Inverter. In: Lecture Notes in Electrical Engineering, pp. 217–224.
- Mandal, R.K., Kale, P.G., 2020. Assessment of different multiclass SVM strategies for fault classification in a PV system. In: Proceedings of the 7th International Conference on Advances in Energy Research. pp. 747–756.
- Mantel, C., Villebro, F., Alves dos Reis Benatto, G., Rajesh Parikh, H., Wendlandt, S., Hossain, K., Poulsen, P.B., Spataru, S., Séra, D., Forchhammer, S., 2019. Machine learning prediction of defect types for electroluminescence images of photovoltaic panels. Applications of Machine Learning <http://dx.doi.org/10.1117/12.2528440>.
- Mekki, H., Mellit, A., Salhi, H., 2016. Artificial neural network-based modelling and fault detection of partial shaded photovoltaic modules. *Simul. Model. Pract. Theory* 67, 1–13.
- Mellit, A., Kalogirou, S., 2008. Artificial intelligence techniques for photovoltaic applications: A review. *Prog. Energy Combust. Sci.* 34 (5), 574–632.
- Mellit, A., Tina, G.M., Kalogirou, S.A., 2018. Fault detection and diagnosis methods for photovoltaic systems: A review. *Renew. Sustain. Energy Rev.* 91, 1–17.
- Miao, W., Xu, Q., Lam, K., Pong, P., Poor, H., 2021. DC arc-fault detection based on empirical mode decomposition of arc signatures and support vector machine. *IEEE Sens. J.* 21 (5), 7024–7033.
- Mills-Price, M., Rourke, M., Kite, D., 2014. Adaptive control strategies and communications for utility integration of photovoltaic solar sites. In: Power and Energy Automation Conference.
- Miwa, M., Yamanaka, S., Kawamura, H., Ohno, H., Kawamura, H., 2006. Diagnosis of a power output lowering of PV array with a (–di/dv)–v characteristic. In: 2006 IEEE 4th World Conference on Photovoltaic Energy Conference. pp. 2442–2445. <http://dx.doi.org/10.1109/WCPEC.2006.279703>.
- Muñoz, M., Correcher, A., Ariza, E., García, E., Ibañez, F., 2015. Fault detection and isolation in a photovoltaic system. In: International Conference on Renewable Energy and Power Quality, la Coruña, Spain.
- Muhammad, N., Zakaria, N.Z., Shaari, S., Omar, A.M., 2017. System performance and detectable faults of a 10-year old 1.1 kWp GCPV system in Malaysia [WWW document]. <https://scilett-fsg.uitm.edu.my>. URL <https://scilett-fsg.uitm.edu.my/images/ManuscriptTemplate/Volume11-1/SL-2017-01-10.pdf> (accessed 4.26.22).
- Muralidharan, S., 2020. Addressing various fault detection and classification in grid tied photovoltaic system using artificial neural network (ANN). *Solid State Technol.* 63 (6), 12511–12523.
- Murugesan, N., Anitha, R., Ganesan, M., 2020. N-semi regular graph-based fuzzy semi-supervised learning approach for fault detection and classification in photovoltaic arrays. *Int. J. Adv. Res. Eng. Technol.* 11 (9), 887–896.
- Natsheh, E., Samara, S., 2020. Tree search fuzzy NARX neural network fault detection technique for PV systems with IoT support. *Electronics* 9 (7), 1087.
- Ndjakomo Essiane, S., Gnetchejo, P., Ele, P., Chen, Z., 2021. Faults detection and identification in PV array using kernel principal components analysis. *Int. J. Energy Environ. Eng.* [Accessed 9 2021].
- Nguyen, X.H., 2015. MATLAB/simulink based modeling to study effect of partial shadow on solar photovoltaic array. *Environ. Syst. Res.* 4 (1).
- Omer, A.M., 2007. Renewable energy resources for electricity generation in Sudan. *Renew. Sustain. Energy Rev.* 11 (7), 1481–1497.
- Omran, A., Said, D., Hussin, S., Ahmad, N., Samet, H., 2020. A novel intelligent detection schema of series arc fault in photovoltaic (PV) system based convolutional neural network. *Period. Eng. Nat. Sci. (PEN)* 8 (3), 1641–1653.
- Onal, Y., Turhal, U.C., 2021. Discriminative common vector in sufficient data case: A fault detection and classification application on photovoltaic arrays. *Eng. Sci. Technol. Int. J.* 24 (5), 1168–1179.

- Patil, D., Bindu, S., 2021. Arc fault detection in DC microgrid using deep neural network. In: 2021 4th Biennial International Conference on Nascent Technologies in Engineering. ICNTE, pp. 1–6.
- Patil, M., Hinge, T., 2019. Improved fault detection and location scheme for photovoltaic system. In: 2019 Innovations in Power and Advanced Computing Technologies. I-PACT.
- Pedersen, E., et al., 2019. Pv array fault detection using radial basis networks. In: 2019 10th International Conference on Information, Intelligence, Systems and Applications. IISA, pp. 1–4. <http://dx.doi.org/10.1109/IISA.2019.8900710>.
- Pillai, D.S., Natarajan, R., 2019. A compatibility analysis on NEC, IEC, and UL standards for protection against line–line and line–ground faults in PV arrays. *IEEE J. Photovolt.* 9 (3), 864–871. <http://dx.doi.org/10.1109/JPHOTOV.2019.2900706>.
- Platon, R., Martel, J., Woodruff, N., Chau, T.Y., 2015. Online fault detection in PV systems. *IEEE Trans. Sustain. Energy* 6 (4), 1200–1207.
- Popovich, V., 2011. Breakage issues in silicon solar wafers and cells. *Photovoltaics International* 12 (May), 49–57.
- Rao, S., Spanias, A., Tepedelenioglu, C., 2019. Solar array fault detection using neural networks. In: 2019 IEEE International Conference on Industrial Cyber Physical Systems. ICPS, pp. 196–200.
- Alves dos Reis Benatto, G., et al., 2020. Drone-based daylight electroluminescence imaging of PV modules. *IEEE J. Photovoltaics* 10 (3), 872–877. <http://dx.doi.org/10.1109/JPHOTOV.2020.2978068>.
- Rezgui, W., Mouss, L.H., Mouss, M.D., Kadri, O., 2014. Electrical faults detection for the intelligent diagnosis of a photovoltaic generator. *J. Electr. Eng.* 1–8.
- Rodrigues, S., Mütter, G., Ramos, H.G., Morgado-Dias, F., 2020. Machine learning photovoltaic string analyzer. *Entropy* 22 (2), 205.
- Rodríguez-Blanco, M.A., et al., 2011. A failure-detection strategy for IGBT based on gate-voltage behavior applied to a motor drive system. *IEEE Trans. Ind. Electron.* 58 (5), 1625–1633.
- Rouani, L., Harkat, M.F., Kouadri, A., Mekhilef, S., 2021. Shading fault detection in a grid-connected PV system using vertices principal component analysis. *Renew. Energy* 164, 1527–1539.
- Sabbaghpur Arani, M., Hejazi, M.A., 2016. The comprehensive study of electrical faults in PV arrays. *J. Electr. Comput. Eng.* 2016, 1–10.
- Sabbaghpur Arani, M., Hejazi, M.A., 2021. On-line faults detection and classification in PV array using Bayesian and k-nearest neighbor classifier. *Energy Eng. Manag.* 10-Jul-2018. [Online]. Available: <http://energy.kashanu.ac.ir/article-1-825-en.html>. (Accessed: 09 November 2021).
- Sabri, N., Tlemçani, A., Chouder, A., 2018. Intelligent fault supervisory system applied on stand-alone photovoltaic system. In: 2018 International Conference on Applied Smart Systems. ICASS, pp. 1–5.
- Sairam, S., Seshadri, S., Marafioti, G., Srinivasan, S., Mathisen, G., Bekiroglu, K., 2021. Edge-based explainable fault detection systems for photovoltaic panels on edge nodes. *Renew. Energy*.
- Salehifar, M., Arashloo, R., Moreno-Equilaz, J., Sala, V., Romeral, L., 2014. Fault detection and fault tolerant operation of a five phase PM motor drive using adaptive model identification approach. *IEEE J. Emerg. Sel. Top. Power Electron.* 2 (2), 212–223.
- Sama, A., 2021. Hello tomorrow – I am a hybrid quantum machine learning. medium. [Online]. Available: <https://andisama.medium.com/hello-tomorrow-i-am-a-hybrid-qml-b70751e36142>. (Accessed: 10 November 2021).
- Samara, S., Natsheh, E., 2019. Intelligent real-time photovoltaic panel monitoring system using artificial neural networks. *IEEE Access* 7, 50287–50299.
- Samara, S., Natsheh, E., 2020. Intelligent PV panels fault diagnosis method based on NARX network and linguistic fuzzy rule-based systems. *Sustainability* 12 (5), 2011.
- Schill, C., Brachmann, S., Koehl, M., 2015. Impact of soiling on IV-curves and efficiency of PV-modules. *Sol. Energy* 100–112, 259–262.
- Schimpf, F., Norum, L.E., 2009. Recognition of electric arcing in the DC-wiring of photovoltaic systems. In: Telecommunications Energy (INTELEC) International IEEE Conference, pp. 1–6.
- Schirone, L., Califano, F., Moschella, U., Rocca, U., 1994a. Fault finding in a 1 MW photovoltaic plant by reflectometry. In: Proceedings of the 24th IEEE Photovoltaic Specialist on Energy Conversion, pp. 846–9.
- Schirone, L., Califano, F.P., Pastena, M., 1994b. Fault detection in a photovoltaic plant by time domain reflectometry. *Prog. Photovolt., Res. Appl.* 2 (1), 35–44.
- Seo, G., Bae, H., Cho, B.H., Lee, K.C., 2012. Arc protection scheme for DC distribution systems with photovoltaic generation. In: 2012 International Conference on Renewable Energy Research and Applications. ICRERA, pp. 1–5.
- Sharma, V., Chandel, S.S., 2013. Performance and degradation analysis for long term reliability of solar photovoltaic systems: A review. *Renew. Sustain. Energy Rev.* 27, 753–767.
- Sheehan, M., Coddington, M., 2014. Pv system codes and standard, interconnection and permitting [www document]. <http://solarplusnw.org>. URL [http://solarplusnw.org/wp-content/uploads/2014/07/PV-System-Codes-and-Standard-Interconnection-Sheehan\\_Final\\_July\\_19.pdf](http://solarplusnw.org/wp-content/uploads/2014/07/PV-System-Codes-and-Standard-Interconnection-Sheehan_Final_July_19.pdf) (accessed 4.26.22).
- Shimakage, T., Nishioka, K., Yamane, H., Nagura, M., Kudo, M., 2011. Development of fault detection system in PV system. In: Proceedings of the 33rd IEEE International Telecommunications Energy Conference. INTELEC, pp. 1–5.
- Silvestre, S., Chouder, A., Karatepe, E., 2013. Automatic fault detection in grid connected PV systems. *Sol. Energy* 94, 119–127.
- Silvestre, S., Silva, M.A., Chouder, A., Guasch, D., Karatepe, E., 2014. New procedure for fault detection in grid connected PV systems based on the evaluation of current and voltage indicators. *Energy Convers. Manage.* 86, 241–249.
- Smith, K., Ran, L., Penman, J., 1997. Real-time detection of intermittent misfiring in a voltage-fed PWM inverter induction-motor drive. *IEEE Trans. Ind. Electron.* 44 (4), 468–476.
- Soffiah, K., Manoharan, P.S., Deepamangai, P., 2021. Fault detection in grid connected PV system using artificial neural network. In: 2021 7th International Conference on Electrical Energy Systems. ICEES, pp. 420–424.
- Solórzano, J., Egido, M.A., 2013. Automatic fault diagnosis in PV systems with distributed MPPT. *Energy Convers. Manage.* 76, 925–934.
- Spataru, S., Sera, D., Kerekes, T., Teodorescu, R., 2012. Detection of increased series losses in PV arrays using fuzzy inference systems. In: 2012 38th IEEE Photovoltaic Specialists Conference, pp. 000464–000469.
- Spataru, S., Sera, D., Kerekes, T., Teodorescu, R., 2015. Diagnostic method for photovoltaic systems based on light I–V measurements. *Sol. Energy* 119, 29–44.
- Stauffer, Y., Ferrario, D., Onillon, E., Hutter, A., 2015. Power monitoring based photovoltaic installation fault detection. In: 2015 International Conference on Renewable Energy Research and Applications. ICRERA, pp. 199–202. <http://dx.doi.org/10.1109/ICRERA.2015.7418695>.
- Steane, A., 1998. Quantum computing. *Rep. Progr. Phys.* 61 (2), 117–173.
- Stellbogen, D., 1993. Use of PV circuit simulation for fault detection in PV array fields. In: Conference Record of the Twenty Third IEEE Photovoltaic Specialists Conference - 1993 (Cat. No. 93CH3283-9), pp. 1302–1307. <http://dx.doi.org/10.1109/PVSC.1993.346931>.
- Sun, M., Lv, S., Zhao, X., Li, R., Zhang, W., Zhang, X., 2018a. Defect detection of photovoltaic modules based on convolutional neural network. *Mach. Learn. Intell. Commun.* 122–132, [Accessed 10 2021].
- Sun, J., Sun, F., Fan, J., Liang, Y., 2017. Fault diagnosis model of photovoltaic array based on least squares support vector machine in Bayesian framework. *Appl. Sci.* 7 (11), 1199.
- Sun, Y., Wang, J., Yang, Q., Li, X., Yan, W., 2018b. Fault diagnosis of photovoltaic module based on extreme learning machine technique. In: Proceedings of the 9th International Multi-Conference on Complexity, Informatics and Cybernetics. IMCIC 2018, pp. 34–39.
- Syafaruddin, E., Karatepe, Hiyama, T., 2011. Controlling of artificial neural network for fault diagnosis of photovoltaic array. In: 2011 16th International Conference on Intelligent System Applications to Power Systems, pp. 1–6.
- Takashima, T., Yamaguchi, J., Ishida, M., 2008. Fault detection by signal response in module strings. In: Proceedings of the 33rd IEEE Photovoltaic Specialists Conference, pp. 1–5.
- Takashima, T., Yamaguchi, J., Otani, K., Kato, K., Ishida, M., 2006. Experimental studies of failure detection methods in PV module strings. In: 2006 IEEE 4th World Conference on Photovoltaic Energy Conference, pp. 2227–2230. <http://dx.doi.org/10.1109/WCPEC.2006.279952>.
- Tina, G.M., Cosentino, F., Ventura, C., 2015. Monitoring and diagnostics of photovoltaic power plants. *Renew. Energy Serv. Mankind* 11, 505–516.
- Triki-Lahiani, A., Bennani-Ben Abdelghani, A., Slama-Belkhouja, I., 2018. Fault detection and monitoring systems for photovoltaic installations: A review. *Renew. Sustain. Energy Rev.* 82, 2680–2692.
- Tsanakas, J.A., Chrysostomou, D., Botsaris, P.N., Gasteratos, A., 2015b. Fault diagnosis of photovoltaic modules through image processing and Canny edge detection on field thermographic measurements. *Int. J. Sustain. Energy* 34 (6), 351–372.
- Tsanakas, J.A., Ha, L.D., Al Shakarchi, F., 2017. Advanced inspection of photovoltaic installations by aerial triangulation and terrestrial georeferencing of thermal/visual imagery. *Renew. Energy* 102, 224–233.
- Tsanakas, J.A., Ha, L., Buerhop, C., 2016. Faults and infrared thermographic diagnosis in operating C-si photovoltaic modules: A review of research and future challenges. *Renew. Sustain. Energy Rev.* 62, 695–709.
- Tsanakas, J.T.A., Vannier, G., Plissonnier, A., Ha, D.L., Barruel, F., 2015a. Fault diagnosis and classification of large-scale photovoltaic plants through aerial orthophoto thermal mapping, 31st European Photovoltaic Solar Energy Conference and Exhibition.
- Uehara, G., Rao, S., Dobson, M., Tepedelenioglu, C., Spanias, A., 2021. Quantum neural network parameter estimation for photovoltaic fault detection. In: 2021 12th International Conference on Information, Intelligence, Systems & Application. IISA, pp. 1–7. <http://dx.doi.org/10.1109/IISA52424.2021.9555558>.
- Usman, M., Ospina, J., Faruque, M., 2020. Fault classification and location identification in a smart DN using ANN and AMI with real-time data. *J. Eng.* 2020 (1), 19–28.
- Van Gompel, J., Spina, D., Develder, C., 2022. Satellite based fault diagnosis of photovoltaic systems using recurrent neural networks. *Appl. Energy* 305.



- Vandemark, A., 2020. Real-time series resistance monitoring of solar PV modules by communicating limited remote measurements to cloud-based algorithm via api. United States N. Web.
- Veerasamy, V., et al., 2021. LSTM recurrent neural network classifier for high impedance fault detection in solar PV integrated power system. *IEEE Access* 9, 32672–32687.
- Verch, S., Muniraju, G., Spanias, A., Tofis, Y., 2021. Feature analysis for PV fault detection neural network using linear PCA and random forest. [Online]. Available: <https://sensip.engineering.asu.edu/wp-content/uploads/2021/09/Skyler-Verch-IRES-final-report-with-citations.pdf>. (Accessed: 09 November 2021).
- Vergura, S., Acciani, G., Amoruso, V., Patrono, G.E., Vacca, F., 2009. Descriptive and inferential statistics for supervising and monitoring the operation of PV plants. *IEEE Trans. Ind. Electron.* 56 (11), 4456–4464. <http://dx.doi.org/10.1109/TIE.2008.927404>.
- Vieira, R.G., Dhimish, M., de Araújo, F.M.U., Guerra, M.I.S., 2020. PV module fault detection using combined artificial neural network and sugeno fuzzy logic. *Electronics* 9 (12), 2150.
- Wang, J., Gao, D., Zhu, S., Wang, S., Liu, H., 2019. Fault diagnosis method of photovoltaic array based on support vector machine. *Energy Sources A: Recov. Util. Environ. Effects* 1–16.
- Wang, Y., Li, Y., Ruan, X., 2016a. High-accuracy and fast-speed MPPT methods for PV string under partially shaded conditions. *IEEE Trans. Ind. Electron.* 63 (1), 235–245.
- Wang, W., Liu, A.C., Chung, H.S., Lau, R.W., Zhang, J., Lo, A.W., 2016b. Fault diagnosis of photovoltaic panels using dynamic current–Voltage characteristics. *IEEE Trans. Power Electron.* 31 (2), 1588–1599. <http://dx.doi.org/10.1109/TPEL.2015.2424079>.
- Wang, L., Liu, J., Guo, X., Yang, Q., Yan, W., 2017. Online fault diagnosis of photovoltaic modules based on multi-class support vector machine. In: 2017 Chinese Automation Congress. CAC.
- Wang, L., Qiu, H., Yang, P., Mu, L., 2021. Arc fault detection algorithm based on variational mode decomposition and improved multi-scale fuzzy entropy. *Energies* 14 (14), 4137.
- Winston, D., et al., 2021. Solar PV's micro crack and hotspots detection technique using NN and SVM. *IEEE Access* 9, 127259–127269.
- Woike, T.W., Stotlar, S.C., Woods, L., 1990. The bypass Diode Assembly: Solar Cell Protection for Space Station Freedom. In: IEEE Conference on Photovoltaic Specialists.
- Wu, Y., Chen, Z., Wu, L., Lin, P., Cheng, S., Lu, P., 2017. An intelligent fault diagnosis approach for PV array based on SA-RBF kernel extreme learning machine. *Energy Procedia* 105, 1070–1076.
- Wu, Y., Lan, Q., Sun, Y., 2009. Application of BP neural network fault diagnosis in solar photovoltaic system. In: 2009 International Conference on Mechatronics and Automation. pp. 2581–2585.
- Xia, K., He, S., Tan, Y., Jiang, Q., Xu, J., Yu, W., 2018. Wavelet packet and support vector machine analysis of series DC ARC fault detection in photovoltaic system. *Trans. Electr. Electron. Eng.* 14 (2), 192–200.
- Yi, Z., Etemadi, A., 2016. A novel detection algorithm for line-to-line faults in photovoltaic (PV) arrays based on support vector machine (SVM). In: 2016 IEEE Power and Energy Society General Meeting. PESGM, pp. 1–4.
- Yi, Z., Etemadi, A.H., 2017a. Fault detection for photovoltaic systems based on multi-resolution signal decomposition and fuzzy inference systems. *IEEE Trans. Smart Grid* 8 (3), 1274–1283.
- Yi, Z., Etemadi, A., 2017b. Line-to-line fault detection for photovoltaic arrays based on multiresolution signal decomposition and two-stage support vector machine. *IEEE Trans. Ind. Electron.* 64 (11), 8546–8556.
- Yin, G., 2005. A distributed generation islanding detection method based on artificial immune system. In: Transmission and Distribution Conference and Exhibition: Asia and Pacific. IEEE/PES, pp. 1–4.
- Yun, L., Bofeng, Y., Dan, Q., Fengshuo, L., 2021. Research on fault diagnosis of photovoltaic array based on random forest algorithm. In: 2021 IEEE International Conference on Power Electronics, Computer Applications. ICPECA.
- Zaki, S., Zhu, H., Fakhri, M., Sayed, A., Yao, J., 2021. Deep-learning-based method for faults classification of PV system. *IET Renew. Power Gener.* 15 (1), 193–205.
- Zaki, S.A., Zhu, H., Yao, J., 2019. Fault detection and diagnosis of photovoltaic system using fuzzy logic control. In: E3S Web of Conferences, Vol. 107. p. 02001.
- Zeineldin, H., El-Saadany, E., Salama, M., 2006. Impact of DG interface control on Islanding detection and non detection zones. *IEEE Trans. Power Deliv.* 21 (3), 1515–1523.
- Zhang, W., Zhang, H., Liu, J., Li, K., Yang, D., Tian, H., 2017. Weather prediction with multiclass support vector machines in the fault detection of photovoltaic system. *IEEE/CAA J. Autom. Sin.* 4 (3), 520–525.
- Zhao, Y., (2010). (thesis). Fault Analysis in Solar Photovoltaic Arrays. The Department of Electrical and Computer Engineering.
- Zhao, Y., Ball, R., Mosesian, J., de Palma, J., Lehman, B., 2015. Graph-based semi-supervised learning for fault detection and classification in solar photovoltaic arrays. *IEEE Trans. Power Electron.* 30 (5), 2848–2858. <http://dx.doi.org/10.1109/TPEL.2014.2364203>.
- Zhao, Q., Shao, S., Lu, L., Liu, X., Zhu, H., 2018. A new PV array fault diagnosis method using fuzzy C-mean clustering and fuzzy membership algorithm. *Energies* 11 (1), 238.
- Zhao, Y., Yang, L., Lehman, B., de Palma, J.-F., Mosesian, J., Lyons, R., 2012. Decision tree-based fault detection and classification in solar photovoltaic arrays. In: 2012 Twenty-Seventh Annual IEEE Applied Power Electronics Conference and Exposition. APEC.
- Ziane, A., Dabou, R., Sahouane, N., Necaibia, A., Mostefaoui, M., Bouraiou, A., Slimani, A., 2020. Detecting partial shading in grid-connected PV station using random forest classifier. In: Artificial Intelligence and Renewables Towards An Energy Transition. pp. 88–95.